

การสังเคราะห์และวิเคราะห์คุณลักษณะของแผ่นฟิล์มพอลิอิมิดแบบร่างแห
โดยใช้โทลิลีนไดไอโซไซยานาท

นายศิริชัย รียเกษ

วิทยานิพนธ์นี้เป็นส่วนหนึ่งของการศึกษาตามหลักสูตรปริญญาวิศวกรรมศาสตรมหาบัณฑิต
สาขาวิชาวิศวกรรมเคมี ภาควิชาวิศวกรรมเคมี
คณะวิศวกรรมศาสตร์ จุฬาลงกรณ์มหาวิทยาลัย
ปีการศึกษา 2549
ลิขสิทธิ์ของจุฬาลงกรณ์มหาวิทยาลัย

SYNTHESIS AND CHARACTERIZATION OF CROSS-LINKED POLYIMIDE FILM USING
TOLYLENE DIISOCYANATE

Mr. Sirichai Reeyakad

A Thesis Submitted in Partial Fulfillment of the Requirements
for the Degree of Master of Engineering Program in Chemical Engineering

Department of Chemical Engineering

Faculty of Engineering

Chulalongkorn University

Academic Year 2006

Copyright of Chulalongkorn University

Thesis Title SYNTHESIS AND CHARACTERIZATION OF CROSS-
LINKED POLYIMIDE FILM USING TOLYLENE
DIISOCYANATE

By Sirichai Reeyakad

Field of Study Chemical Engineering

Thesis Advisor Associate Professor ML. Supakanok Thongyai, Ph.D.

Accepted by the Faculty of Engineering, Chulalongkorn University in
Partial Fulfillment of the Requirements for the Master's Degree

.....Dean of the Faculty of
Engineering
(Professor Direk Lavansiri, Ph.D.)

THESIS COMMITTEE

..... Chairman
(Associate Professor Suttichai Assabumrungrat, Ph.D.)

..... Thesis Advisor
(Associate Professor ML. Supakanok Thongyai, Ph.D.)

..... Member
(Associate Professor Seeroong Prichanont, Ph.D.)

..... Member
(Assistant Professor Bunjerd Jongsomjit, Ph.D.)

..... Member
(Sirirat Wacharawichanant, Ph.D.)

ศิริชัย รียเกษ: การสังเคราะห์และวิเคราะห์คุณลักษณะของแผ่นฟิล์มพอลิอิมิดแบบ
 ร้างแหโดยใช้โทลิลีนไดไอโซไซยานาท (SYNTHESIS AND CHARACTERIZA-
 TION OF CROSS-LINKED POLYIMIDE FILM USING TOLYLENE
 DIISOCYANATE) อ. ที่ปรึกษา: รศ. ดร. มล. ศุภกนก ทองใหญ่, 84 หน้า

งานวิจัยนี้ได้ทำการสังเคราะห์ และวิเคราะห์คุณลักษณะของแผ่นฟิล์มพอลิอิมิดแบบร่าง
 แห โดยปฏิกิริยาระหว่างไดไอโซไซยานาทกับหมู่ไฮดรอกซิลที่อยู่ในสายโซ่ของพอลิอิมิด ซึ่ง
 สามารถยืนยันได้โดยอินฟราเรดสเปกตรัม ในระหว่างกระบวนการให้ความร้อนของพอลิอิมิด
 แบบร่างแหพบว่าเกิดการสลายตัวของคาร์บอนไดออกไซด์ที่อยู่ในส่วนของสายโซ่ยูริเทน ซึ่งทำให้
 เกิดรูพรุนในแผ่นฟิล์ม โดยการเกิดรูพรุนภายในแผ่นฟิล์มสามารถยืนยันได้โดยค่าคงที่ไดอิเล็กตริก
 พบว่าเมื่อปริมาณโทลิลีนไดไอโซไซยานาทมากขึ้นค่าคงที่ไดอิเล็กตริกจะมีค่าลดลง โดยจากการ
 เปรียบเทียบคุณสมบัติของแผ่นฟิล์มพบว่า PI50-C1.0 มีคุณสมบัติที่เหมาะสมที่สุดเนื่องจากมีค่า
 สมบัติทางกลที่ดีและค่าคงที่ไดอิเล็กตริกที่มีค่าต่ำ จากผลของการวิเคราะห์คุณสมบัติทางกลที่
 คุณสมบัติต่างๆ พบว่า PI50-C1.0 มีคุณสมบัติทางกลที่ดีอย่างเห็นได้ชัดเจนนที่อุณหภูมิสูง
 (มากกว่า 350 องศาเซลเซียส) ซึ่งเป็นการยืนยันการเกิดโครงสร้างแบบร่างแห อย่างไรก็ตาม
 PI50-C1.0 ยังแสดงค่าความเค้นที่ต่ำกว่า PI50 ที่อุณหภูมิห้อง แสดงถึงอิทธิพลของรูพรุนที่มี
 มากกว่าโครงสร้างแบบร่างแห ทำยที่สุดจากการวิเคราะห์ลักษณะพื้นผิว และรูพรุนโดยเครื่อง
 SEM ไม่พบความแตกต่างระหว่าง PI50 กับ PI50-C1.0 ซึ่งสามารถอธิบายได้ว่ารูพรุนที่เกิดขึ้น
 จากคาร์บอนไดออกไซด์มีขนาดเล็กมากเกินกว่ากำลังขยายของเครื่อง SEM

ภาควิชา.....วิศวกรรมเคมี.....
 สาขาวิชา.....วิศวกรรมเคมี.....
 ปีการศึกษา.....2549.....

ลายมือชื่อนิสิต.....
 ลายมือชื่ออาจารย์ที่ปรึกษา.....

4870487321: MAJOR CHEMICAL ENGINEERING

KEY WORD: POLYIMIDE, DIELECTRIC, CROSS-LINKED, POROUS FILM,
DIISOCYANATE

SIRICHAI REEYAKAD: SYNTHESIS AND CHARACTERIZATION OF
CROSS-LINKED POLYIMIDE FILM USING TOLYLENE DIISO-
CYANATE. THESIS ADVISOR: ASSOC. PROF. ML. SUPAKANOK
THONGYAI, Ph.D., 84 pp.

Cross-linked polyimide films were synthesized by the reaction between diisocyanate groups and hydroxyl functional groups in polyimide structure, which was confirmed by IR. During the thermal treatment of the cross-linked polyimide, the thermal labile component (CO_2) in the urethane segments was decomposed which might generate pores in the film. The presence of the pores was confirmed from the dielectric constant of the film. The dielectric constant of the films decreased with the increase of TDI loading. By comparing the properties of the films, the PI50-C1.0 exhibited optimum mechanical and good dielectric properties. The cross-linked structure was also confirmed by DMA. The PI50-C1.0 showed excellent storage and loss modulus especially in the high temperature range (above 350°C) due to the characteristic of cross-linked structure. Moreover, the results of tensile stress test showed that the PI50-C1.0 exhibited lower tensile strength than the PI50 because the presence of pore in PI50-C1.0 might influence to strength greater than the effect of cross-linked structure. Finally, the SEM cross sectional images can not be observed the different between PI50 and PI50-C1.0. This might be based on that the very small size of pores, which were generated by carbon dioxide.

Department Chemical Engineering

Field of study Chemical Engineering

Academic Year 2006

Student's signature

Advisor's signature

ACKNOWLEDGEMENTS

I would like to express my deeply gratitude to my advisor, Associate Professor Dr. ML. Supakanok Thongyai, Ph.D. to his continuous guidance, enormous number of invaluable discussions, helpful suggestions, warm encouragement, patience to correct my writing and all supporting. I am grateful to Associate Professor Suttichai Assabumrungrat, Ph.D., Assistant Professor Seeroong Prichanont, Ph.D., Associate Professor Bunjerd Jongsomjit, Ph.D. and Sirirat Wacharawichanant, Ph.D. for serving as chairman and thesis committees, respectively, whose comments were constructively and especially helpful.

Sincere thanks are made to Mektec Manufacturing Corporation for using Differential Scanning Calorimetry (TGA), Universal Testing Machine, Dynamic Mechanical Analysis (DMA) and digital hot-plate stirrer

Sincere thanks to all my friends and all members of the Center of Excellent on Catalysis & Catalytic Reaction Engineering (Petrochemical Engineering Research Laboratory), Department of Chemical Engineering, Chulalongkorn University for their assistance and friendly encouragement.

Finally, I would like to dedicate this thesis to my parents and my families, who generous supported and encouraged me through the year spent on this study.

CONTENTS

	PAGE
ABSTRACT(IN THAI).....	iv
ABSTRACT(IN ENGLISH).....	v
ACKNOWLEDGEMENTS.....	vi
CONTENTS.....	vii
LIST OF FIGURES.....	x
LIST OF TABLES.....	xiii
CHAPTERS	
I INTRODUCTION.....	1
1.1 The Objective of This Thesis.....	4
1.2 The Scope of This Thesis.....	4
II THEORY.....	5
2.1 Synthesis of polyimides.....	5
2.1.1 Two-step method via poly(amic acid)s.....	5
2.1.1.1 Formation of poly(amic acid)s.....	6
2.1.1.2 Reactivity of monomers.....	7
2.1.1.3 Effect of solvents.....	10
2.1.1.4 Side reactions and effect of other factors.....	11
2.1.1.5 Thermal imidization of poly(amic acid).....	12
2.1.2 One-step method.....	15
2.1.2.1 High-temperature solution polymerization.....	15
2.1.2.2 Low-temperature solution polymerization.....	17
2.2 Processes for making films and coatings.....	18
2.3 Isocyanates.....	18
2.3.1 Reactions of isocyanates.....	19
2.4 Electrical properties.....	20
2.4.1 Dielectric Constant.....	20
2.4.2 Dissipation Factor.....	21

	PAGE
CHAPTER	
III LITERATURE REVIEWS.....	23
3.1 Polyimide.....	23
3.2 Phenylethynyl containing imide oligomer.....	24
3.3 Cross-linked polyimide.....	26
3.4 Porous polyimide film.....	30
IV EXPERIMENT.....	31
4.1 Equipments and Chemicals.....	31
4.1.1 Chemicals.....	31
4.1.2 Equipments.....	32
4.2 Preparation of polyimide capped with non-reactive end groups.....	36
4.3 Preparation of cross-linked polyimide.....	38
4.4 Preparation of cross-linked polyimide films.....	38
4.5 Characterization Instruments.....	38
4.5.1 Infrared Spectroscopy (FTIR).....	38
4.5.2 Thermogravimetric analysis (TGA).....	39
4.5.3 Dynamic Mechanical Analysis (DMA).....	39
4.5.4 Tensile testing machine.....	40
4.5.5 Dielectric properties.....	41
4.5.6 Scanning Electron Microscope (SEM).....	41
4.6 Research methodology.....	42
V RESULTS AND DISCUSSION.....	43
5.1 Preparation of polyimide.....	43
5.2 Preparation of cross-linked polyimide.....	44
5.3 Preparation of cross-linked polyimide films.....	45
5.4 Physical properties of cross-linked polyimide films.....	47
5.5 Dielectric properties.....	48
5.6 Thermal Properties.....	50
5.7 Mechanical Properties.....	53
5.7.1 Dynamic mechanical properties.....	53

	PAGE
CHAPTER	
5.7.2 Tensile mechanical properties.....	56
5.8 Morphology.....	59
VI CONCLUSIONS AND RECOMMENDATIONS.....	61
6.1 Conclusions.....	61
6.2 Recommendations.....	62
REFERENCES.....	63
APPENDICES.....	66
APPENDIX A.....	67
APPENDIX B.....	69
APPENDIX C.....	76
VITA.....	84

LIST OF FIGURES

FIGURE	PAGE
2.1 Preparation of Kapton polyimide.....	5
2.2 Reaction mechanism of imide formation.....	6
2.3 Resonance effect on phthalic anhydride group.....	7
2.4 Major reaction pathways involving poly(amic-acid) formation.....	11
2.5 Schematic representation of typical isothermal imidization kinetic curves at various temperatures.....	13
2.6 Mechanism of thermal ring closure of amic acid to imide.....	14
2.7 Reaction of dicyanomethylidene phthalide with aniline.....	17
2.8 Polymerization of bisdicyanomethylidene derivative of PMDA with ODA.....	17
2.9 Structure of Diisocyanates.....	19
2.10 Polyurethane addition reaction.....	19
2.11 Electrode arrangement for testing dielectric constant.....	20
2.12 Electrode arrangement for testing dissipation factor.....	21
2.13 Vector diagram of equivalent parallel circuit for a laminate.....	21
3.1 Structure of 6FDA/TFDB polyimide.....	23
3.2 Structure of perfluorinate polyimide.....	24
3.3 Structure of PETI-5.....	25
3.4 Structure of cross-linked polyimide based on hexamethylene diisocyanate.....	27
3.5 Structure of end cross-linked polyimide.....	28
3.6 Structure of cross-linked polyimide based on diphenylmethane diisocyanate.....	29
4.1 Glove box.....	32
4.2 Schlenk line.....	33
4.3 Schlenk tube.....	34
4.4 Inert gas supply system.....	34
4.5 Vacuum pump.....	35
4.6 Reaction vessel.....	35
4.7 Preparation of polyimide capped with non-reactive end groups.....	37

FIGURE	PAGE
4.8 Dynamic Mechanical Analysis (DMA) Equipment.....	40
4.9 Universal Testing Machine equipment.....	41
4.10 Flow diagram of research methodology.....	42
5.1 FTIR spectra of a) PI25 b) PI50 c) PI75 d) PI100.....	44
5.2 FT-IR spectra of a) Polyimide solution in NMP b) Polyimide solution after TDI added c) Polyimide solution after TDI added 30 min.....	45
5.3 Thermogravimetric analyses of polyimide solution in NMP of a) PI100 b) PI100-C1.0.....	46
5.4 Optical images of polyimide films a) PI25 b) PI25-C0.1 c) PI25-C0.5 d) PI25-C1.0.....	48
5.5 Dielectric constant of polyimide films.....	49
5.6 TGA thermogram of the polyimide films.....	51
5.7 DMA curves (storage modulus (E') and temperature) for PI50 and PI50-C1.0.....	54
5.8 DMA curves (loss modulus (E'') and temperature) for PI50 and PI50-C1.0.....	55
5.9 DMA curves ($\tan\delta$ and temperature) for PI50 and PI50-C1.0.....	55
5.10 Decomposition mechanism of urethane component.....	56
5.11 Tensile strength of PI50.....	57
5.12 Tensile strength of PI50-C1.0.....	57
5.13 Comparison of Tensile strength of PI50 and PI50-C1.0.....	58
5.14 SEM images of surface of a) PI50 b) PI50-C1.0 and cross section of c) PI50 d) PI50-C1.0.....	59
A.1 FTIR spectra of PI25 series.....	67
A.2 FTIR spectra of PI50 series.....	67
A.3 FTIR spectra of PI75 series.....	68
A.4 FTIR spectra of PI100 series.....	68
B.1 DMA curve of PI25.....	69
B.2 DMA curve of PI25-C0.1.....	69
B.3 DMA curve of PI25-C0.5.....	70
B.4 DMA curve of PI25-C1.0.....	70
B.5 DMA curve of PI50.....	71
B.6 DMA curve of PI50-C0.1.....	71

FIGURE	PAGE
B.7 DMA curve of PI50-C0.5.....	72
B.8 DMA curve of PI50-C1.0.....	72
B.9 DMA curve of PI75.....	73
B.10 DMA curve of PI75-C0.1.....	73
B.11 DMA curve of PI75-C0.5.....	74
B.12 DMA curve of PI100.....	74
B.13 DMA curve of PI100-C0.1.....	75
C.1 TGA curve of PI25.....	76
C.2 TGA curve of PI25-C0.1.....	76
C.3 TGA curve of PI25-C0.5.....	77
C.4 TGA curve of PI25-C1.0.....	77
C.5 TGA curve of PI50.....	78
C.6 TGA curve of PI50-C0.1.....	78
C.7 TGA curve of PI50-C0.5.....	79
C.8 TGA curve of PI50-C1.0.....	79
C.9 TGA curve of PI75.....	80
C.10 TGA curve of PI75-C0.1.....	80
C.11 TGA curve of PI75-C0.5.....	81
C.12 TGA curve of PI75-C1.0.....	81
C.13 TGA curve of PI100.....	82
C.14 TGA curve of PI100-C0.1.....	82
C.15 TGA curve of PI100-C0.5.....	83
C.16 TGA curve of PI100-C0.5.....	83

LIST OF TABLES

TABLE	PAGE
2.1 Electron affinity of aromatic anhydrides.....	8
2.2 Basicity pK_a of diamines and their reactivity toward PMDA.....	9
2.3 Rates of amic acid formation at 30°C and effects of solvents.....	10
2.4 Infrared Absorption Bands of Imides and Related Compound.....	15
4.1 Conditions and parameter for running DMA.....	39
5.1 Physical properties of polyimide films.....	47
5.2 Dielectric constant of polyimide films.....	49
5.3 Void fraction of polyimide films.....	50
5.4 Thermal properties of the polyimide films.....	53
5.5 Tensile properties of PI50 and PI50-C1.0.....	59

CHAPTER I

INTRODUCTION

The last twenty-five years of this century have seen a flurry of activity in the synthesis and development of high performance and high temperature polymers. This has been in large part due to need for advanced materials required for a diverse range of applications including aerospace, automotive and microelectronic industries. These applications often demand a unique combination of properties including high glass transition temperatures, toughness, good adhesion, oxidative and thermal stability, and low dielectric constant.

From this standpoint, polyimides as a class of materials are very promising due to an array of desirable characteristics that these materials possess including excellent mechanical properties, wear resistance, radiation resistance, inertness to solvents, hydrolytic stability, low dielectric constants, high breakdown voltage, low losses over a wide range of frequency, good adhesion strengths, low thermal expansion, and long-term stability. Indeed significant advances have been made in the diverse field of polyimides in the past five decades and today these versatile materials find use in a broad range of applications. These functions include the usages as structural adhesive to bond wing panels and fuselage of both civilian and military aircraft, as interlayer dielectrics in microelectronic applications and as coatings in optoelectronic applications.

The synthesis of an aromatic polyimide was first reported in 1908 but it was not until the late 1950s that DuPont developed a successful commercial route to high-molecular-weight polyimides. The first commercial polyimide was introduced by DuPont in the late 1960s. Since then this field has blossomed, and there has been a high tempo of R&D activity in synthesizing an array of polyimides with requisite properties for a given application and in devising new methods of characterization. Concomitantly, a legion of polyimides have become available with many and different characteristics to satisfy requirements for various applications. [1]

One of the most important applications of polyimide thin films is used as the interlayer dielectric. The utmost importance for the microelectronic applications is the lowness of dielectric constant and high dielectric breakdown voltage of polyimides. In electronic packing, low dielectric materials minimize cross talk and maximize signal propagation speed in devices. Hence, the development of polyimides with increasingly lower dielectric constants has been the focus of several investigations. In particular, fluorinated polyimides have received extensive attention due to their lower dielectric constants suitable for the microelectronic applications. Chern et al. [3-5] and Matsuura et al. [8, 9] mainly interested in fluorine introduction to polyimide structure in order to decrease dielectric constant. They reported that the incorporation of fluorine into polyimide structure has been intensively explored in the past decade and also fluorine amount increasing has been found to generally lower the dielectric constant and moisture absorption. On the other hand Cassidy et al. [2] has reported the effect of fluorination on polyamide whose dielectric constant nearly in the range of 2.6–3.0.

An alternative approach, Yamazaki et al. [10] has offered that cross-linked polyimide thin films may be interesting because the gel structure is expected to make porous polyimides which can be used as low dielectric material. Recently, a novel cross-linked polyimide (CPI) has been prepared by imidization of cross-linked poly(amic-acid). [11, 12] Unfortunately, the shrinkage due to the thermal imidization of cross-linked poly(amic-acid) could lead to drop in the performance of the materials. Currently, porous polyimide films were vary interested because the presence of voids in their films can reduce the overall dielectric constant. There are several ways to prepare porous materials such as the decomposition of thermally labile component of polymer blends or block copolymers [13, 14], the introduction of carbon micro-spheres or hollow silica tubes [15], the introduction of silica particles follow by the etching of HF [16]. However, the limitations of porous materials are generally the distribution of pore, the uncontrollable pores size and the low mechanical properties. Therefore, the low dielectric materials, which have good mechanical properties and very small pore size, are celled for next generation of electronic devices.

This research involves the study and synthesis of cross-linked polyimide film to decrease dielectric constant and to improve mechanical properties. With this purpose, the polyimide containing functional groups in the main chain and cross-linked polyimide film will be synthesized. Firstly, the polyimide containing phthalic anhydride end capped was synthesized by using one step method polymerization then reacted with various amount of diisocyanate as cross-linking agents in order to obtain corresponding cross-linked structures. The effects of cross-linking modification on the thermal stability and physical properties of the cross-linked films were studied. Furthermore, preliminary studies on the electrical properties such as dielectric constant of TDI based cross-linked films were investigated.

1.1 Objectives of the thesis

- 1.1.1. To synthesize cross-linked polyimide films based on tolylene diisocyanate.
- 1.1.2. To improve dielectric properties of the conventional polyimide film for microelectronic applications.

1.2 Scope of the thesis

1.2.1 Study and synthesize polyimides derived from 4,4'-(hexafluoroisopropylidene)diphthalic anhydride (6FDA), phthalic anhydride (PA), 3,3'-dihydroxy-4,4'-diaminobiphenyl (HAB) and 3,4'-oxidianiline (3,4'-ODA) by using one-step method polymerization.

1.2.2. Synthesize the cross-linked polyimide based on tolylene diisocyanate (TDI).

1.2.3. Characterize the cross-linked polyimide film properties by conventional techniques: FTIR, TGA, DMA, SEM, Tensile properties and dielectric properties measurement.

CHAPTER II

THEORY

2.1 Synthesis of Polyimides [1]

2.1.1 Two-step method via poly(amic acid)s

The majority of polyimides possess extended rigid planar aromatic and heteroaromatic structures and are infusible and insoluble. The earlier pioneers at DuPont Co. coped with this common problem of intractability generally associated with high-temperature polymers by synthesizing the soluble polymer precursor, namely "poly(amic acid)" and converting it to the final polyimide. Figure 2.1 shows an example of the synthesis of Kapton polyimide. This highly elegant process made it possible to bring the first significant commercial polyimide products into the market and it is still the method of choice in majority of applications. However, the seemingly simple process involves several elementary reactions interrelated in a complex scheme. In the following sections important parameters that govern these complex interrelations will be discussed in terms of reaction mechanisms in relation to the chemical and physical natures of monomers and intermediates as well as solvents involved.

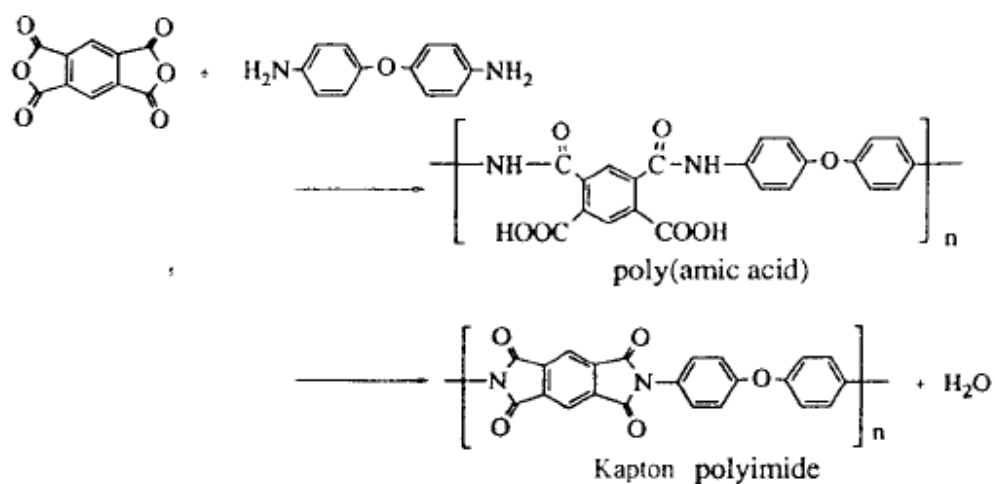


Figure 2.1 Preparation of Kapton polyimide

2.1.1.1 Formation of Poly(amic acid)s

When a diamine and a dianhydride are added into a dipolar aprotic solvent such as *N,N*-dimethylacetamide, poly(amic acid) is rapidly formed at ambient temperatures. The reaction mechanism involves the nucleophilic attack of the amino group on the carbonyl carbon of the anhydride group, followed by the opening of the anhydride ring to form amic acid group as illustrated in Figure 2.2

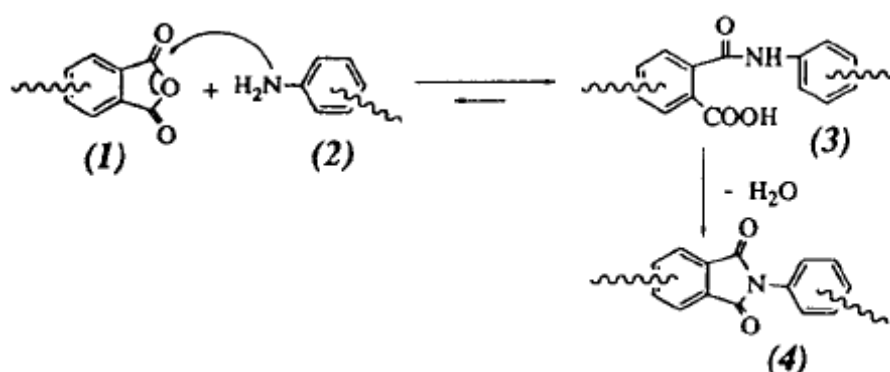


Figure 2.2 Reaction mechanism of imide formation

The most important aspect of this process is that it is an equilibrium reaction. Often it appears to be an irreversible reaction because a high-molecular-weight poly(amic acid) is readily formed in most cases as long as pure reagents are used. This is because the forward reaction is much faster than the reverse reaction, often by several orders of magnitude. If the large reaction rate difference is not met, the high-molecular-weight poly(amic acid) is not formed. Therefore, it is important to examine the driving forces that favor the forward reaction over the reverse reaction. It should also be noted that the acylation reaction of amines is an exothermic reaction and that the equilibrium is favored at lower temperatures. The forward reaction in dipolar solvents is a second-order reaction and the reverse reaction is a first-order reaction. Therefore, the equilibrium is favored at high monomer concentrations to form higher molecular-weight poly(amic acid)s

2.1.1.2 Reactivity of Monomers

As mentioned earlier the mechanism of poly(amic acid) formation is a nucleophilic substitution reaction at one of the carbonyl carbon atoms of the dianhydride with diamine. Therefore, it is expected that the reaction rate is primarily governed by the electrophilicity of the carbonyl groups of the dianhydride and the nucleophilicity of the amino nitrogen atom of the diamine. Phthalic anhydride group is not an acid in Bronsted's sense, but it is a strong electron acceptor and, therefore, a relatively strong Lewis acid. The two carbonyl groups are situated at the ortho position to each other and their strong electron-withdrawing effect activates each other towards nucleophilic reaction. The effect is particularly enhanced by the preferred carbonyl conformation locked in the coplanar aromatic ring as illustrated by the resonance structures in Figure 2.3

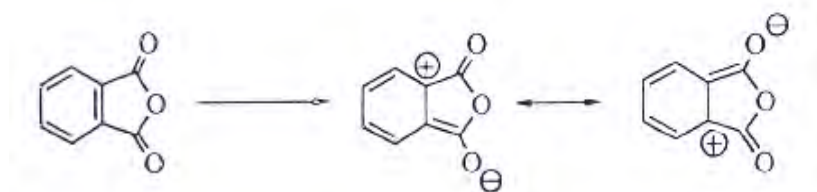
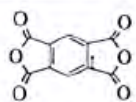
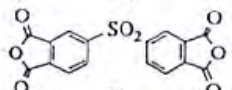
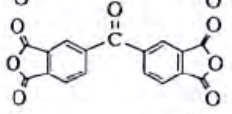
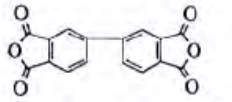
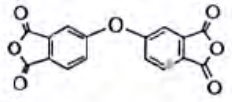
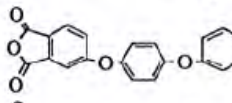
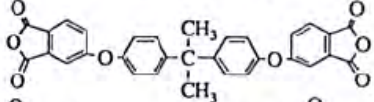
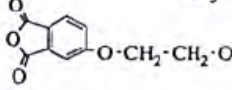


Figure 2.3 Resonance effect on phthalic anhydride group.

Among commonly available dianhydrides pyromellitic dianhydride (PMDA), 1,2,4,5-benzenetetracarboxylic dianhydride, is the most reactive. It possesses four carbonyl groups attached to the same benzene ring in a coplanar conformation and, therefore, shows the strongest tendency to accept an electron.

The electrophilicity of carbonyl carbons of each dianhydride can be measured in terms of the electron affinity, a tendency to accept an electron, of the molecule. As shown in Table 2.1, earlier investigators quantified electron affinity (E_a) for various dianhydrides by polarographic measurement and demonstrated that the rate of acylation reaction of 4,4'-diaminodiphenyl ether and a model compound 4-aminodiphenyl ether was closely correlated with the E_a value.

Table 2.1 Electron affinity of aromatic anhydrides.


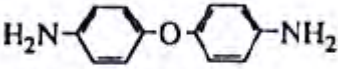

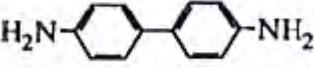
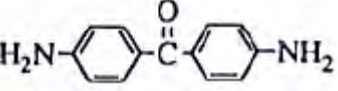
Dianhydrides	Abbreviation	E_a (eV)
1. 	PMDA	1.90
2. 	DSDA	1.57
3. 	BTDA	1.55
4. 	BPDA	1.38
5. 	ODPA	1.30
6. 	HQDA	1.19
7. 	BPADA	1.12
8. 	EDA	1.10

Because of the strong electron-accepting property of dianhydrides and high electron density of amino groups of many diamines, quantum chemical analysis predicts that a charge transfer interaction and electrostatic interaction between dianhydrides and diamines contribute significantly to the reactivity. The acylation of a diamine with a dianhydride is preceded by a charge transfer interaction in which diamine is a donor and dianhydride an acceptor. It is a common observation that the reaction mixture exhibits a strong color of charge transfer complex at the beginning, and that the color gradually fades as the acylation proceeds. For dianhydrides with the bridged bisphthalic anhydride structure (dianhydrides 2, 3, and 5-8 in Table 2.1), the bridge group strongly influences E_a of the dianhydride. Compared with BPDA, which lacks a bridge group, the electron-withdrawing bridge groups such as SO_2 and $\text{C}=\text{O}$ increase the E_a value substantially, while electron-donating groups such as ethers decrease it. The reactivity of ether-containing dianhydrides (6-8 in Table 2.1) is significantly reduced so that they are practically not affected by the atmospheric

moisture while PMDA and 3,3', 4,4'-benzophenonetetracarboxylic dianhydride (BTDA) must be handled under strictly moisture-free conditions at all times.

Unlike the E_a value of dianhydrides, the ability of diamines to give off an electron, the ionization potential (I), does not seem to correlate well in a simple manner, although the reaction rates of diamines towards a given dianhydride generally increase with increase in their ionization potential. The reactivity of diamines instead correlates well with its basicity (pK_a) in a Hammett's relation. The reaction rates (k) of various diamines toward PMDA are shown in Table 2.2 in relation to their pK_a .

Table 2.2 Basicity pK_a of diamines and their reactivity toward PMDA.

Diamine	pK_a	$\log k$
	6.08	2.12
	5.20	0.78
	4.80	0
	4.60	0.37
	3.10	-2.15

The structure of diamines seems to influence the rate of acylation reaction more than the variation in dianhydride structure. It should be noted that the rate constants differ by four orders of magnitude between amines with electron-donating substituents and those with electron-withdrawing ones. If relatively less reactive dianhydrides such as ether-containing dianhydride are reacted with 4,4'-diaminodiphenylsulfone or 4,4'-diaminobenzophenone, it is expected that the molecular weight of the resulting poly(amic acid)s would be lower.

2.1.1.3 Effect of Solvents

Solvents used in the formation of poly(amic acid)s play an important role. Most commonly used solvents are dipolar aprotic amide solvents such as *N,N*-dimethylformamide (DMF), *N,N*-dimethylacetamide (DMAc), *N*-methylpyrrolidinone (NMP), and tetramethylurea (TMU). Sulfoxides such as dimethylsulfoxide (DMSO) can be used. However, lesser thermal stability and difficulty in removing it in the following imidization process argue against its use. One of the important properties of these solvents is the basicity (Lewis' base). It is interesting and worthy to note that the starting reagents are weakly basic aromatic amine and nonprotic anhydride, and yet the product is a strong protic acid. In other words, the starting mixture is basic and the product is an acid. The orthoamic acid is a relatively strong carboxylic acid because of the electron-withdrawing effect of the orthoamide group and the stabilization by internal hydrogen bonding of dissociated carboxylate with amide hydrogen. The strong acidbase interaction between the amic acid and the amide solvent is a major source of exothermicity of the reaction and one of the most important driving forces. Therefore, it is expected that the rate of poly(amic acid) formation is generally faster in more basic and more polar solvents. The rate of reaction measured for phthalic anhydride and 4-phenoxyaniline increased with solvent in the order of tetrahydrofuran (THF) < acetonitrile < DMAc (Table 2.3).

Table 2.3 Rates of amic acid formation at 30°C and effects of solvents.

Anhydrides	Solvents	k_1 (1/mol·s)	k_2 (1/mol·s ²)
Phthalic anhydride	DMAc	0.0850	–
	Acetonitrile	0.00102	33.63
	THF	0.000387	7.17
	<i>m</i> -Cresol	0.685	7.34
Tetrahydrophthalic anhydride	DMAc	0.000583	0.0378
	Acetonitrile	0.00750	0.116
	THF	0.158	2.16
	<i>m</i> -Cresol	0.0412	7.92

k_1 , rate constant of second-order reaction; k_{-1} , rate constant of reverse reaction; k_2 , rate constant of autocatalytic reaction.

2.1.1.4 Side Reactions and Effect of Other Factors

As discussed above, the formation of poly(amic acid) is primarily governed by the reactivity of monomers and the nature of solvent used. However, close analysis reveals that there are several minor but important reactions accompanying the main reaction. These side reactions may become significant under certain conditions, particularly when the acylation reaction of diamine is relatively slow because of low monomer reactivity or low monomer concentration. The major pathways involved in the formation of poly(amic acid) are illustrated in Figure 2.4

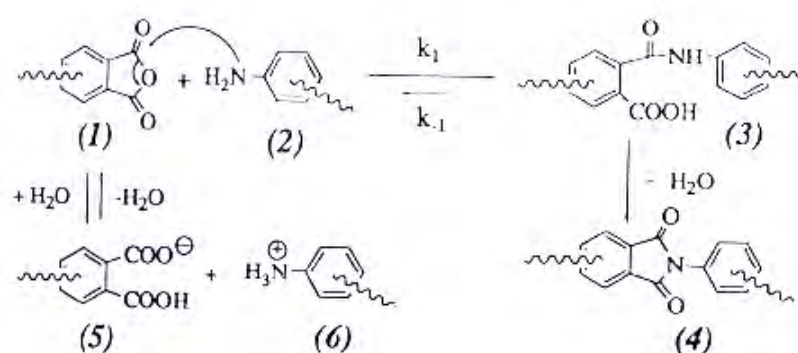


Figure 2.4 Major reaction pathways involving poly(amic-acid) formation. k_1 , rate constant for PAA formation; k_{-1} , rate constant for reverse reaction.

The main reaction is an equilibrium reaction determined by acylation (k_1) and deacylation (k_{-1}) reactions. The latter is also described as an intramolecular acidolysis to form an anhydride. This unique feature is the result of ortho neighboring effect. In contrast, the acylation of an amine with benzoic anhydride is an irreversible reaction under the same reaction condition. In Figure 2.4, the general structure of poly(amic acid)s is considered as a class of polyamides with pendant carboxylic groups at ortho positions. Aromatic polyamides, such as Nomex, which lack ortho carboxylic groups, are very stable under conditions of poly(amic acid) synthesis.

Although they are structurally similar, poly(amic acid)s are known to undergo hydrolytic degradation even at ambient temperatures. When poly(amic acid)s are in solution a small amount of anhydride groups always exist in an equilibrium concentration. However small, it plays an important role in the hydrolytic degradation

of poly(amic acid). In the presence of water the anhydride group is hydrolyzed to form ortho dicarboxylic group. The reaction is driven by the enhanced nucleophilicity of water in a dipolar aprotic solvent and by strong acid-base interaction of the product with the dipolar solvent. The ortho dicarboxylic group thus remains stabilized as one of the end groups of the poly(amic acid) and does not revert to the anhydride. As the anhydride group is consumed, the more is produced to reestablish the equilibrium. The effect of water on the molecular weight of poly(amic acid)s during polymerization, and the effect of added water on the molecular weight of the already polymerized poly(amic acid)s in solution, are well documented. Although the common source of water is in the solvents and the monomers containing water as an impurity, it should be noted that the water is also formed in situ by the imidization of amic acid groups. Although the rate of the imidization, and therefore the formation of water, is relatively slow at ambient temperatures, it is still significant enough to cause a gradual decrease in molecular weight over a long period of time.

2.1.1.5 Thermal Imidization of Poly(amic acid)

Conversion of poly(amic acid)s to the corresponding polyimides is most commonly performed thermally in "solid state." This method is suitable for preparation of thin objects such as films, coatings, fibers, and powders in order to allow the diffusion of by-product and solvent without forming bristles and voids in the final polyimide products. The cast films are dried and heated gradually up to 250-350°C, depending upon the stability and glass transition temperature (T_g) of the polymer. Too rapid a heating may cause the formation of bubbles in the sample. When a DMAc solution of poly(amic acid) is cast and "dried" at ambient temperature to a nontacky state, the resulting film still contains a substantial amount of the solvent (typically up to 25% by weight, depending on the drying conditions). In the subsequent heating, imidization reaction takes place not in a true solid state but rather in a very concentrated viscous solution, at least during the initial and intermediate stages of thermal imidization. The presence of residual solvent plays an important role. The imidization proceeds faster in the presence of dipolar amide solvents. The observation is attributed to the specific solvation to allow the favorable conformation of amic acid group to cyclize. It may be also explained by the plasticizing effect of the solvent to increase the mobility of the reacting functional groups. The favorable

property of amide solvent also suggests that its basicity to accept protons may be responsible for the specific effect. The proton of the carboxylic group is strongly hydrogen-bonded to the carbonyl group of the amide solvent. The cyclization of *o*-carboxamide group results in dehydrogen bonding and release of the solvent molecule along with water of condensation. The thermal imidization process of poly(amic acid)s is complex, and it has not been possible to describe it by simple kinetic expression. The imidization process involves several interrelated elementary reactions, and dynamically changing physical properties such as diffusion rate, chain mobility, solvation, and acidity. Such complex concurrent events make it difficult to analyze the system in simple terms. The isothermal imidization kinetics is shown schematically in Figure 2.5.

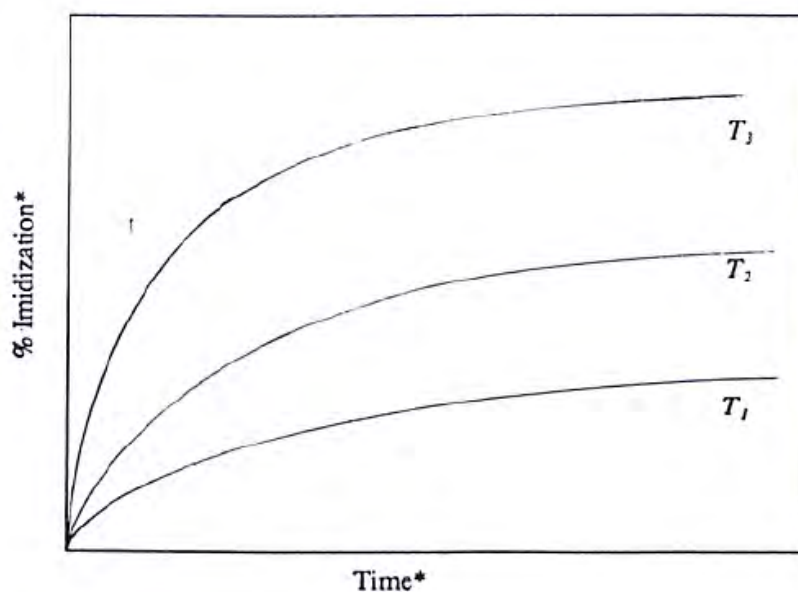


Figure 2.5 Schematic representation of typical isothermal imidization kinetic curves at various temperatures ($T_1 < T_2 < T_3$).

The imidization proceeds rapidly at the initial stage and tapers off at a plateau, a typical diffusion-limited kinetic process. As the degree of imidization increases, the T_g or stiffness of the polymer chain increases. When the T_g approaches the reaction temperature, the imidization rate slows down markedly. At a higher temperature, a higher degree of imidization is attained. The initial rapid stage of imidization is attributed to the ring closure of amic acid in the favorable conformation (a), as shown in Figure 2.6.

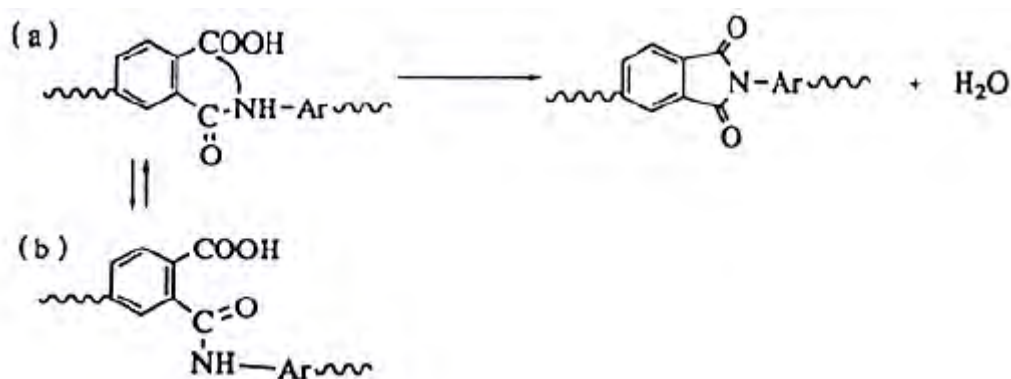


Figure 2.6 Mechanism of thermal ring closure of amic acid to imide.

The slower rate in the later stage of imidization is attributed to the unfavorable conformation (b), which has to rearrange to conformation (a) before ring closure. Such a conformational rearrangement requires rotational motion of the adjoining polymer chain and strongly bound solvent molecules.

Analytical methods useful to determine the degree of chemical transformations in the solid state are limited. The most commonly used method is infrared spectroscopy. Some of the absorption bands useful for the quantitative or qualitative analysis of imidization are listed in Table 2.4. Several characteristic absorption bands are used for the quantification of five-membered aromatic imides. The strongest absorption occurs at 1720 cm^{-1} (C=O symmetrical stretching). However, the band partially overlaps with strong carboxylic acid band (1700 cm^{-1} , C=O) of poly(amic acid). The more useful bands of imide groups are 1780 cm^{-1} (C=O asymmetrical stretching), 1380 cm^{-1} (C-N stretching), and 725 cm^{-1} (C=O bending). The absorption of anhydrides also occurs at 1780 and around 720 cm^{-1} . When a mixture of imide and anhydride groups is analyzed, these bands may partially overlap with those of imide group, requiring proper correction. The carboxylic acid bands, 1700 cm^{-1} (C=O) and $2800\text{--}3200\text{ cm}^{-1}$, (OH), and amide bands, 1660 cm^{-1} (C=O, amide I), 1550 cm^{-1} (C-NH, amide II) and bands at $3200\text{--}3300\text{ cm}^{-1}$ (NH) often appear as broad peaks, particularly when they are strongly associated with hydrogen bonds. Nevertheless, they are useful for the qualitative assessment during imidization process.

Table 2.4 Infrared Absorption Bands of Imides and Related Compound

	Absorption band (cm^{-1})	Intensity	Origin
Aromatic imides	1780	S	C=O asym. Stretch
	1720	VS	C=O svm. Stretch
	1380	S	C-N stretch
	725		C=O bending
Isoimides	1795-1820	S	Iminolactone
	1700	M	Iminolactone
	921-934	VS	Iminolactone
Amic acids	2900-3200	M	COOH and NH_2
	1710	S	C=O (COOH)
	1660 amide I	S	C=O (CONH)
	1550 amide II	M	C-NH
Anhydrides	1820	M	C=O
	1780	S	C=O
	720	S	C=O
Amines	~3200 two bands	W	NH, symmetrical structure (ν_s)
			NH, asymmetrical structure (ν_{as})
			$\nu_s = 345.53 + 0.876\nu_{as}$

VS, very strong; S, strong; M, medium; W, weak

2.1.2 One-step method

2.1.2.1 High-Temperature Solution Polymerization

A single-stage homogeneous solution polymerization technique can be employed for polyimides which are soluble in organic solvents at polymerization temperatures. In this process, a stoichiometric mixture of monomers is heated in a high boiling solvent or a mixture of solvents in a temperature range of 140-250°C where the imidization reaction proceeds rapidly. Commonly used solvents are nitrobenzene, benzonitrile, α -chloronaphthalene, *o*-dichlorobenzene, trichlorobenzenes, and phenolic solvents such as, *n*-cresol and chlorophenols in addition to dipolar aprotic amide solvents. Toluene is often used as a cosolvent to facilitate the removal of the water of condensation. During polymerization, water is distilled off continually as an azeotrope along with the solvent. Preparation of high-molecular-

weight poly(amic acid) is not necessary in this procedure. Imidization still proceeds via amic acid intermediate. However, the concentration of amic acid group is very small at any time during the polymerization because it is unstable at high temperature and rapidly imidizes, or reverts to amine and anhydride. Because water is formed as the result of the imide formation, some of the anhydride groups are rapidly hydrolyzed to o-dicarboxylic acid. When a mixture composed of diamine, dianhydride, and a solvent is heated, a viscous solution is formed at intermediate temperature of 30-100°C. The composition of the product is mainly poly(amic acid). At this stage, phase separation is usually observed in nonpolar solvents such as chlorinated aromatic hydrocarbons. However, on raising the temperature to 120-160°C, a vigorous evolution of water occurs and the reaction mixture suddenly becomes homogeneous. At this stage the product is essentially a low molecular-weight polyimide having o-dicarboxy and amino end groups. Thereafter, a slow stepwise polycondensation takes place according to the reaction between the end groups. Gerashchenko et al. studied one-step solution polycondensation in nitrobenzene employing soluble polyimide system based on 9,9-bis(4-aminophenyl)fluorene with PMDA or 4,4'-oxydiphthalic anhydride. The kinetic profile was composed of a fast second-order reaction at initial stage and the following slow first-order reaction. The high-temperature solution imidization in nitrobenzene showed that it was a second-order reaction. Similar results were also reported by Vinogradova et al. Lavrov et al. studied imidization of a model compound N-phenylphthalamic acid to N-phenylphthalimide in various solvents. The rate profile showed an initial fast second-order kinetic and much slower second-order reaction after 40-60% conversion. The rate was slower in basic aprotic amide solvents and faster in acidic solvent in-cresol. In general, imidization reaction has been shown to be catalyzed by acid. Kreuz et al. observed that thermal imidization of poly(amic acid)s was catalyzed by tertiary amines. High-temperature solution polymerization in m-cresol is often performed in the presence of high boiling tertiary amines such as quinoline as catalyst. Dialkylaminopyridines and other tertiary amines were effective catalysts in neutral solvents such as dichlorobenzene. Alkali metal and zinc salts of carboxylic acids, and salts of certain organophosphorus compounds were also very efficient catalysts in one-step polycondensation of polyimides.

2.1.2.2 Low-Temperature Solution Polymerization

Kim and Moore synthesized a dicyanomethylidene derivative of phthalic anhydride, as shown in Figure 2.7. The compound reacted with aniline in NMP to produce an intermediate of amic acid analog that gradually transformed during 24 h at room temperature to N-phenylphthalimide, coproducing malonitrile as condensation byproduct. Subsequently, bis(dicyanomethylidene) derivative of PMDA and ODA were reacted in NMP to afford poly(amic acid) analog intermediate, which underwent partial imidization at room temperature in the homogeneous solution, as illustrated in Figure 2.8.

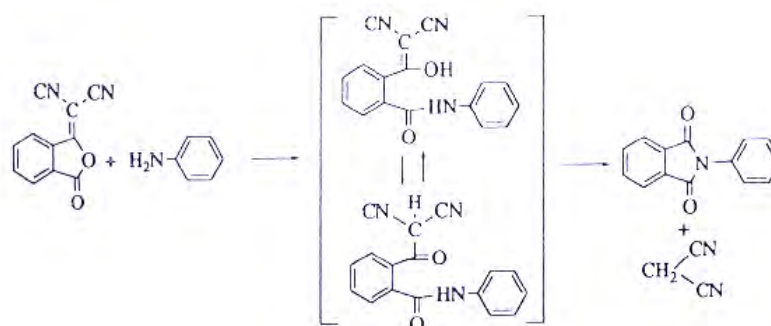


Figure 2.7 Reaction of dicyanomethylidene phthalide with aniline.

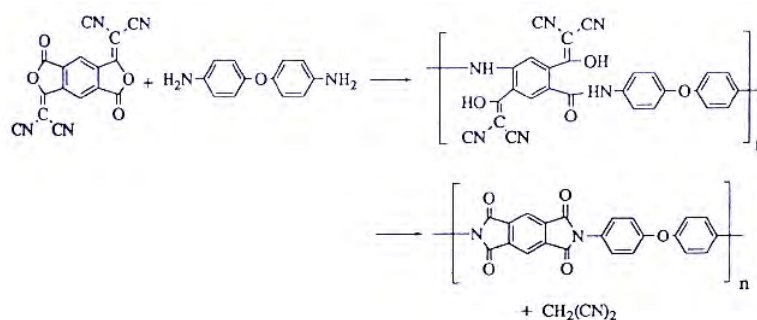


Figure 2.8 Polymerization of bisdicyanomethylidene derivative of PMDA with ODA

The extent of imidization reached approximately 75% over 24 h, after which time the polymer began to precipitate. The solid-state imidization of films prepared from the poly(amic acid) analog intermediate behaved similarly to that of poly(amic acid). However, the imidization could be achieved at lower temperature; it was nearly complete at 120°C in 20 h.

2.2 Processes for making films and coatings

The synthesis of aromatic polyimides from dianhydrides and diamines can be carried out either a one-step or two-step method. In the classic (two-step) method, a tetracarboxylic dianhydride (or functional derivative) is added to a solution of a diamine in a polar aprotic solvent, such as N-methylpyrrolidone (NMP), at 15-75°C to form a soluble poly(amic acid). The poly(amic acid) is cyclodehydrated (imidized) to the corresponding insoluble polyimide by either heating at temperatures in excess of 300°C (thermal imidization) or through the addition of chemical dehydrating agents (chemical imidization). Since the polyimide is insoluble, films or coatings are generally prepared from the poly(amic acid). Polyimides that are soluble in organic solvents can be prepared using a one-step method in which the dianhydride and diamine are stirred at 180-220°C in a high-boiling-point organic solvent. The synthesis of the poly(amic acid) precursor and its imidization to the polyimide occur spontaneously. Low-molecular-weight soluble polyimide oligomers terminated by reactive end groups can also be prepared. These "addition" polyimides are then polymerized in situ by heating. This discussion will focus only on polyimides prepared using the two-step method using a thermal (as opposed to chemical) imidization process. The six steps in the preparation of coatings by thermal cure are:

1. Substrate preparation
2. Application of the adhesion promoter
3. Deposition of the precursor solution onto the substrate
4. Drying the coating to remove solvent and allow the substrate to be handled
5. Patterning the coating
6. Curing the coating to remove any remaining solvents and to complete the conversion of the precursor to the polyimide

2.3 Isocyanates [30]

Diisocyanate products are required for making elastomers, whilst high functionality MDI (diisocyanato-diphenylmethane)-rich in polyisocyanates is desirable for the manufacture of rigid foams and binding materials. Within the latter group,

wide variation in the molecular weight distribution and functionality is possible, giving considerable control over reactivity, viscosity, and application properties.

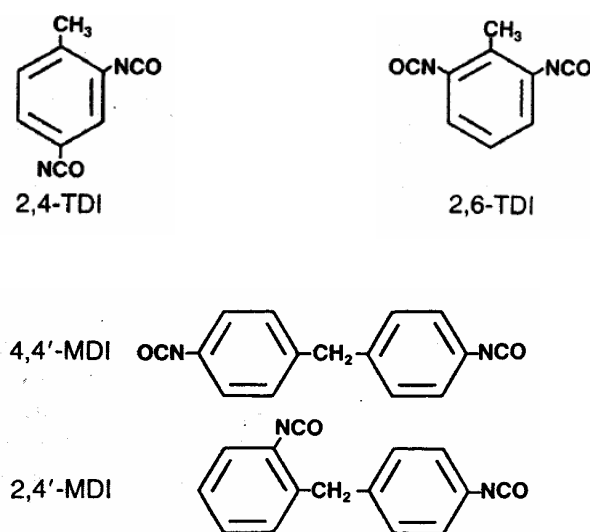


Figure 2.9 Structure of Diisocyanates

Aliphatic diisocyanates, which are much less reactive than the aromatic diisocyanate, are therefore used for applications requiring high resistance to yellowing. Those most widely available are 1-isocyanato-3-isocyanatomethyl-3,5,5-trimethylcyclohexane (isophorone diisocyanate or IPDI), 1,6-diisocyanato-hexane (hexamethyl diisocyanate or HDI) and 4,4-diisocyanato-dicyclohexylmethane (hydrogenate MDI or HMDI). The isomeric diisocyanates, 2,4- and 1,3-di(isocyanato-dimethyl-methyl)-benzene (m- and p- tetramethyl xylene diisocyanate or m- and p-TMXDI), which behave like aliphatic diisocyanates, are also available.

2.3.1 Reactions of isocyanates

With polyols : the reaction of di- or poly-isocyanates with polyols form polyurethanes :

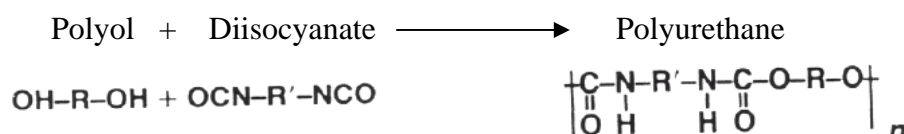


Figure 2.10 Polyurethane addition reaction

The reaction is exothermic. The rate of the polymerization reaction depends upon the structure of both the isocyanate and the polyol. Aliphatic polyols with primary hydroxyl end groups are the most reactive. They react with isocyanates 10 times faster than similar polyols with secondary hydroxyl groups. Phenol reacts with isocyanates more slowly and the resulting urethane groups are easily broken on heating to yield the original isocyanate and the phenol. This reversible reaction is used in manufacture of “blocked” isocyanates which are activated by heating. The isocyanate group (-NCO) can react with any compound containing “active” hydrogen atom and diisocyanates may therefore be used to modify many other product.

2.4 Electrical properties

2.4.1 Dielectric Constant [31]

Dielectric constant is the ratio of the capacitance of a capacitor with a given dielectric to the capacitance of the same capacitor with air as dielectric (Figure 2.11). It is calculated from the capacitance as read on a capacitance bridge, the thickness of the sample and the area of the electrode.

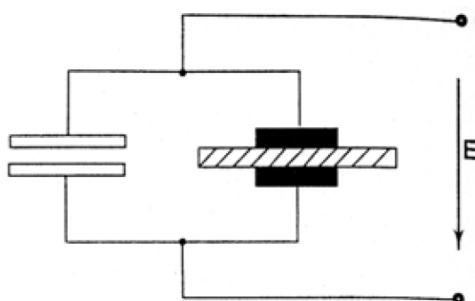


Figure 2.11 Electrode arrangement for testing dielectric constant

The dielectric constant is also referred to as Permittivity and being a ratio, is a dimensionless entity. The dielectric constant measures the ability of an insulating material to store electrostatic energy. It varies with the thickness, temperature, humidity, frequency and chemical composition of the material. The effects of temperature and frequency variations on the dielectric constant vary for different materials.

2.4.2 Dissipation Factor

The dissipation factor of an insulating material is the ratio of the total power loss (in watts) in the material to the product of the voltage and current in the capacitor in which the material is the dielectric. It varies with frequency, moisture, temperature, etc. and is a dimensionless entity. Expressed in another way, the dissipation factor is the ratio of parallel reactance to parallel resistance. It is measured with the electrode arrangement as shown in Figure 2.12 where as Figure 2.13 shows the vector diagram of the equivalent parallel circuit.

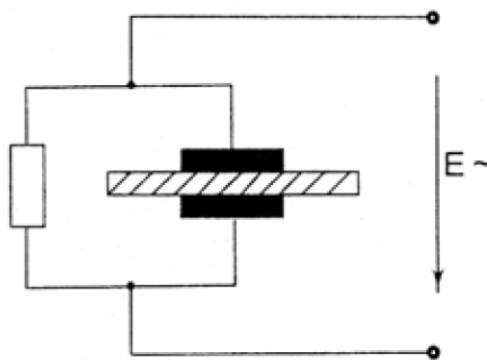


Figure 2.12 Electrode arrangement for testing dissipation factor

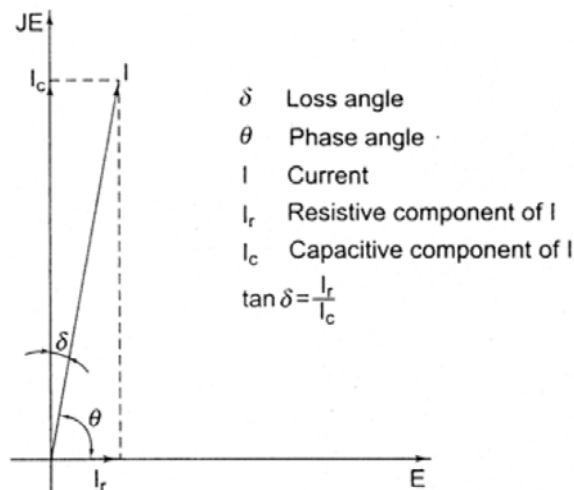


Figure 2.13 Vector diagram of equivalent parallel circuit for a laminate

The dissipation factor is expressed as $\tan \delta$ (the tangent value of loss angle δ). The dissipation is directly related to the resistive power loss in a laminate. Therefore, for an electronic circuit operating at a high power loss, it is desirable to use laminates

with a low dissipation factor. The value of the dissipation factors for various combinations of fillers and resins are:

Paper phenolic laminates	0.02-0.08
Glass epoxy laminates	0.01-0.03
Glass PTFE laminates	0.0008-0.005

The dissipation factor of a laminate varies with the frequency, temperature and moisture absorbed. This implies that the dissipation factor given in data sheet must be related to the condition under which it has been determined.

CHAPTER III

LITERATURE REVIEWS

3.1 Polyimide

Tohru Matsuura, et al. [8] synthesized new fluorinated polyimides by the reaction of 2,2'-bis(trifluoromethyl)-4,4'-diaminobiphenyl (TFDB) with 2,2-bis(3,4-dicarboxy phenyl) hexafluoropropane dianhydride (6FDA) or pyromellitic dianhydride (PMDA). The polyimide 6FDA/TFDB from the reaction of TFDB with 6FDA has high optical transparency and high solubilities in several solvents such as N,N-dimethylacetamide (DMAc), tetrahydrofuran (THF), acetone, and ethyl acetate. In addition, it has a low dielectric constant of 2.8 at 1 MHz, a low refractive index of 1.556 at 589.3 nm, and a low water absorption rate of 0.2%. The polyimide PMDA/TFDB prepared from the reaction of TFDB with PMDA has not only a low dielectric constant of 3.2 and a low refractive index of 1.647, but also a low coefficient of thermal expansion (CTE) of -5×10^{-6}

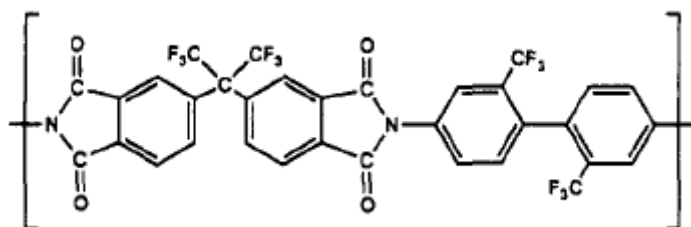


Figure 3.1 Structure of 6FDA/TFDB polyimide

Shinji Ando, Tohru Matsuura, and Shigekuni Sasaki [9] synthesized a perfluorinated polyimide that has T_g over 260 °C and a high optical transparency over the entire optical communication wavelengths. Their high thermal stability and optical transparency are due to their fully aromatic molecular structure and the absence of C-H bonds. The use of a diamine, which has a relatively high reactivity, and a new perfluorinated dianhydride, which has a flexible structure, makes it possible to obtain a tough and flexible perfluorinated polyimide film. In addition, this polymer has a low dielectric constant. Perfluorinated polyimides are promising for usage as optoelectronic materials.

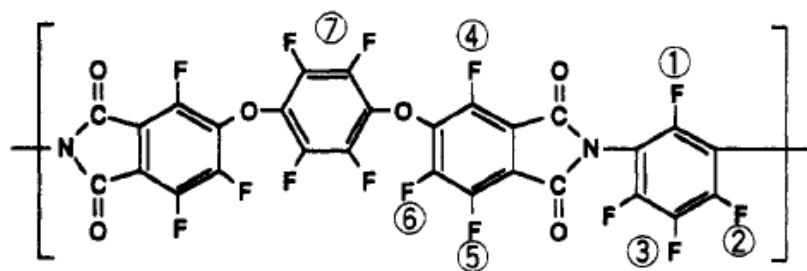


Figure 3.2 Structure of perfluorinate polyimide

Der-Jang Liaw, Feng-Chyuan Chang, Man-Kit Leung, et al. [17] successfully prepared a series of new noncoplanar polyimides and polyamides based on biphenyldiamine containing a naphthalene group by the condensation method with various tetracarboxylic dianhydrides and aromatic dicarboxylic acids. The introduction of a naphthalene group into the polymer backbone resulted in polyimides and polyamides with excellent solubility and mechanical properties. These polymers exhibited the characteristic of thermal stability by the naphthalene group and reduce the glass transition temperature of the rigid-rod-like structure which could improve the processing characteristics. These properties can make these polyimides and polyamides attractive for practical applications such as processable high-temperature engineering plastics because of the bulky and noncoplanar naphthalene groups in the polymer chain.

3.2 Phenylethynyl containing imide oligomer

P. M. Hergenrother, J. W. Connell and J. G. Smith Jr. [18] prepared amide acid and imide oligomers containing pendent and terminal phenylethynyl groups at calculated molecular weight of 5000. The cured oligomer exhibit high T_g and high unoriented thin film tensile properties. Adhesive panels and carbon fiber laminates were readily fabricated under 1.4 MPa. Titanium tensile shear specimens fabricated from one composition exhibited excellent retention of room temperature properties when tested at 232°C. Preliminary composite properties of one system exhibited high open whole compressive strengths with excellent retention of strength when wet tested at 177°C.

P.M. Hergenrother, J.W. Connell, J.G. and Smith Jr. [19] investigated imide oligomers containing phenylethynyl groups. Phenylethynyl groups were placed on the ends of oligomers of different molecular weights (1250, 2500 and 5000 g/mol), pendent along the backbone of oligomers and both pendent and terminal on oligomers. 4-Phenylethynylphthalic anhydride (PEPA) was used to place phenylethynyl groups on the ends of the oligomers and 3,5-diamino-4'-phenylethynyl benzophenone (DPEB) was used to introduce pendent phenylethynyl groups along the oligomeric backbone. Upon heating above 300°C, the phenylethynyl groups react to provide chain extension, branching and crosslinking. Several of these materials exhibited excellent properties as adhesives and composite matrices. The lower molecular weight oligomers exhibit better compression moldability than the higher molecular weight version.

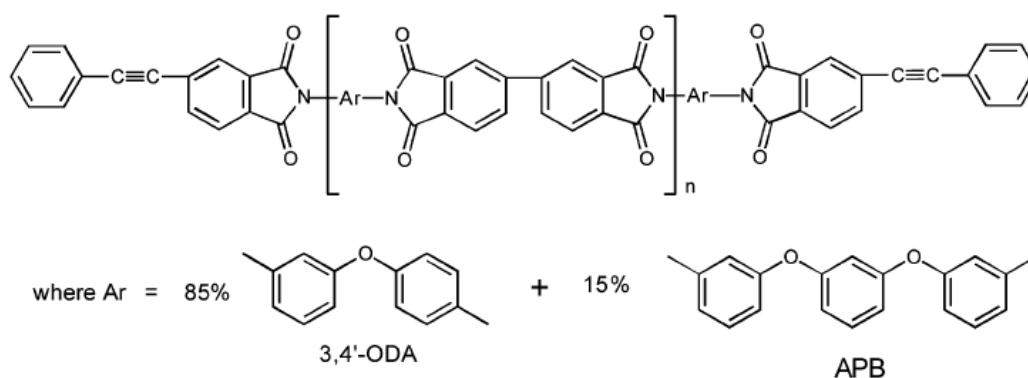


Figure 3.3 Structure of PETI-5

Paul M. Hergenrother and Craig M. Thompson [20] investigated naphthylethynyl terminated imide oligomers. The naphthylethynyl terminated imide oligomers were compared with the corresponding phenylethynyl terminated imide oligomers. The replacement of the phthalimide groups with naphthalimide groups showed that the phenylethynyl end-cap reacted at a lower temperature than the naphthylethynyl end-cap. Four aryl ethynyl terminated imide oligomers having the same imide backbone and molecular weight but different terminal units were prepared and the properties of the cured polymers compared. Phenylethynyl endcapped or naphthylethynyl end-capped oligomers, cured at 340 or 371 °C, exhibited similar tensile properties in thin films.

C. D. Simone and D. A. Scola [21] synthesized and characterized phenylethynyl (PE) end-capped polyimides derived from 4,4'-(2,2,2-trifluoro-1-phenylethylidene) diphthalic anhydride (3FDA), 4,4'-(hexafluoroisopropylidene) diphthalic anhydride (6FDA), and 3,3',4,4'-biphenylene dianhydride (s-BPDA). Phenylethynyl end-capped 3FDA and 6FDA oligomides demonstrate lower minimum viscosities than BPDA oligomides. The PE-3F and PE-6F oligomers also show greater viscosity stability at elevated temperature 310 °C than s-BPDA oligomides. The lower viscosities can be explained by the presence of the bulky groups CF₃ and phenyl on 3FDA and two CF₃ groups on 6FDA relative to the planar configuration of the s-BPDA dianhydride. The greater viscosity stability of the PE-3F and PE-6F oligomers over the s-BPDA oligomers at 310 °C may be explained by the decreased electron density and hence lower reactivity of the ethynyl group in the PE-3F and PE-6F oligomers due to the influence of fluorine in the polymer chain.

3.3 Cross-linked polyimide

Min Zuo and Tsutomu Takeichi [22] prepared a novel type of poly (urethane–imide) was prepared by a reaction of a polyurethane prepolymer and a soluble polyimide containing hydroxyl functional group. Polyurethane prepolymer was prepared by a reaction of polyester polyol and 2,4-tolylenediisocyanate and then end-capped with phenol. Transparent poly(urethane–imide) films were obtained, which suggests some miscibility between polyurethane and polyimide. This was also confirmed from the viscoelastic analysis. Poly(urethane–imide)s showed excellent solvent-resistance as a result of the formation of network structure, and the films had the properties of either plastic or elastomer depending on the chemical structure and crosslink density. Introducing polyimide component into polyurethane improved decomposition temperature of polyurethane for more than 30°C. Urethane linkage in the poly(urethane–imide) are split at ca. 150°C and isocyanate groups are generated. The unique equilibrium reaction of urethane linkage in the poly(urethane–imide) can be applied such as high temperature adhesives.

Osamu Yamazaki, Takashi Yamashita and Kazuyuki Horie [23] provided a new method to prepare poly(amide acid)gels by the reaction of a poly(amide acid) with diisocyanates as crosslinking agent. From the change in the IR spectra, the key

process of crosslinking was determined to be the decarboxylation from the reaction product of the carboxyl group and isocyanate group. The amounts of diisocyanates added gave a little effect on gelation, but the kinds of diisocyanates have an effect on the gelation time. The gels change their volume with varying the composition of the NMP-water mixed solvent.

Jionghao He, Kazuyuki Horie and Rikio Yokota [24] synthesized swollen gels with rigid polyimide. The crosslinking reaction proceeded between hydroxyl groups on the polyimide chains and isocyanate groups in a crosslinker. The average molecular weight between crosslinking points M_c , was calculated based on both swelling and viscoelastic measurements of the polyimide gels. As for the equilibrium swelling data, a concentration-dependent form of the Flory–Huggins parameter has been applied to calculate the M_c . The values of M_c from equilibrium swelling and viscoelastic measurement have been found to be in agreement. By comparing M_c with the results of $^1\text{H-NMR}$, the percentages of effective and ineffective linkages have been evaluated quantitatively for all the polyimide gels. It has been found that the elastically effective crosslinking is less than 20%.

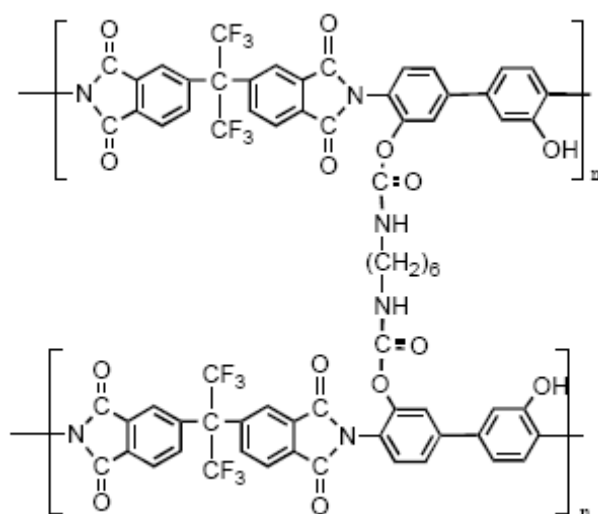


Figure 3.4 Structure of cross-linked polyimide based on hexamethylene diisocyanate

Jionghao He, Kazuyuki Horie, Rikio Yokota and Feifeng He [25] developed the approach of end-crosslinking with an imide linkage to increase the amount of effective junctions and obtain polyimide gels with high modulus. Methylenedianiline oligomer (pMDA), which has an average amino functionality of 2.6, was used as an

amine comonomer as well as a crosslinker to react with 4,4'-(hexafluoroisopropylidene)-diphthalic anhydride (6FDA), 4,4'-oxydiphthalic anhydride (ODPA) and 3,3',4,4'-biphenyltetracarboxylic dianhydride (BPDA) to make different polyimide gels. High compression moduli greater than 1 MPa were found for the ODPA/pMDA polyimide gels at their equilibrium swollen states in N-methylpyrrolidone (NMP). BPDA/pMDA gels did not swell in NMP, while 6FDA/pMDA gels swelled significantly and finally dissolved in NMP. The equilibrium swelling ratio and compression moduli for as-prepared and equilibrium swollen states were correlated to the chemical structure and initial monomer concentrations of the polyimide gels, and found to agree quite well with the prediction of the scaling theory.

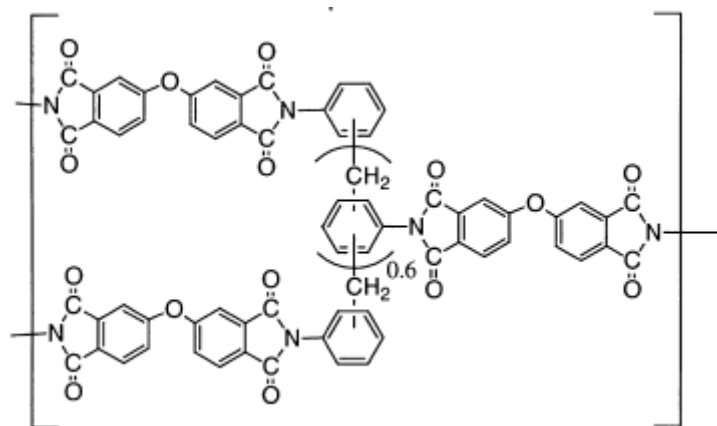


Figure 3.5 Structure of end cross-linked polyimide

Seung-Jin Yang, Choonkeun Lee, Wonbong Jang, et. al [26] prepared poly(epoxy imide) by a reaction between a hydroxyl-group-containing soluble copolyimide and commercial epoxy resin at 200 °C for 2 hr. Poly(epoxy imide) thin films exhibited higher thermal stability and lower dielectric constants than commercial filp-chip package material (U300). The thermal stability increased with increasing crosslink density and decreasing bulky CF₃ groups. The dielectric constants of the poly(epoxy imide)s were 1.1-1.3 times lower than that of U300, and this is highly desirable for the microelectronic packaging industry. The dielectric constant dramatically decreased when bulky CF₃ groups were added and when the functionalities of epoxy resins decreased.

Huseyin Deligoza, Saadet Ozgumus and Tuncer Yalcinyuva [27] prepared a novel cross-linked polyimide film by imidization of cross-linked poly(amic acid) (CPAA). The dielectric constant and dielectric loss of the conventional and novel cross-linked polyimide films were found to be frequency and temperature dependent. It was found that this type of cross-linked polyimide is very promising for electrical applications due to its good thermal stability, excellent solvent resistance, low dielectric constant, low moisture absorption and stability in a various regions of frequencies. So this type of novel polyimide films can be used as alternative dielectric layers in the microelectronic industry.

Huseyin Deligoza, Tuncer Yalcinyuva and Saadet Ozgumus [28] prepared four different types of cross-linked polyimides based on 4,4-diphenylmethane diisocyanate (MDI) by the reaction of different types of conventional poly(amic acid) intermediates with MDI as a cross-linking agent. Subsequently, they were thermally imidized in order to obtain corresponding cross-linked polyimide structure. The results of FTIR-ATR showed that MDI can effectively react with carboxylic acid groups of PAA to form cross-linked polyimide films. The results showed that all CPI films have good insulating properties such as high dielectric breakdown voltage, low loss factor, leakage density and excellent physical properties.

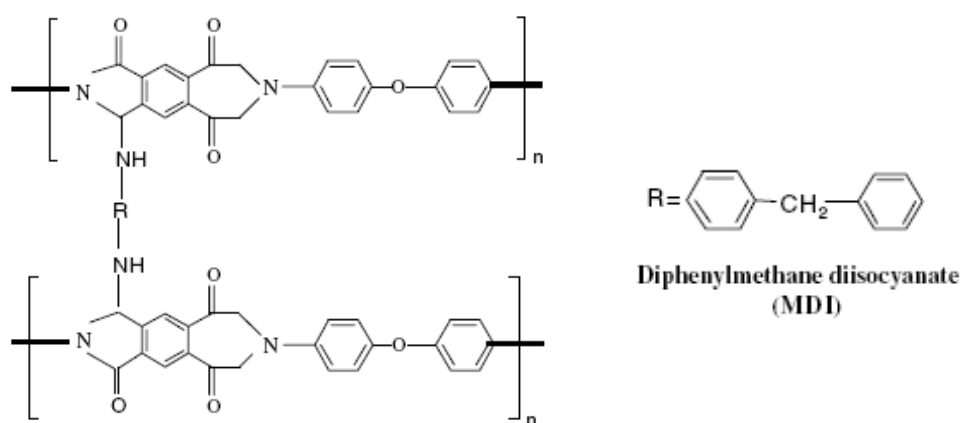


Figure 3.6 Structure of cross-linked polyimide based on diphenylmethane diisocyanate

3.4 Porous polyimide film

P. Santhana Gopala Krishnan, Chia Zheng Cheng, et al. [14] prepared nanoporous polyimide films in two steps. The first step is the preparation of poly(urethane-imide) films by casting blend solutions containing various weight percentages of poly(amic-acid) and phenol blocked polyurethane prepolymer. In the second step, these films were thermally treated above 300°C to give nanoporous polyimide films. During thermal treatment, less thermally stable urethane domains decomposed, leaving porous polyimide films. The presence of pores was confirmed by scanning electron microscopy (SEM). The dielectric constant of the polyimide film was found to decrease with increasing amounts of urethane content.

Feng-Chih Chang, Yuan-Jyh Lee, et al. [29] described a novel method for preparing nanoporous polyimide films through the use of a hybrid PEO-POSS template. First, nanoporous foams are generated by blending polyimide as the major phase with a minor phase consisting of the thermally labile PEO-POSS nanoparticles. The labile PEO-POSS nanoparticles would undergo oxidative thermolysis to release small molecules as byproducts that diffuse out of the matrix to leave voids into the polymer matrix. They achieved significant reductions in dielectric constant (from $k = 3.25$ to 2.25) for the porous PI hybrid films, which had pore sizes in the range of 10-40 nm.

Lizhong Jiang, et al. [16] demonstrated a new methodology of preparing polyimide porous films with pore sizes in the nanometer regime. This is a novel, versatile approach for the production of ultralow dielectric constant polymer films. Microphase-separated hybrid films comprised of a polyimide as the matrix or dominant phase with silica as the dispersible phase have been prepared by sol-gel route. The hybrid films were designed in such a way as to control the size of the silica; by the way the tensile strength of the hybrid film was improved. Upon a HF etching treatment, the silica particles in the matrix of PI were removed, leaving pores with a size and shape dictated by the initial hybrid morphology. The dielectric constant of the porous films decreased greatly, owing to the introduction of pores, however the tensile strength decreased accordingly.

CHAPTER IV

EXPERIMENT

The experimental procedures in this study were divided into five parts as follows,

- (i) Chemicals and Equipments
- (ii) Polyimides preparation
- (iii) Cross-linked polyimide via diisocyanate
- (iv) Films preparations
- (v) Characterization of all Cross-linked polyimide products

The details of each part were described below.

4.1 Equipments and Chemicals

4.1.1 Chemicals

1. 4,4'-(hexafluoroisopropylidene) diphthalic anhydride (6FDA, 99.0%) was purchased from Sigma-Aldrich Inc.
2. 3,4'-oxydianiline (ODA, 97.0%) was purchased from Sigma-Aldrich Inc.
3. 3,3'-Dihydroxy-4,4'-diaminobiphenyl (HAB) was purchased from ChrisKev Co., Inc.
4. Phthalic anhydride (PA, >98.0%) was purchased from Merck Ltd.
5. Toluene diisocyanate (TDI, mixture of 2,4- and 2,6-isomer, 95.0%) was purchased from Sigma-Aldrich Inc.
6. N-methylpyrrolidone (NMP, >99.5%) was purchased from Merck Ltd.
7. Toluene (C₇H₈) polymerization grade was received from Esso chemical (Thailand) Co., Ltd. It was dried over dehydrated CaCl₂ and was distilled over sodium/benzophenone under argon atmosphere.
8. Benzophenone (purity 99.0%) was obtained from Fluka Chemie A.G. Switzerland.
9. Methanol (Commercial grade) was purchased from SR lab.

10. Argon gas (Ultra High Purity, 99.999%) was purchased from Thai Industrial Gas Co., Ltd. (TIG) and was purified by passing through the column packed with molecular sieve 3 Å, BASF Catalyst R3-11G, sodium hydroxide (NaOH) and phosphorus pentoxide (P_2O_5) to remove traces of oxygen and moisture.

4.1.2 Equipments

All types of equipments used in the polyimide film and cross-linked polyimide film preparation are listed below:

4.1.2.1 Polyimide synthesis part

(a) Glove box

Glove Box MBRAUN MB 200B with oxygen and moisture analyzer was used for transferring solid reagents under inert atmosphere and for storing air-sensitive reagents. The oxygen and moisture levels are normally below 1 ppm inside the glove box. The glove box is shown in Figure 4.1.

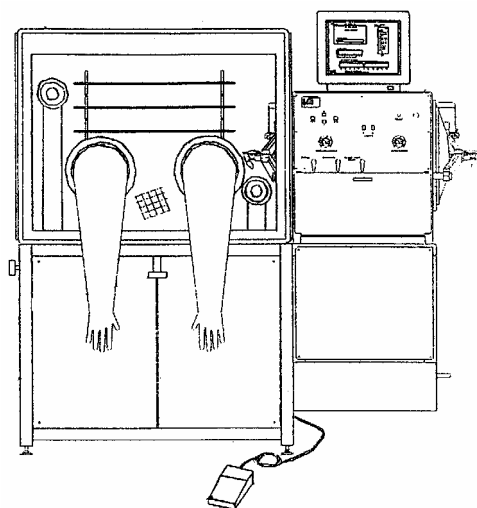


Figure 4.1 Glove box

(b) Schlenk line

Schlenk line consisted of vacuum line connected to vacuum pump and argon line for purging when reagents are transferred. The schlenk line was shown in Figure 4.2.

(c) Schlenk Tubes

A schlenk tube is a tube with a glass ground joint and a side arm with three way glass valve. Sizes of the Schlenk tubes used were 50, 100, and 200 mL. They were used for synthesis of cross-linked polyimide and collect materials which were sensitive to oxygen and moisture.

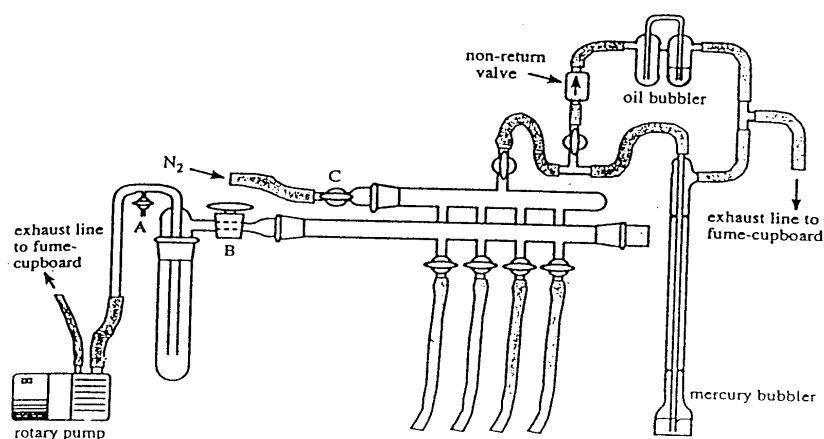


Figure 4.2 Schlenk line

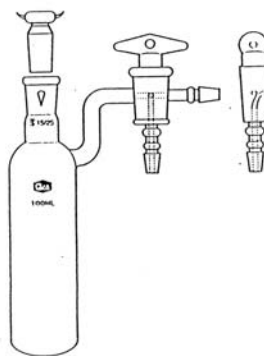


Figure 4.3 Schlenk tube

(d) The inert gas supply

The inert gas (argon) was passed through columns of oxygen trap (BASF catalyst, R3-11G), moisture trap (molecular sieve), sodium hydroxide (NaOH) and phosphorus pentoxide (P_2O_5) for purifying ultra high purity argon before used in Schlenk line and solvent distillation column. The inert gas supply system is shown in Figure 4.4.

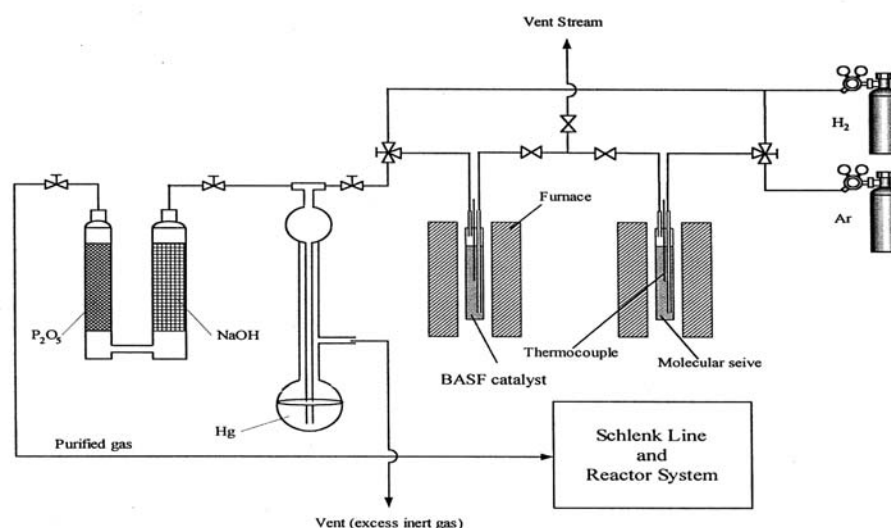
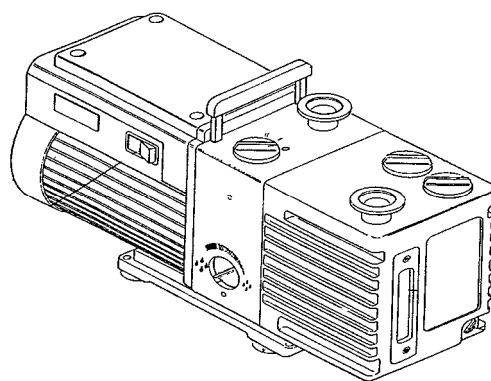


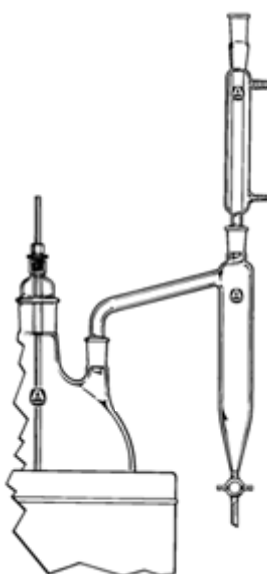
Figure 4.4 Inert gas supply system

(e) The vacuum pump

The Vacuum pump model 195 from Labconco Corporation was used. A pressure of 10^{-1} to 10^{-3} mmHg was adequate for the vacuum supply to the vacuum line in the Schlenk line. The vacuum pump is shown in Figure 4.5.

**Figure 4.5** Vacuum pump**(f) Reactor**

A three-necked, round bottom flask equipped with an argon inlet, a thermometer, a magnetic stir bar and a condenser with a Dean-stark trap was used as the reaction vessel.

**Figure 4.6** Reaction vessel

(g) Magnetic stirrer and Hot plate

The magnetic stirrer and hot plate Model RCT Basic from IKA Labortechnik were used.

4.1.2.2 Film preparation Part

(a) Vacuum oven

A Cole-Parmer vacuum oven model 282A was used for removing solvent. This vacuum oven is programmable. All functions can be set from digital panel and display their status on LCD. The temperature, pressure and time are controllable.

(b) Temperature controlled oven

A Carbolite LHT5/30 (201) Temperature controlled oven was used in these experiments. The maximum working temperature of this machine is 500°C. This equipment was used for thermal treated the film.

4.2 Preparation of a series of polyimide capped with non-reactive end groups

Various kinds of polyimide capped with non-reactive end groups were prepared by the reaction of 6FDA, diamine mixtures of HAB and 3,4'-ODA and PA in NMP as shown in Figure 4.7. The content of hydroxyl groups in the polyimide was controlled by adjusting the ratio of diamine monomers HAB and 3,4'-ODA. Here, we coded polyimides as PI25, PI50, PI75 and PI100 to indicate the percent of HAB in diamine mixtures

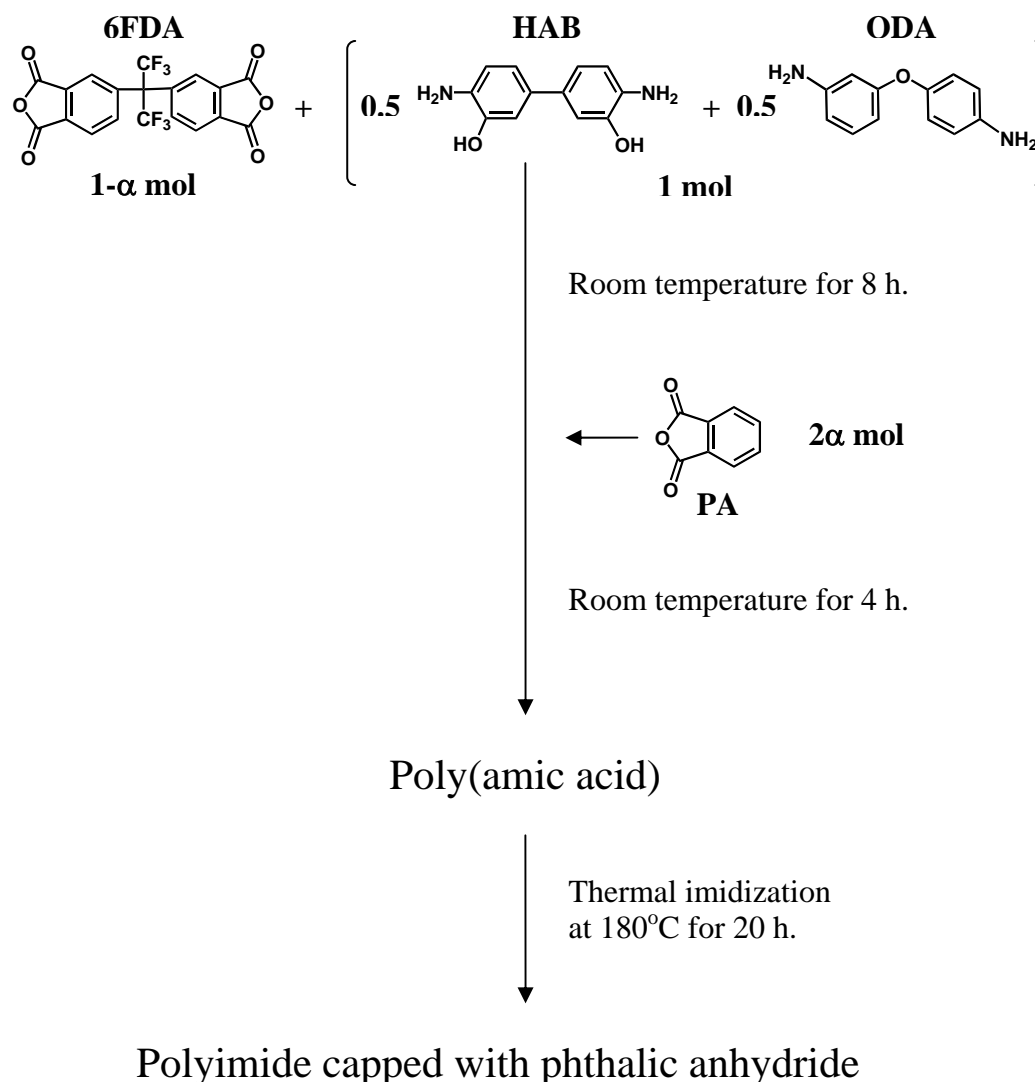


Figure 4.7 Preparation of polyimide capped with non-reactive end groups

A typical example, the preparation of PI50 is shown below. A three-necked, round bottom flask equipped with an argon inlet, a thermometer, a magnetic stir bar and a condenser with a Dean-stark trap was used as the reaction vessel. HAB (1.5039 mmol, 0.3248 g), 3,4'-ODA (1.5039 mmol, 0.3008 g) and 6 mL of NMP were added to a reaction vessel. The mixture was stirred at ambient temperature until the diamines were completely dissolved. Next, 6FDA (3.0000 mmol, 1.3326 g) solution in NMP with about 10% solids (w/w) was added. This solution was stirred under argon atmosphere for 8 h at room temperature. Subsequently, PA (0.0156 mmol, 0.0023) was added and reacted for another 4 h to obtain the PA end capped poly(amic acid). Toluene 20 mL was added to the reaction solution to remove water by azeotropic

distillation. This required approximately 20 h at 180°C to complete the reaction. After cooling down, the solution was precipitated in 500 mL of a 1:1 methanol/deionized water mixture. The precipitated polyimide was filtered and dried in vacuum at 150°C for 15 h.

4.3 Preparation of cross-linked polyimide

Three series of cross-linked polyimides with NCO/OH equal to 0.1, 0.5 and 1.0 were prepared according to the procedure is described below. The polyimide was dissolved in NMP to give a 10% solution. Then, polyimide solution and TDI solution in NMP were mixed in various NCO/OH ratio to obtain cross-linked polyimides with three different cross-linking density, NCO/OH = 0.1, 0.5 and 1.0, which were coded as PI50-C0.1, PI50-C0.5 and PI50-C1.0 respectively.

4.4 Preparation of cross-linked polyimide films

Cross-linked polyimide solutions were cast on a well cleaned glass substrates and the solvent was evaporated under vacuum at 50°C for 10 h. The cast films were thermally treated at 100°C, 150°C and 300°C for 1 h each in a temperature controlled oven. After the thermal treatment the films were removed from the glass substrate by immersing into water and dried at 100°C for 24 h. All prepared films were obtained as transparent, dark brown to yellow colored and flexible.

4.5 Characterization Instruments

4.5.1 Infrared Spectroscopy (FTIR)

Infrared survey spectra were recorded with Nicolet 6700 FTIR spectrometer. The scanning ranged from 400 to 4000 cm^{-1} with scanning 64 times at room temperature. The film samples were measured by grip with the sample holder. For the powder samples, the spectra were performed on the pallet sample of KBr powder.

4.5.2 Thermogravimetric analysis (TGA)

Thermogravimetric analysis (TGA) thermograms were performed using a SDT Analyzer Model Q600 from TA Instruments, USA. in the temperature range of 50-600°C at a heating rate of 10°C/min and N₂ (or O₂) flow rate of 100 ml/min. The weight of the TGA samples was controlled in the range of 3-10 mg.

4.5.3 Dynamic Mechanical Analysis (DMA)

Dynamic mechanical properties of all polyimide products were determined by using Dynamic Mechanical Analysis (DMA) with a Perkin-Elmer Pyris Diamond DMA. The samples were cut for standard DMA samples (10x25 mm). Condition and parameters were shown in Table below.

Table 4.1 Conditions and parameter for running DMA

Conditions and parameter	Value
Sample size(w x l) (mm)	10 x 20
DMS Measurement Mode	Tension
Temperature Control Mode	Ramp (5.0 °C/min)
DMS frequency (Hz)	1.0, 5.0, 10.0
Temperature range	50 to 350 °C
L Amplitude (µm)	10
Minimum Tension/Compression Force(mN)	200
Tension/Compression Force gain	1.5
Force Amplitude Default Value (mN)	4000
Nitrogen as carrier gas (ml/min)	100

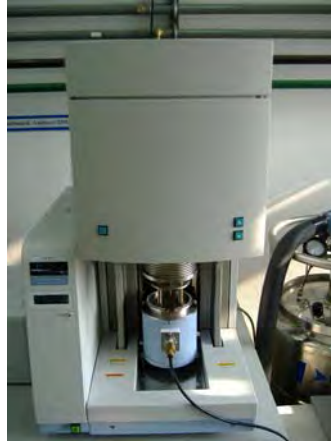


Figure 4.8 Dynamic Mechanical Analysis (DMA) Equipment

4.5.4 Tensile testing machine

Tensile properties were characterized using an Instron universal testing machine with a test speed of 12.5 mm/min. The tests were conducted according ASTM D 882-02.

The tensile testing machine of a constant-rate-of-crosshead movement is used. It has a fixed or essentially stationary member carrying one grip, and a moveable member carrying a second grip. Self-aligning grips employed for holding the test specimen between the fixed member and moveable member prevent alignment problems. An extension indicator is used to determine the distance between two designated points located within the gauge length of the test specimen as the specimen is stretched.



Figure 4.9 Universal Testing Machine equipment

4.5.5 Dielectric properties

The dielectric properties of the polyimide films were obtained via the capacitance method and were measured at room temperature and 500 mV with an Agilent E 4980A Precision LCR Meter. The films for dielectric properties analysis were cut into 15x15 mm specimens.

4.5.6 Scanning Electron Microscope (SEM)

The morphologies of the films were studied by Scanning Electron Microscope (SEM), JSM-6400 Scanning Microscope. The films were fractured under liquid nitrogen and mounted on sample stud for the cross sectional view.

4.6 Research Methodology

Research methodology of flow diagram is shown in Figure 4.10

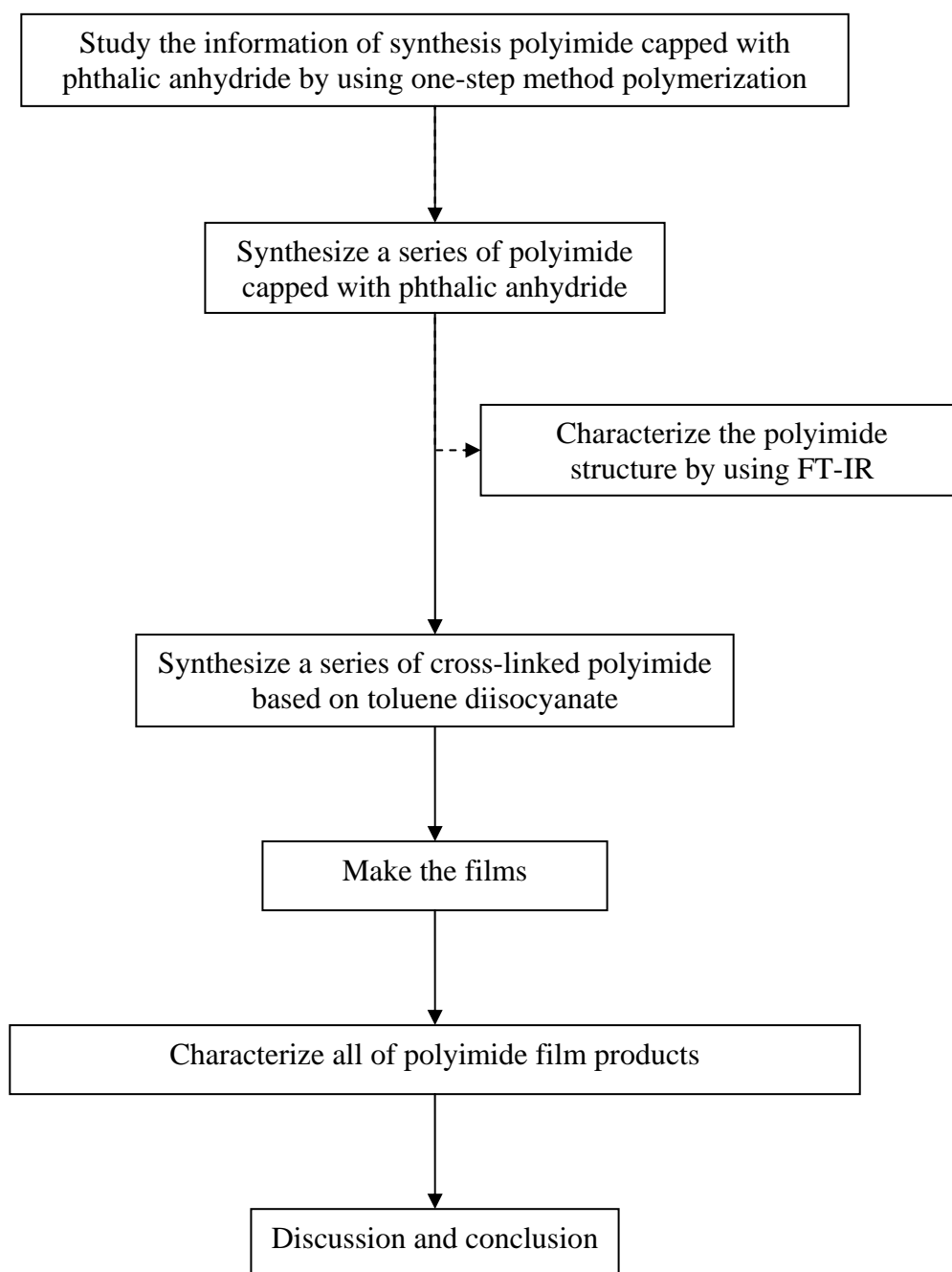


Figure 4.10 Flow diagram of research methodology

CHAPTER V

RESULTS AND DISCUSSION

The purpose of this research is to synthesize low dielectric polyimide film. This chapter provides the identification information of the polyimide films and the characterization information of cross-linked polyimide films. The thermal properties, mechanical properties, dielectric properties and morphology of the polyimide films were obtained and verified.

5.1 Preparation of polyimide

Four series of polyimide based on 6FDA, HAB, 3,4'-ODA and PA were prepared by one-step method polymerization. After the imidization process, the structures of the four series of polyimide were analyzed with FTIR. The completion of the imidization was confirmed with FTIR (4000-400 cm^{-1}) as show in Figure 5.1 The characteristic imide groups are observed at 1785 cm^{-1} for C=O asymmetric stretching vibrations, at 1720 cm^{-1} for C=O symmetric stretching vibrations, at 1380 cm^{-1} for C-N stretching vibrations and at 725 cm^{-1} for C=O bending vibrations. The carbonyl group (C=O) in CONH stretching band around 1660 cm^{-1} was not observed in Figure 5.1, which indicates the successful thermal imidization of the four series of polyimide.

Moreover, the broad absorption around 3400 cm^{-1} was also observed, which attributes to the presence of hydroxyl functional groups in polyimide backbone. For all four series, the intensity of broad absorption around 3400 cm^{-1} increased with the increase of HAB content due to the increase of OH functional groups.

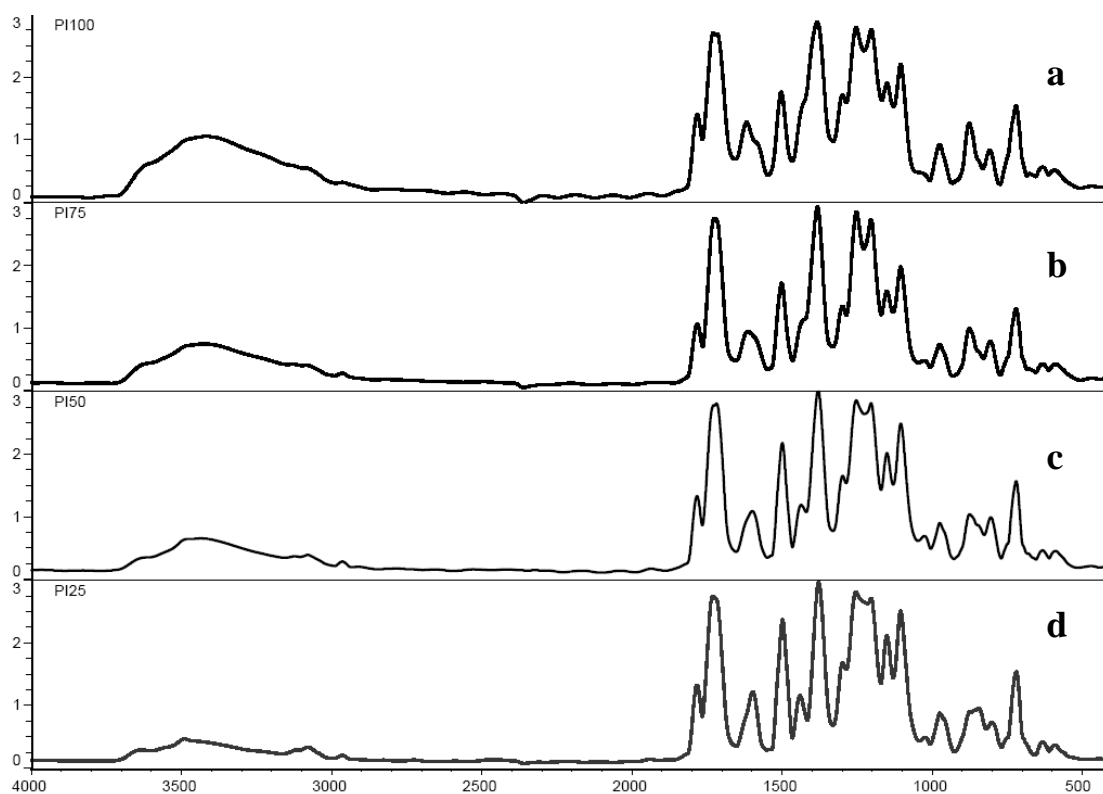


Figure 5.1 FTIR spectra of a) PI100 b) PI75 c) PI50 d) PI25

5.2 Preparation of cross-linked polyimide

This research intends to prepare a series of cross-linked polyimide by simple reaction which is based on a reaction between toluene diisocyanates and hydroxyl functional groups in a polyimide. The ratios of TDI loading (0.1, 0.5 and 1.0) were calculated from the mole of NCO added per the mol of OH occupied in the polyimide. For example, the ratio of one indicated that all of the OH groups containing were reacted with the isocyanate groups. Therefore, no free OH groups appeared. During the addition of TDI into polyimide solution, we used FTIR for monitoring the advancement of the reaction of TDI as show in Figure 5.2. From the figure, the characteristic peaks for the TDI at 2250 cm^{-1} was presented after the addition of TDI. After 30 min of reaction, the characteristic absorption of isocyanate groups (NCO) at 2250 cm^{-1} almost disappeared. These FTIR spectra confirm that isocyanate groups completely reacted with hydroxyl functional groups in the polyimide to form cross-linked polyimide. In addition, it's hard to confirm the existing of urethane linkage by FTIR because the characteristic broad peak for the N-H of urethane at 3340 cm^{-1} is overlapped with the hydroxyl groups in polyimide at 3400 cm^{-1}

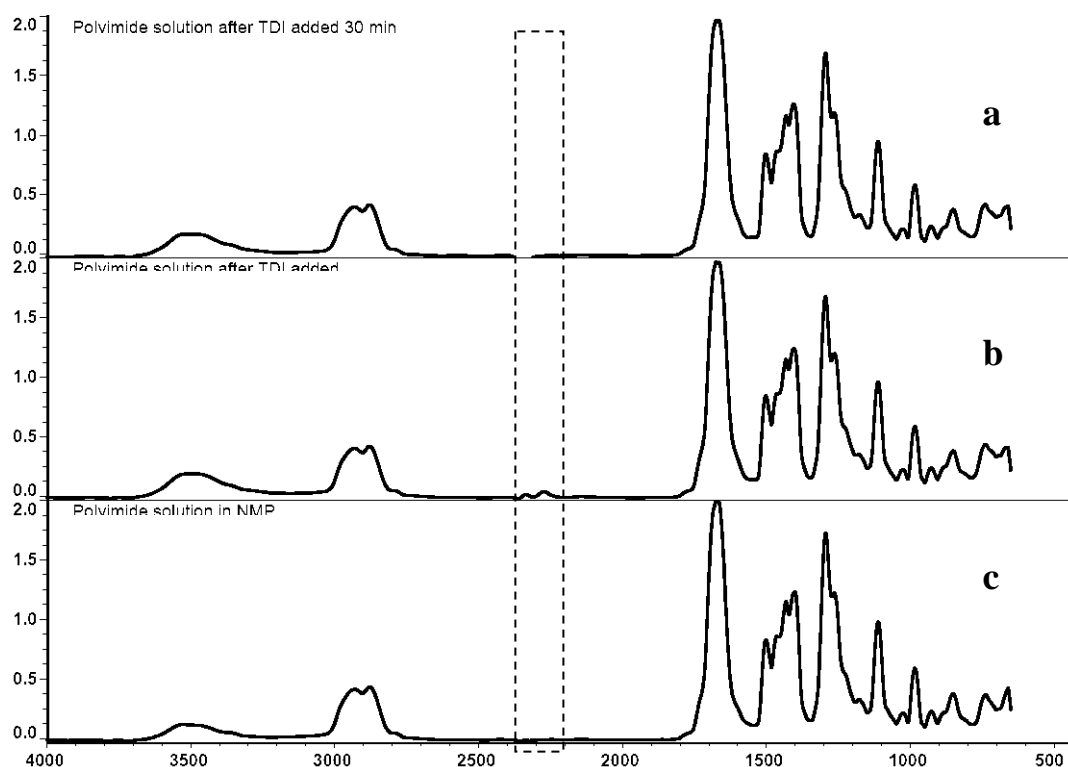


Figure 5.2 FT-IR spectra of a) Polyimide solution after TDI added 30 min b) Polyimide solution after TDI added c) Polyimide solution in NMP

5.3 Preparation of cross-linked polyimide films

To monitor the phenomenon during thermal treatment step, the polyimide and cross-linked polyimide solution were examined with TGA. These TGA samples were prepared by the partial evaporation of NMP solvent in polyimide solution and examined before thermal treatment process. The example of the decomposition profile is shown in Figure 5.3 for the PI100 and PI100-C1.0 solution in NMP.

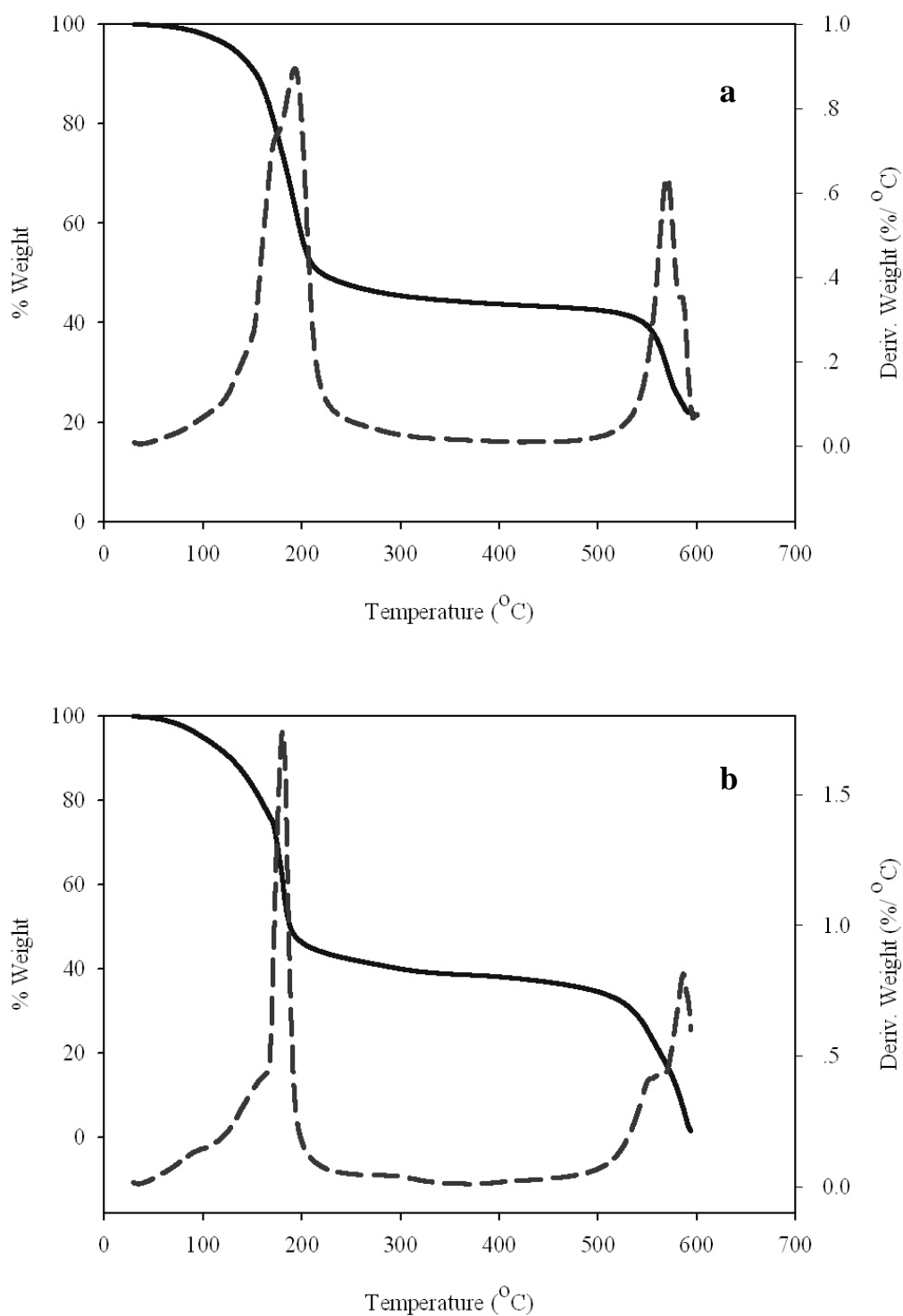


Figure 5.3 Thermogravimetric analyses of polyimide solution in NMP of a) PI100 b) PI100-C1.0

From the TGA curves, it was found that the decomposition occurred in three stages in TGA curves of the PI100-C1.0 solution in NMP. At a heating rate of

10°C/min of TGA in oxygen atmosphere, the first decomposition occurred in the temperature range 100 to 210°C which is due to the evaporation of the NMP solvent. The second stage took place in the temperature range 230 to 300°C which corresponds to the decomposition of thermally labile urethane component. The third stage occurred above 500°C which is due to the decomposition of the imide component.

In the other hand, TGA curves of the PI100 solution in NMP show that only two steps decomposition occurred. Therefore, partial decomposition of the poly(urethane-imide) solution at 230 to 300°C could lead to the decomposition of the urethane part only.

5.4 Physical properties of cross-linked polyimide films

Figure 5.4 and Table 5.1 illustrate the physical properties and the optical images of polyimide films respectively. All prepared films were obtained as transparent, dark brown to yellow colored and flexible except PI75-C1.0, PI100-C0.5 and PI100-C1.0 that were brittle.

Table 5.1 Physical properties of polyimide films

Polymer	Pure	C 0.1	C 0.5	C 1.0
PI25	O	O	O	O
PI50	O	O	O	O
PI75	O	O	O	X
PI100	O	O	X	X

O is flexible, X is brittle

It can be explain that the increase in urethane component bring about the reduction of flexibility due to the decomposition of urethane component in polyimide film. Moreover, Figure 5.4 indicates that the incorporation of too much urethane component leads to the increase in thermally labile component, also causes the dark color of the films.

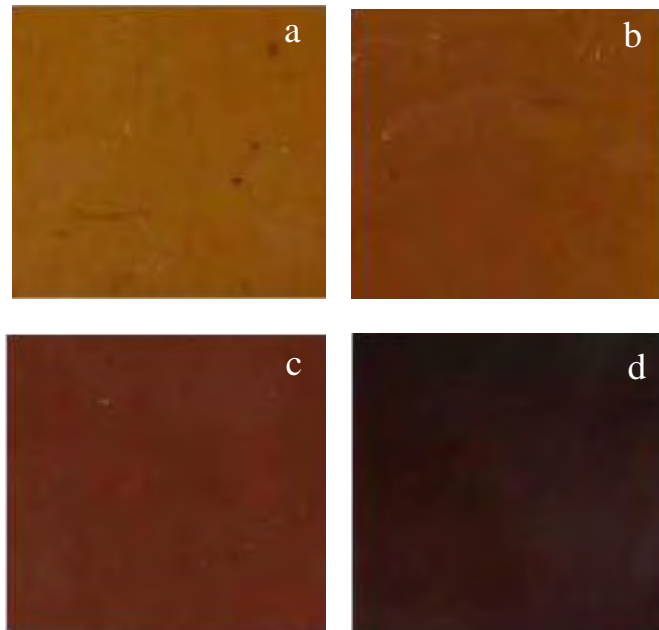


Figure 5.4 Optical images of polyimide films a) PI25 b) PI25-C0.1 c) PI25-C0.5 d) PI25-C1.0

5.5 Dielectric properties

Lower dielectric constants are one of the most desirable properties of next generation electronic devices. Table 5.2 and Figure 5.5 show the dielectric constants of the polyimide films calculated by the following equation:

$$k = \frac{Ct}{\epsilon_0 A} \quad (5.1)$$

where C is the measured capacitance, t is the thickness of the sample, A is the area of the film and ϵ_0 is the permittivity of the free space (8.854×10^{-12} MKS unit).

Table 5.2 Dielectric constant of polyimide films

Polymer	Dielectric constant at 1 MHz			
	Pure	C 0.1	C 0.5	C 1.0
PI25	3.17	3.06	3.05	2.87
PI50	3.22	3.15	3.02	2.83
PI75	3.40	3.23	3.13	2.57
PI100	3.55	3.29	3.15	-

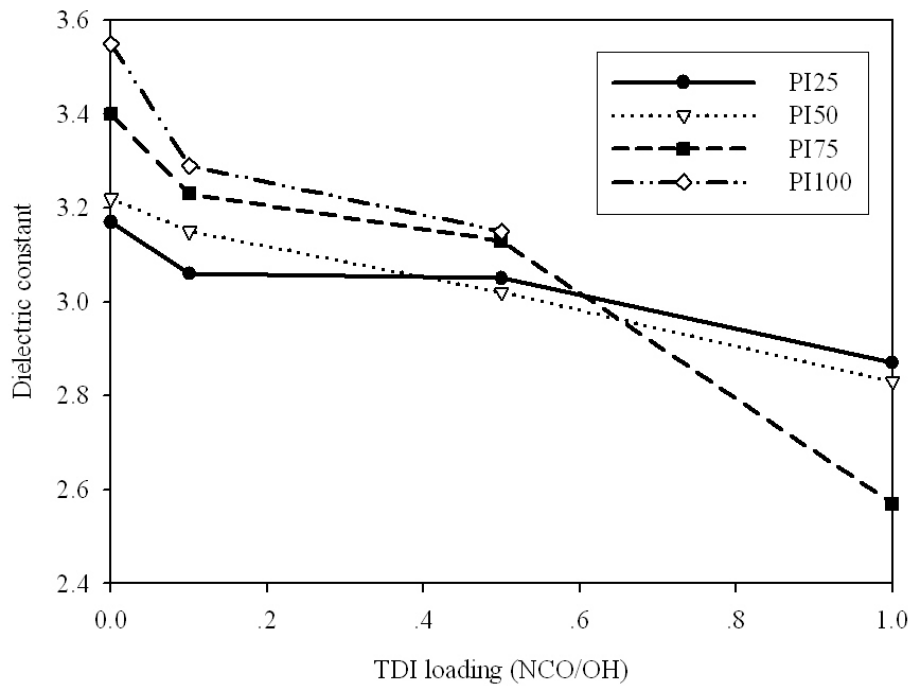


Figure 5.5 Dielectric constant of polyimide films

In case of PI100-C1.0, the film became brittle after thermal treatment. Therefore, dielectric constant was not determined for this sample. From Figure 5.5, it was found that the dielectric constant increased with the increase of hydroxyl group content (PI100>PI75>PI50>PI25). This can be explained on the basis that the hydroxyl group is normally hydrophilic lead to easy absorption of water, which being highly polar, also causes the dielectric constant increase dramatically.

For all the four series (PI25, PI50, PI75 and PI100), the dielectric constant decreased with the increase the TDI loading. Especially, the dielectric constant decreased greatly for PI75-C1.0. In order to elucidate the reason, the air volume percentages of the films were calculated by using Bruggeman's equation (According to Xiaodong Wang et al 2007) [15]:

$$f_p \frac{k_p - k_e}{k_p + 2k_e} + f_a \frac{k_a - k_e}{k_a + 2k_e} = 0 \quad (5.2)$$

where k_p , k_e and k_a are the dielectric constant of the pure polyimide film, the effective dielectric constant of the film and the dielectric constant of the air, respectively, and f_p

and f_a are the volume fraction of the polyimide and the air, respectively. Table 5.3 illustrates the volume fraction of the air in the polyimide films.

Table 5.3 Void fraction of polyimide films

Polymer	Air volume in polyimide films ^a (v/v %)			
	Pure	C 0.1	C 0.5	C 1.0
PI25		3.93	3.97	10.82
PI50		2.43	7.00	13.78
PI75		5.45	8.70	27.64
PI100		8.02	12.12	-

^a The air volume of porous polyimide films was calculated according to Bruggeman's equation.

From this result, it can be explained that the lower dielectric constant was due to the degradation of the more thermally labile urethane component during thermal treatment which might create pores in the film. These pores were occupied with air, which has the dielectric constant of one, resulting in the decrease of the overall dielectric constant. By comparing in columns (C0.1 and C0.5), the void increased with the increase of OH groups content but the dielectric constant did not decrease accordingly. This can be attributed that the OH groups also exhibited strong influence as same as the contained void.

Although PI75-C1.0 has the lowest dielectric constant, it exhibits poorly mechanical properties. In this research, we chose PI50-C1.0 and PI50 to characterize the evaluated properties and to elucidate the effect of cross-linked structure because the PI50-C1.0 exhibited optimum mechanical and good dielectric properties.

5.6 Thermal Properties

The thermal properties of the films were investigated by TGA under nitrogen atmosphere. The TGA were examined after thermal treatment process (300°C) which was different from the Topic 5.3 because the NMP solvent and the thermally labile

component have been removed during the thermal treatment. Both of TGA thermograms of PI50 and PI50-C1.0 were shown in Figure 5.6.

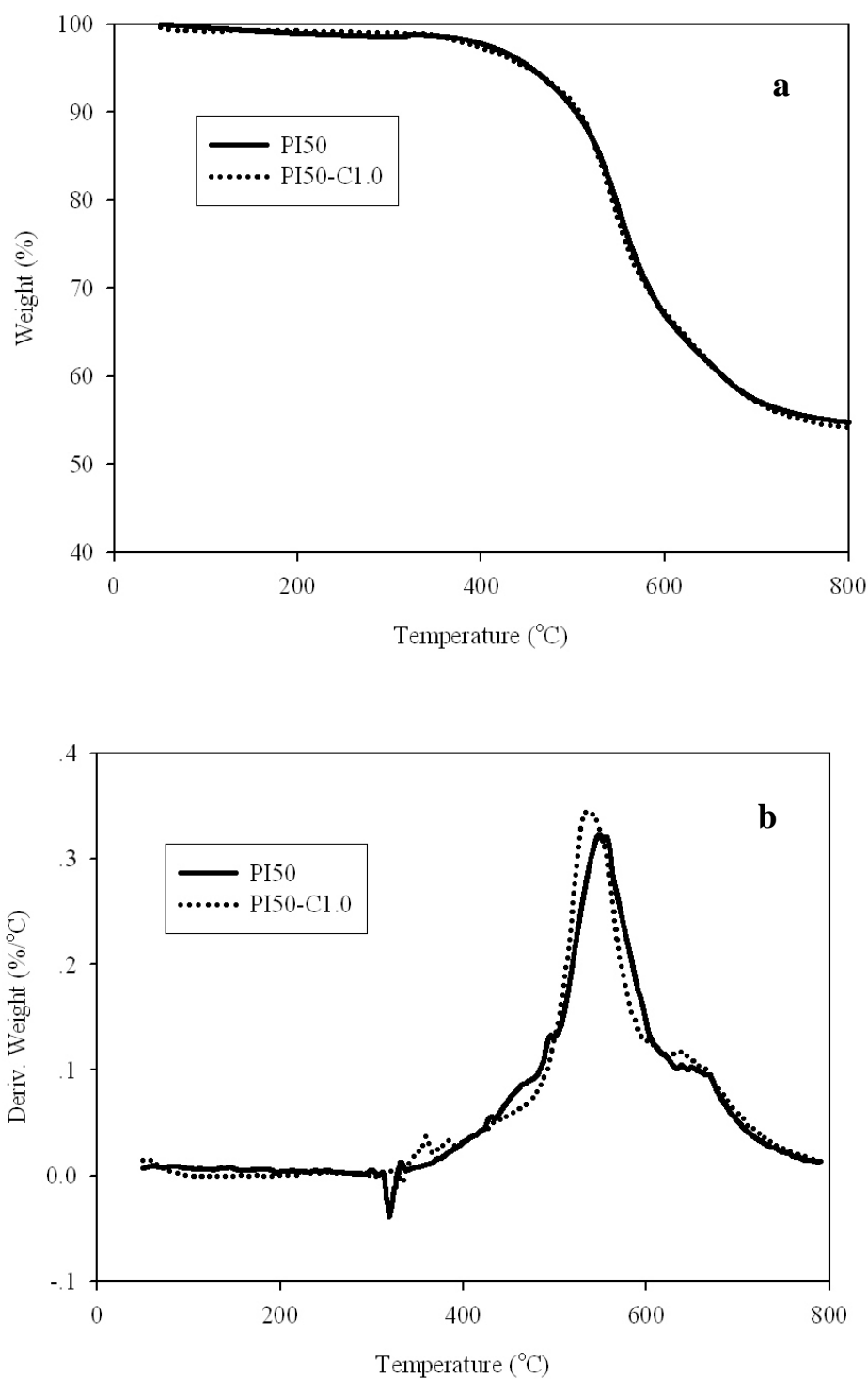


Figure 5.6 TGA thermogram of the polyimide films

From the TGA thermograms, it was seen that PI50 exhibited a 5% weight loss at 453°C and 10% weight loss was about 503°C and PI50-C1.0 shown the values of 451°C and 507°C respectively. Char yield of the PI50 reported at 800°C was 54.8% by weight and the PI50-C1.0 reported at 800°C was approximately 54.2% by weight. The values were approximately the same. This can be explicated that the carbon dioxide in urethane component in PI50-C1.0 was completely removed after thermal treatment which was discussed further in DMA results (Topic 5.7.1). Therefore, the intrinsic structure of PI50-C1.0 might become approximately the same as PI50 resulted in the thermal properties were relatively identical. To elucidate the differences in figure 5.6 b) plots of derivative weight versus temperature of both the PI50 and PI50-C1.0. The peak of derivative weight curves means the highest rate of decomposition. It was found that the highest rates of decomposition occurred 548°C and 535°C for PI50 and PI50-C1.0 respectively. It can be implied that the lower bond energy of C-N (293 kJ/mol) contained more in cross-linked structure (PI50-C1.0), which was compared with C=C (614 kJ/mol), can be decomposed at lower temperature when those were based on the same weight. [32] In other word, for the same weight, the PI50-C1.0 has less total bond energy than the PI50. Therefore, with the same ramp rate (constant energy input), the PI50-C1.0 will reach the maximum derivative weight before PI50 because it consumed less energy to break the bond in the samples.

Table 5.4 Thermal properties of the polyimide films

Polymer	Thermal properties		
	T 5% (°C) ^a	T 10% (°C) ^b	Char yield (%) ^c
PI50	453	503	54.8
PI50-C1.0	451	507	54.2

^a The temperature where 5% weight loss occurred.

^b The temperature where 10% weight loss occurred.

^c Weight of residue polyimide at 800°C.

5.7 Mechanical Properties

5.7.1 Dynamic mechanical properties

In this research, the dynamic mechanical properties of the polyimide films were performed as a function of temperature. Figure 5.7, Figure 5.8 and Figure 5.9 represent the storage modulus, the loss modulus and $\tan \delta$ of the polyimide films respectively. It could be observed that the storage modulus and loss modulus of the PI50-C1.0 were quite similar with PI50 in the temperature range of 50-350°C. The large decrease in the storage modulus at temperature above 330°C indicated the beginning of the corresponding glass transition region of each specimen. In the other hand, the PI50-C1.0 exhibited higher the storage modulus and loss modulus than the PI50 in the high temperature range (above 350°C). Thermal stability of the polyimide films can be seen from the slope of the glassy stage modulus in the DMA thermograms.

Furthermore, the higher slope of the glassy state modulus implied the greater thermal instability of the polymer films. This phenomenon might indicate that the decomposition mechanism of urethane component did not remove entire urethane segment. As a result, the cross-linked structure of PI50-C1.0 still occurred in the polyimide structure after the thermal treatment. As we well know, cross-linking changes and generally improves mechanical properties. The improvements from uncrosslinked are almost significant above the glass transition temperature of uncrosslinked polymer. After the large decrease at T_g , the dynamic modulus of cross-linked polymer does not decrease further with increasing temperature.[33] Moreover, the glass transition temperature increases with the increase of cross-link density. The phenomenon is also good agreement with the reported by Namita Roy Choudhury and Matthew Oaten (2005) [34], who studied the Silsesquioxane-Urethane hybrid film. They proposed that the thermal decomposition of the urethane segment can be explained as in the following Figure 5.10. Comparing to our research, the pore may be created by the formation of carbon dioxide and the cross-linked structure may be created by the secondary amine from urethane component.

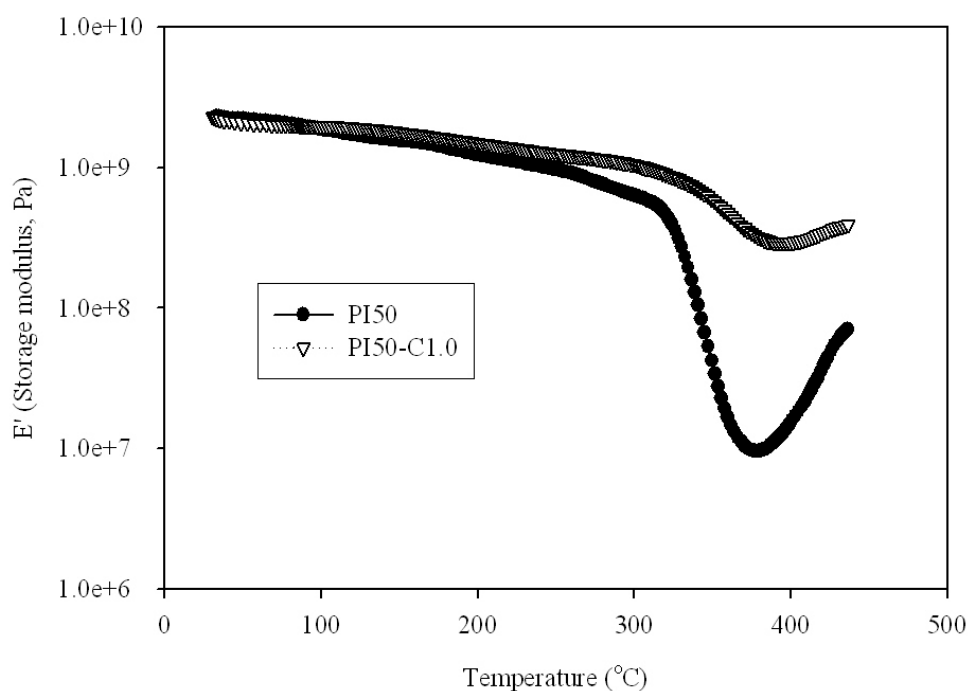


Figure 5.7 DMA curves (storage modulus (E') and temperature) for PI50 and PI50-C1.0

From $\tan \delta$ curves, the glass transition temperature of PI50 and PI50-C1.0 displayed 355°C and 383°C respectively. The results were consistent with the storage modulus and loss modulus. The higher glass transition temperature was due to the rigidity of cross-linked structure of PI50-C1.0.

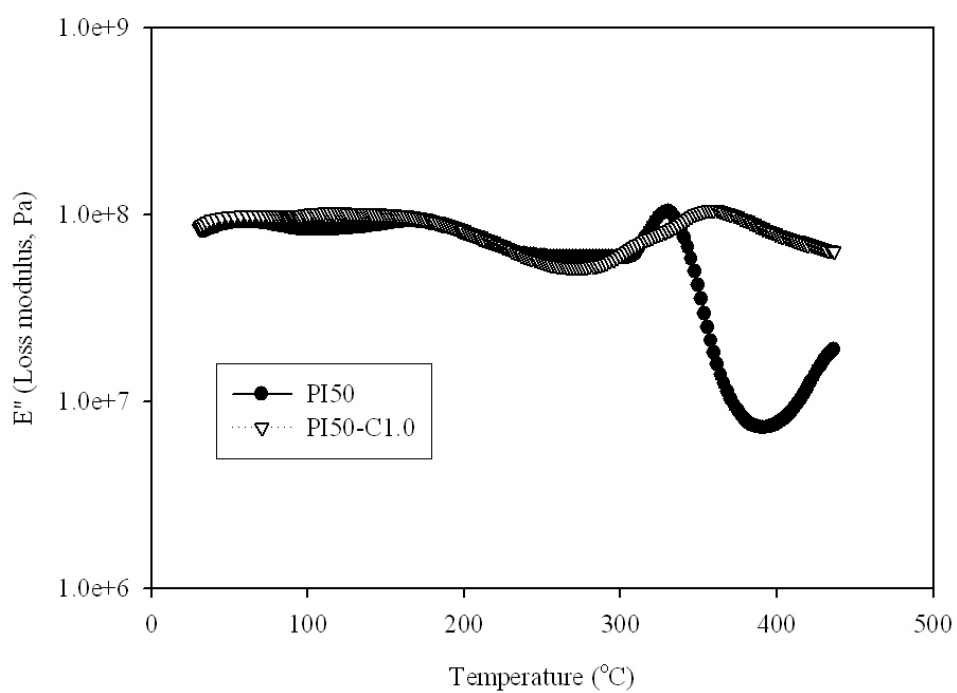


Figure 5.8 DMA curves (loss modulus (E'') and temperature) for PI50 and PI50-C1.0

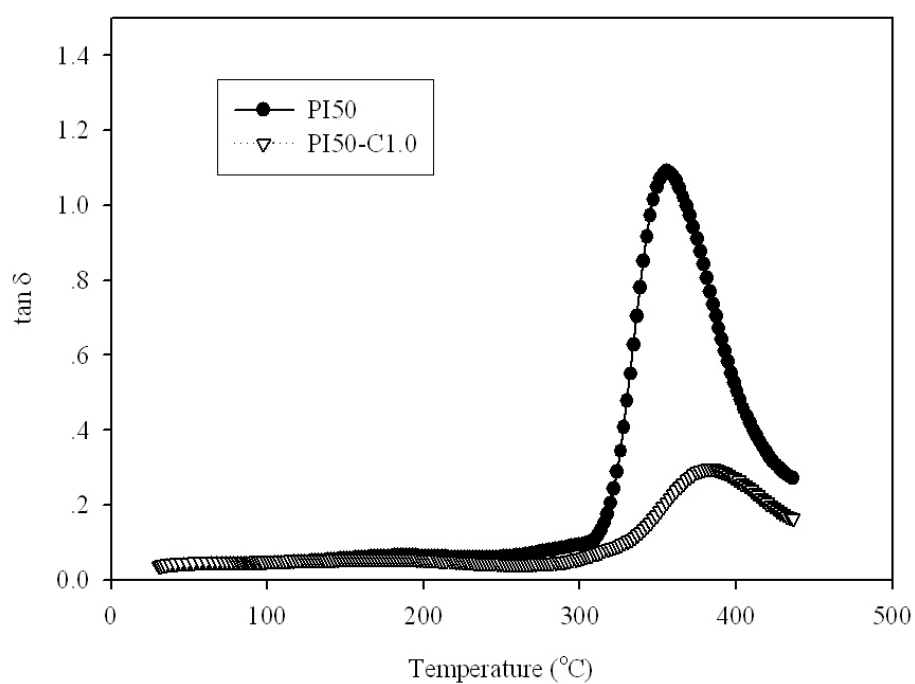


Figure 5.9 DMA curves ($\tan \delta$ and temperature) for PI50 and PI50-C1.0

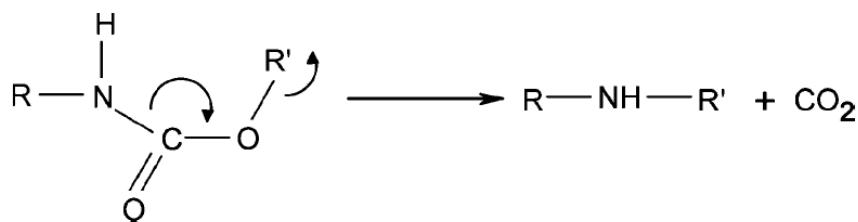


Figure 5.10 Decomposition mechanism of urethane component

Based on DMA results, the PI50-C1.0 demonstrated that the higher glass transition temperature, the higher storage modulus and loss modulus at high temperature region (above 350°C) than the PI50 might due to the characteristics of cross-linked structure as the remnant of urethane bond.

5.7.2 Tensile mechanical properties

The tensile mechanical properties were measured by tensile testing machine at room temperature and each sample of polyimide films was tested for five samples. Figure 5.11 and Figure 5.12 show the tensile stress and tensile strain of PI50 and PI50-C1.0 respectively. The results of each sample are in the same vicinity (small difference) because if the sample has any little defect (bubbles, cracks, scratch) it will definitely affect the tensile strength results.

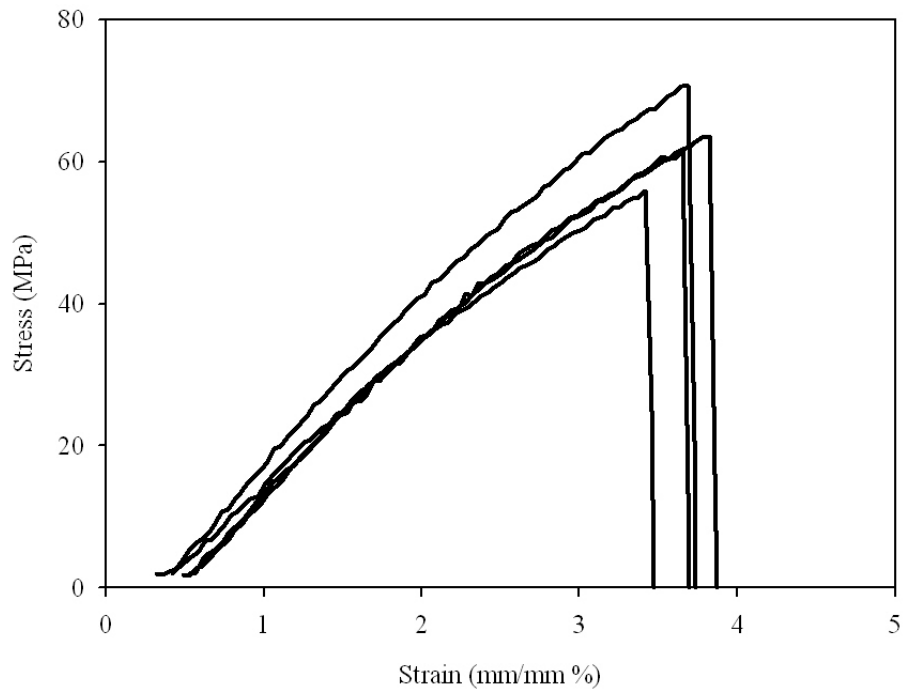


Figure 5.11 Tensile strength of PI50

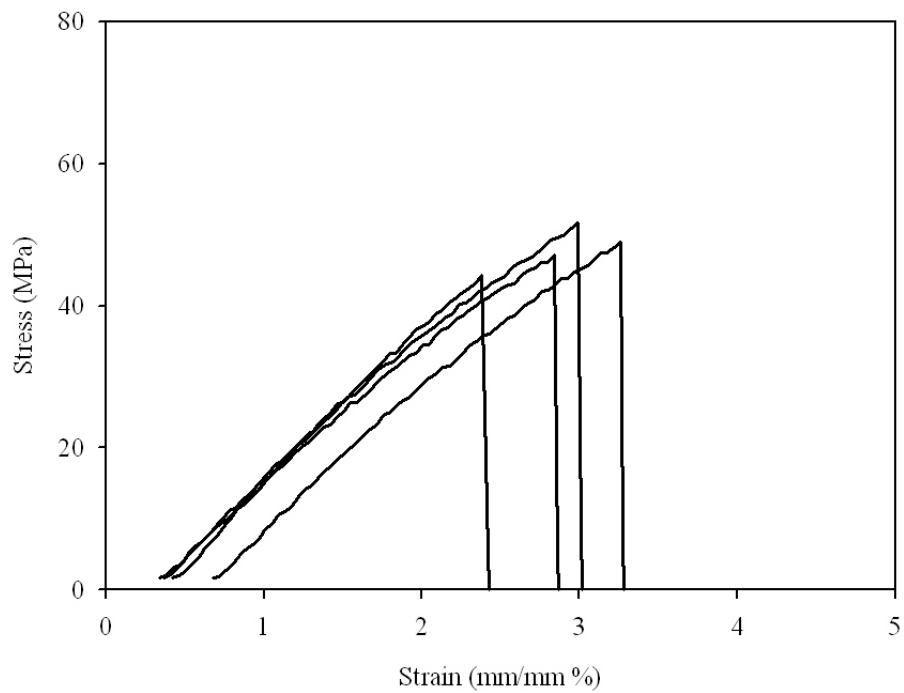


Figure 5.12 Tensile strength of PI50-C1.0

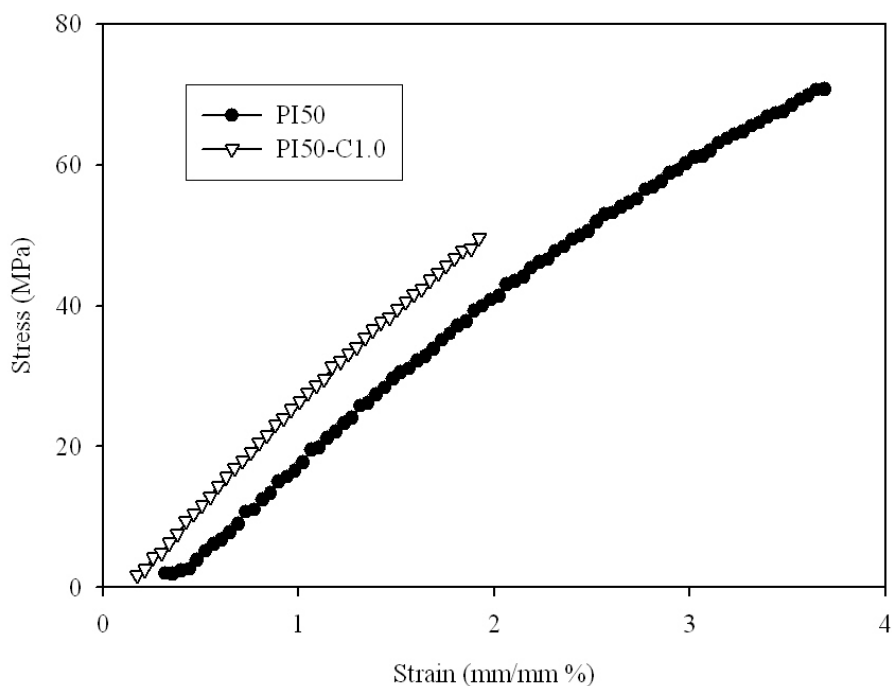


Figure 5.13 Comparison of Tensile strength of PI50 and PI50-C1.0

Table 5.5 Tensile properties of PI50 and PI50-C1.0

Polymer	Tensile properties		
	Tensile stress at Break (Standard) (MPa)	Modulus (E-modulus) (MPa)	Toughness ^a (MPa)
PI50	65.2	2,357	133.7
PI50-C1.0	49.2	3,144	65.2

^a Calculated by the area under stress-strain curve.

The results of tensile stress tests of the PI50 and the PI50-C1.0 are evaluated in Figure 5.13 and Table 5.5. By comparing with PI50 and PI50-C1.0, the PI50 exhibited the higher tensile strength than PI50-C1.0. This can also be explained that the tensile properties show the bulk properties at room temperature. Therefore the presence of pore in PI50-C1.0 might influence to strength greater than the effect of cross-linked structure, led to the reduction in strength of the PI50-C1.0. Additionally, the PI50-C1.0 exhibited the lower elongation at break, the lower toughness and the higher modulus than the PI50 as a result of the stiffness of cross-linked structure that

balance with the void weakness in the samples. The results also agree with the characteristics of cross-linked structure as described in the DMA results. Moreover, we were highly confident that if the tensile properties were performed at high temperature (above 350°C), the PI50-C1.0 would exhibit the tensile properties greater than the PI50 because the PI50 will subject to the decrease in mechanical properties at glass transition temperature while PI50-C1.0 will less affect the mechanical properties because it has higher T_g and crosslink structures.

5.8 Morphology

Figure 5.14 displays the SEM images of the polyimide films. According to picture a) and b), these show the same surface morphology of the polyimide films. Both of the PI50 and PI50-C1.0 exhibited the smooth surface.

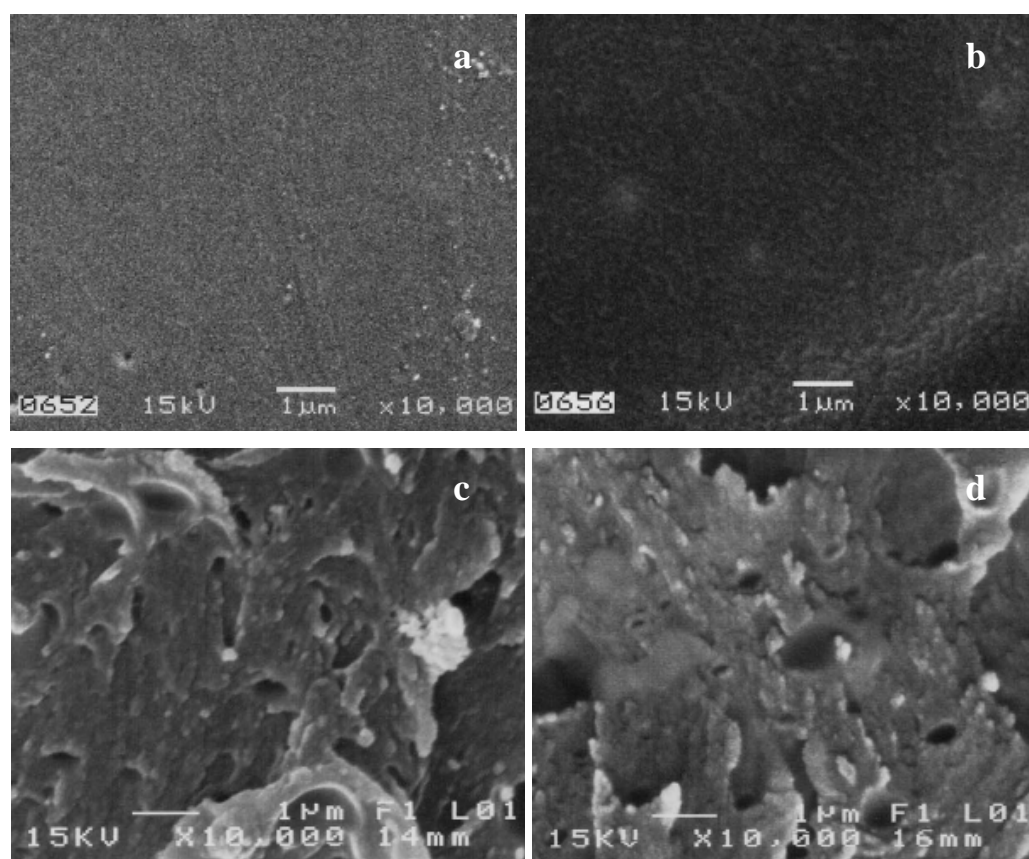


Figure 5.14 SEM images of surface of a) PI50 b) PI50-C1.0 and cross section of c) PI50 d) PI50-C1.0

In the other hand, picture c) and d) show the cross sectional images of the polyimide films. Both of SEM cross sectional images displayed the presence of pores. The similar SEM picture implied that the cause of pore has come from the same effect regardless of the isocyanate added. The presence of pores could be explained by the evaporation of NMP solvent during the thermal treatment process. As we discussed above, the decomposition of urethane component in the PI50-C1.0 might generate pores in the film because of CO₂ formed. Therefore, unfortunately, the SEM cross sectional images can not be observed the different between PI50 and PI50-C1.0. This might be based on that the very small size of pores, which were generated by carbon dioxide, could not be observed due to the limitation of SEM resolution. However the different in the void imply the existing of the small pore of CO₂ because all the samples have subjected to the same sample preparation and the similar pore created by NMP will be the same while the difference in dielectric constant arises because of the pore of CO₂ which correspond to the extra urethane linkages.

CHAPTER VI

CONCLUSIONS AND RECOMMENDATIONS

6.1. CONCLUSIONS

From this work, it can be concluded as follows:

1. The cross-linked polyimide films can be synthesized by the reaction between diisocyanate groups and hydroxyl functional groups in polyimide structure, which was confirmed by FTIR, follow by thermal treatment to obtain cross-linked polyimide films.
2. From monitoring the phenomenon during the thermal treatment by TGA, the PI100-C1.0 exhibited the little shoulder in the temperature range 230-300°C due to the decomposition of CO₂ in the urethane segments, which might generate pore in the film.
3. The dielectric constant of the films decreased with the increase of TDI loading as a result of the presence of pore in the cross-linked polyimide films. Although the PI75-C1.0 has the lowest dielectric constant, it exhibits poorly mechanical properties. Therefore, we chose PI50-C1.0 and PI50 to characterize the evaluated properties and to elucidate the effect of cross-linked structure because the PI50-C1.0 exhibited optimum mechanical and good dielectric properties.
4. The cross-linked structure was also confirmed by DMA. The PI50-C1.0 showed excellent storage and loss modulus in the high temperature range (above 350°C) due to the characteristic of cross-linked structure.
5. The results of tensile stress test showed that the PI50-C1.0 exhibited lower tensile strength than the PI50 because the presence of pore in PI50-C1.0 might influence to strength greater than the effect of cross-linked structure.

6. The SEM cross sectional images can not be observed the different between PI50 and PI50-C1.0. This might be based on that the very small size of pores, which were generated by carbon dioxide, could not be observed due to the limitation of SEM resolution.

6.2 RECOMMENDATIONS

From the results in this work, the further investigation in the following subjects will be useful.

1. Further characterize on the morphology of PI50-C1.0 by the TEM and AFM will be advantage to identification of pore generated by carbon dioxide.
2. Vary the cross-linking agent which has the difference of molecular size such as hexamethylene diisocyanate (HDI) and characterize their properties.
3. Further study on the effect of TDI loading (not only 0.1, 0.5 and 1.0) and investigates the mechanical properties compare to the uncross-linked polyimide and justify the optimum content.

REFERENCES

- [1] Ghosh, M.K. and Mittal, K.L. **Polyimides, fundamentals and applications**. New York: Mercel-Dekker, 1996.
- [2] Boston, H.G., Reddy, V.S., Cassidy, P.E., Fitch, J.W., Stoakley, D. and Clair, A.K. New aromatic diacids containing the trifluoromethyl group and their polyamides. **High Perform Polymer** 9(1997): 323-332.
- [3] Chern, Y.T. and Shiue, H.C. Low dielectric constants of soluble polyimides based on adamantane. **Macromolecules** 30(1997): 4646–4651.
- [4] Chern, Y.T. and Shiue, H.C. Low dielectric constants of soluble polyimides derived from the novel 4,9-bis[4-(4-aminophenoxy)phenyl]diamantine. **Macromolecules** 30(1997): 5766–5772.
- [5] Chern, Y.T. Low dielectric constant polyimides derived from novel 1,6-bis[4-(4-aminophenoxy)phenyl]diamantine. **Macromolecules** 31(1998): 5837–5844.
- [6] Hougham, G., Tesero, G. and Shaw, J. Synthesis and properties of highly fluorinated polyimides. **Macromolecules** 27(1994): 3642–3649.
- [7] Hougham, G., Tesero, G., Viehbeck, A. and Chapple-Sokol, JD. Polarization effects of fluorine on the relative permittivity in polyimides. **Macromolecules** 27(1994): 5964–5971.
- [8] Matsuura, T. and Hasuda, Y. Polyimide derived from 2,2'-bis(trifluoromethyl)-4,4'-diaminobiphenyl. 1. Synthesis and characterization of polyimides prepared with 2,2-bis(3,4-dicarboxyphenyl) hexafluoro- propane dianhydride or pyromellitic dianhydride. **Macromolecules** 24(1991): 5001-5005.
- [9] Matsuura, T., Ando, S. and Sasaki, S. Per fluorinated polyimide synthesis. **Macromolecules** 25(1992): 5858-5860.
- [10] Yamazaki, O., Yamashita, T. and Horie, K. Preparation and properties of poly(amide acid) gels. **Reactive and Functional Polymers** 43(2000): 173–181.
- [11] Deligoza, H., Ozgumus, S. and Yalcinyuva, T. A novel cross-linked polyimide film: synthesis and dielectric properties. **Polymer** 46(2005): 3720–3729.

- [12] Deligoza, H., Ozgumus, S., Yalcinyuva, T. and Yildirim, S. Preparation, characterization and dielectric properties of 4,4-diphenyl-methane diisocyanate (MDI) based cross-linked polyimide films. **European Polymer Journal** 42(2006): 1370–1377.
- [13] Takeichi, T., Yamazaki, Y. and Zuo, M. Preparation of porous carbon films by the pyrolysis of poly(urethane-imide) films and their pore characteristics. **Carbon** 39(2001): 257-265.
- [14] Santhana, P., Krishnan, G. and Cheng, C.Z. Preparation of nanoporous polyimide films from poly(urethane-imide) by thermal treatment. **Macromolecular Materials and Engineering** 288(2003): 730-736.
- [15] Wang, X. and Lin, J. Novel low k polyimide/mesoporous silica composite films: Preparation, microstructure, and properties. **Polymer** 48(2007): 318-329.
- [16] Jiang, L., Liu, J., Wu, D., Li, H. and Jin, R. A methodology for the preparation of nanoporous polyimide films with low dielectric constants. **Thin Solid Films** 510(2006): 241 – 246.
- [17] Liaw, D.J., Chang, F.C. and Leung, M.K. High thermal stability and rigid rod of novel organosoluble polyimides and polyamides based on bulky and noncoplanar naphthalene-biphenyldiamine. **Macromolecules** 38(2005): 4024-4029.
- [18] Hergenrother, P.M., Connell, J.W. and Smith, J. Imide oligomers containing pendent and terminal phenylethynyl groups. **Polymer** 38(1996): 4657-4665.
- [19] Hergenrother, P.M., Connell, J.W. and Smith, J. Phenylethynyl containing imide oligomers. **Polymer** 41(2000): 5073-5081.
- [20] Hergenrother, P.M. and Thompson, C.M. Aryl ethynyl terminated imide oligomers and their cured polymers. **Macromolecules** 35(2002): 5835-5839.
- [21] Simone, D.C. and Scola, D.A. Phenylethynyl end-capped polyimides derived from 4,4'-(2,2,2-trifluoro-1-phenylethylidene)diphthalic anhydride, 4,4'-(hexafluoroisopropylidene) diphthalic anhydride, and 3,3',4,4'-bi phenylene dianhydride: Structure-viscosity relationship. **Macromolecules** 36(2003): 6780-6790.
- [22] Zuo, M. and Takeichi, T. Preparation and characterization of poly (urethane-imide) films prepared from reactive polyimide and polyurethane prepolymer. **Polymer** 40(1999): 5153-5160.

- [23] Yamazaki, O., Yamashita, T. and Horie, K. Preparation and properties of poly(amide acid) gels. **Reactive and Functional Polymers** 43(2000): 173–181.
- [24] He, J., Horie, K. and Yokota, R. Characterization of polyimide gels cross-linked with hexamethylene diisocyanate. **Polymer** 41(2000): 4793-4802.
- [25] He, J., Horie, K. and Yokota, R. Preparation of end-crosslinked polyimide gels with high moduli. **Polymer** 42(2001): 4063-4072.
- [26] Yang, S.J., Lee, C. and Jang, W. Synthesis and characterization of poly (epoxy-imide) crosslinked networks. **Journal of Polymer Science: Part B: Polymer Physics** 42(2004): 4293-4302.
- [27] Deligoza, H., Ozgumus, S. and Yalcinyuva, T. A novel cross-linked polyimide film: synthesis and dielectric properties. **Polymer** 46(2005): 3720–3729.
- [28] Deligoza, H., Ozgumus, S., Yalcinyuva, T. and Yildirim, S. Preparation, characterization and dielectric properties of 4,4-diphenyl-methane diisocyanate (MDI) based cross-linked polyimide films. **European Polymer Journal** 42(2006): 1370–1377.
- [29] Lee, Y.J. and Huang, J.M. Low-dielectric, nanoporous polyimide films prepared from PEO-POSS nanoparticles. **Polymer** 46(2005): 10056-10065.
- [30] Wood, G. **The ICI Polyurethanes Handbook**. New York: John Wiley & Sons, 1987.
- [31] Khandpur, R.S. **Printed Circuit Boards: Design, Fabrication and Assembly**. New York: McGraw-Hill, 2006.
- [32] Brown, T.L. **Chemistry**. New Jersey: Prentice Hall, 2000.
- [33] Murayama, T. **Dynamic Mechanical Analysis of polymeric materials**. Amsterdam: Elsevier Scientific Publishing, 1982.
- [34] Choudhury, N.R. and Oaten, N. Silsesquioxane-Urethane hybrid for thin film application. **Macromolecules** 38(2005): 6392-6401.

APPENDICES

Appendix A

FT-IR Characterization

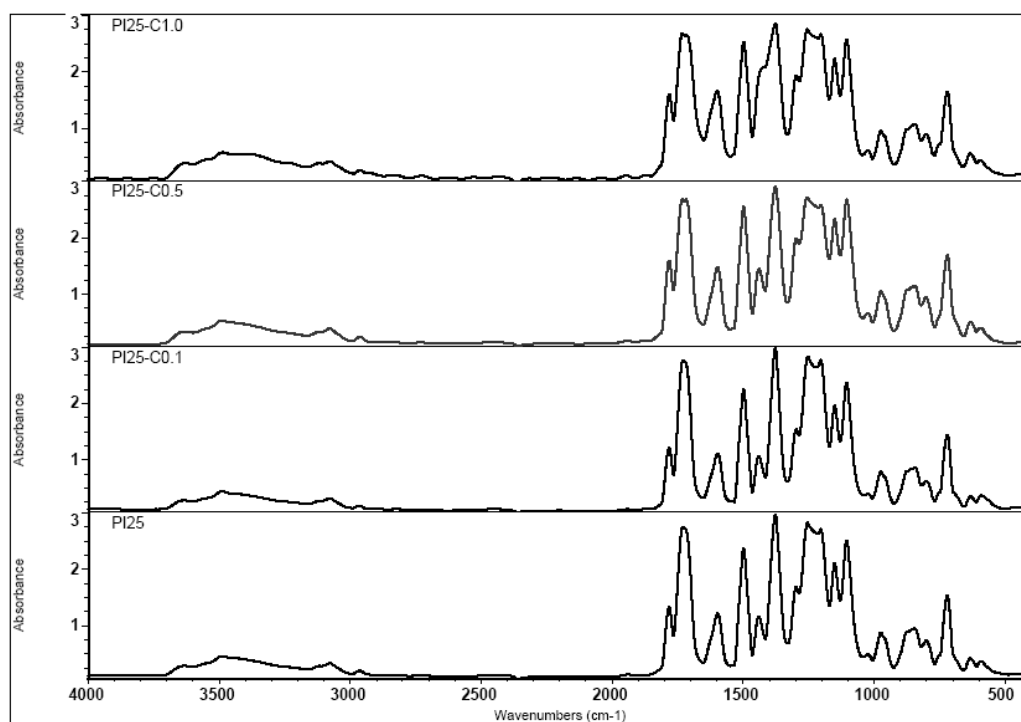


Figure A.1 FTIR spectra of PI25 series

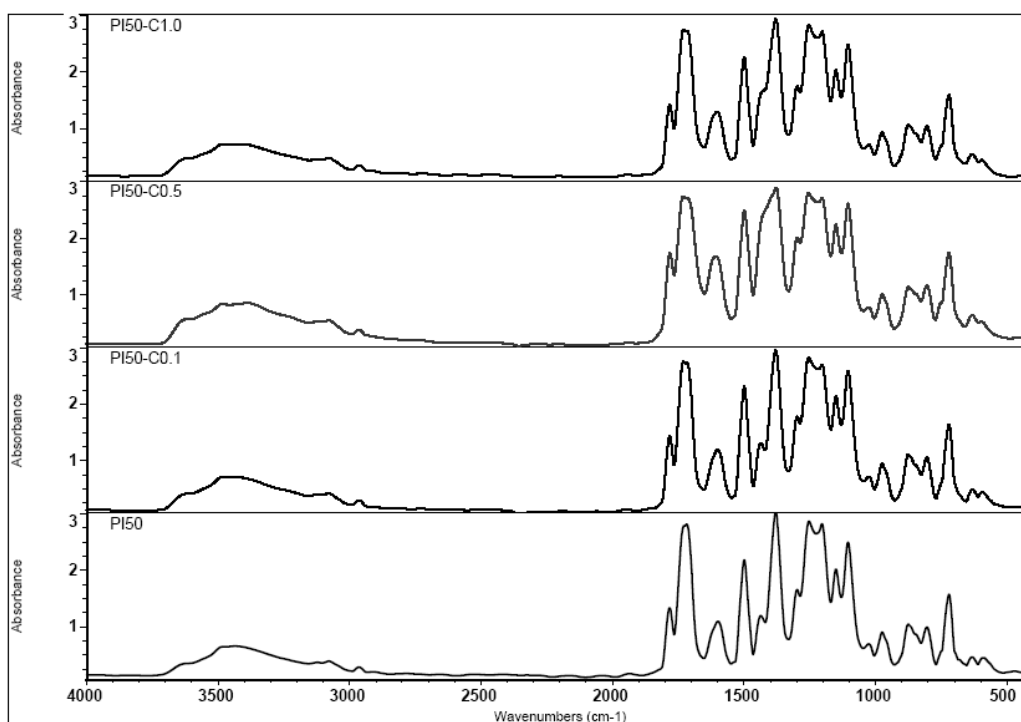


Figure A.2 FTIR spectra of PI50 series

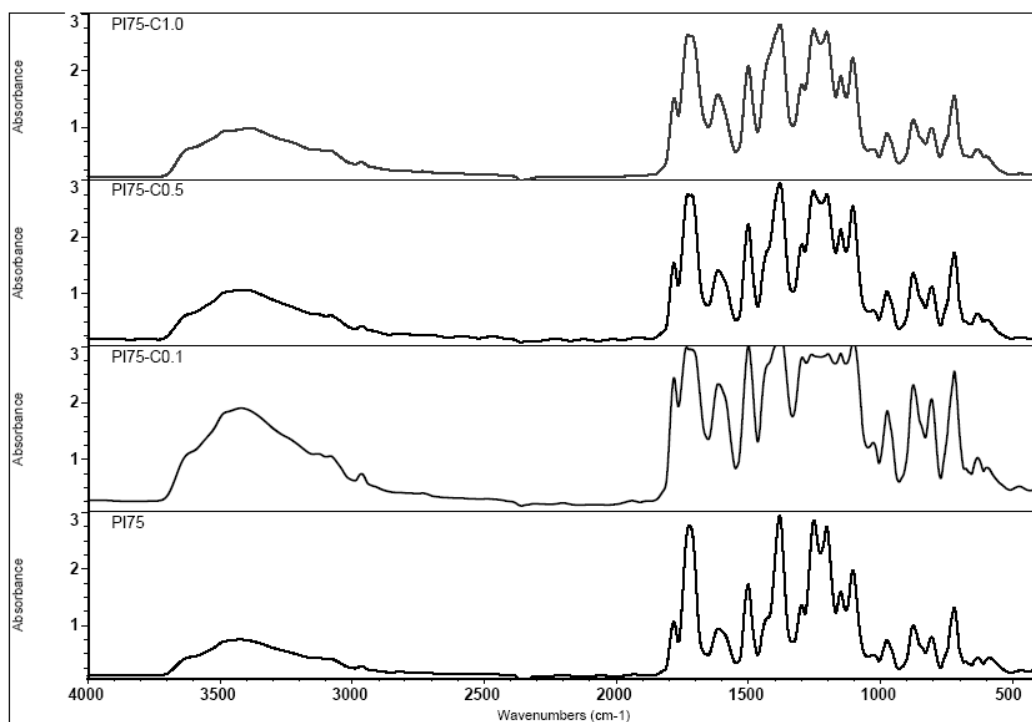


Figure A.3 FTIR spectra of PI75 series

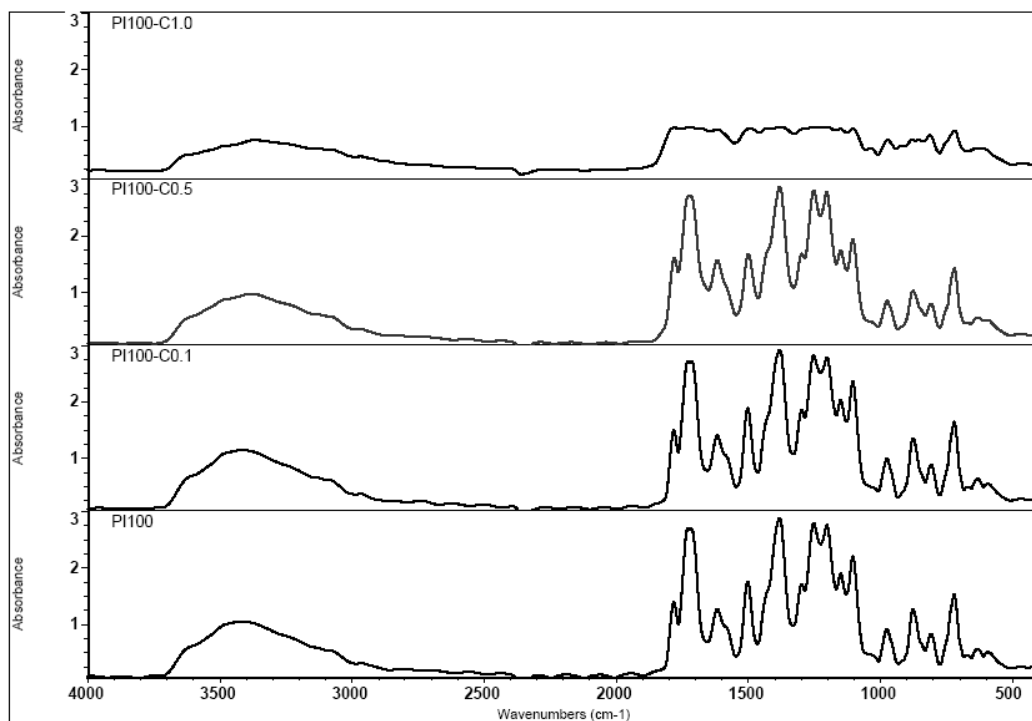


Figure A.4 FTIR spectra of PI100 series

Appendix B
DMA Characterization under N₂ atmosphere

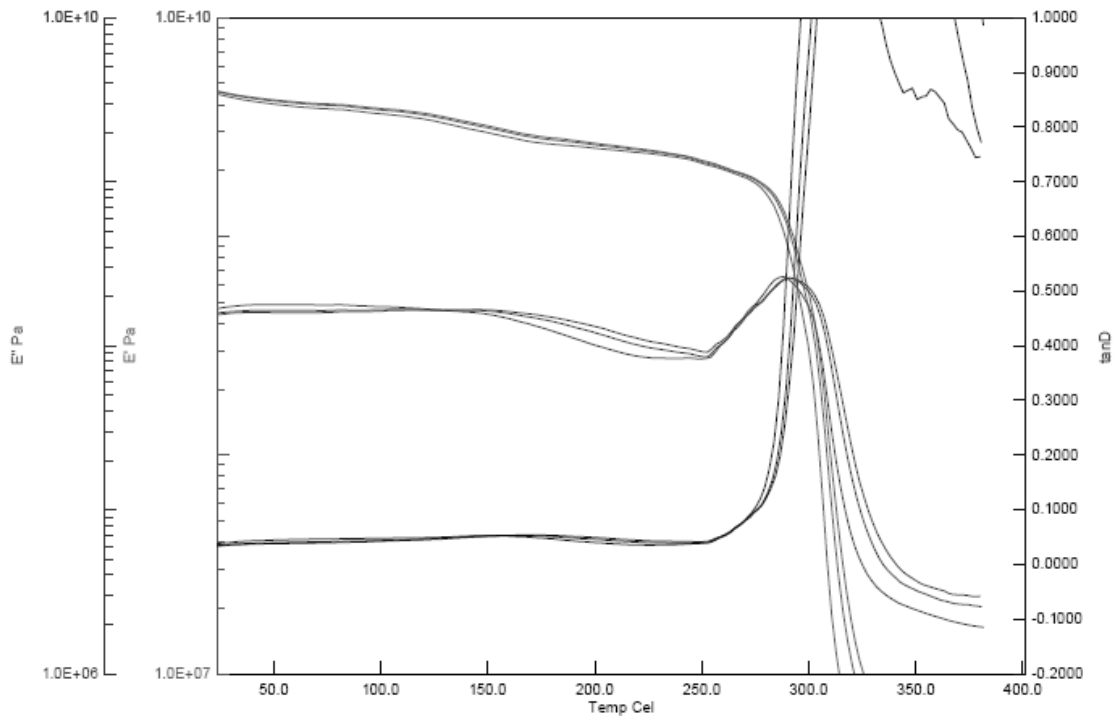


Figure B.1 DMA curve of PI25

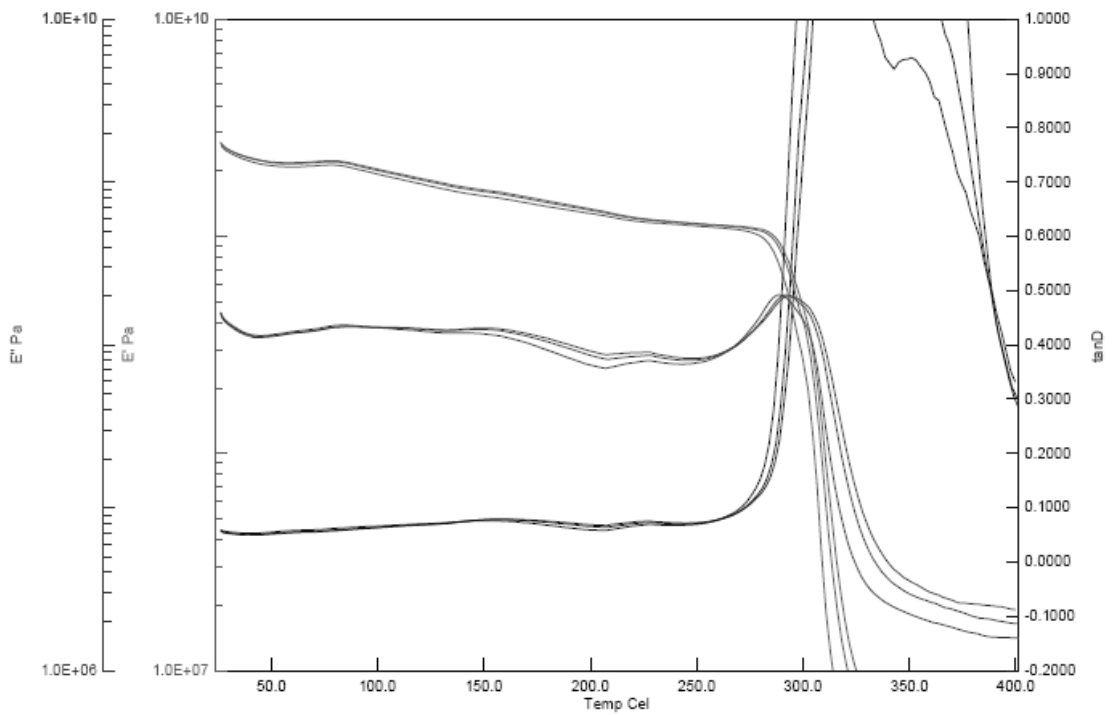


Figure B.2 DMA curve of PI25-C0.1

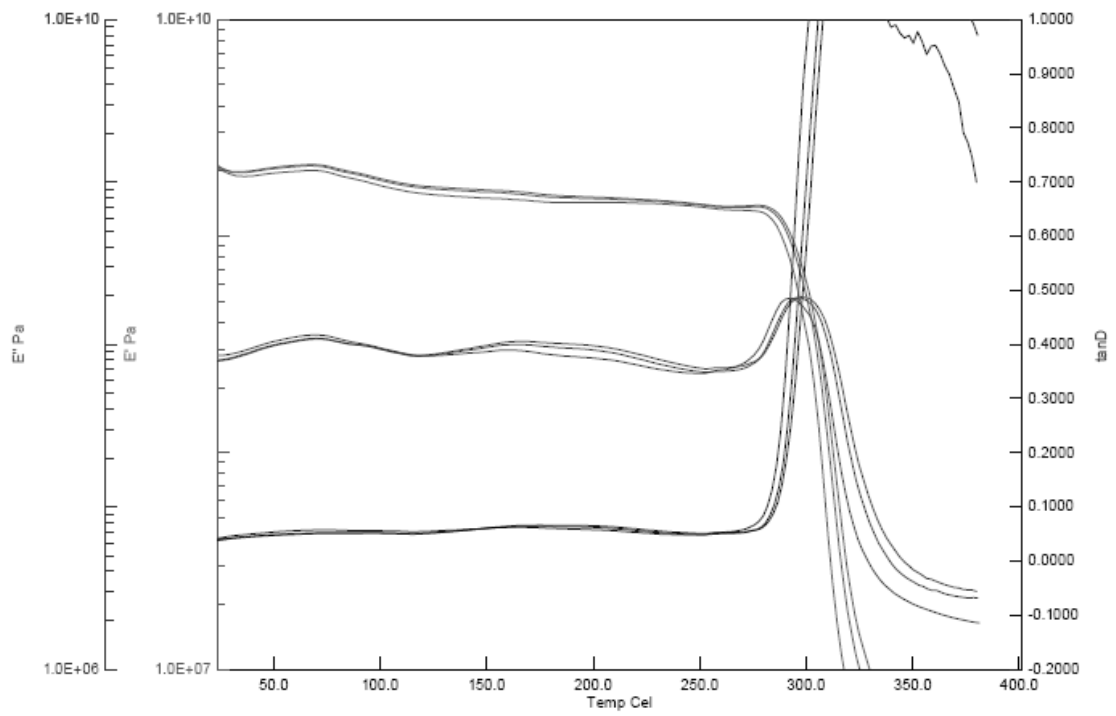


Figure B.3 DMA curve of PI25-C0.5

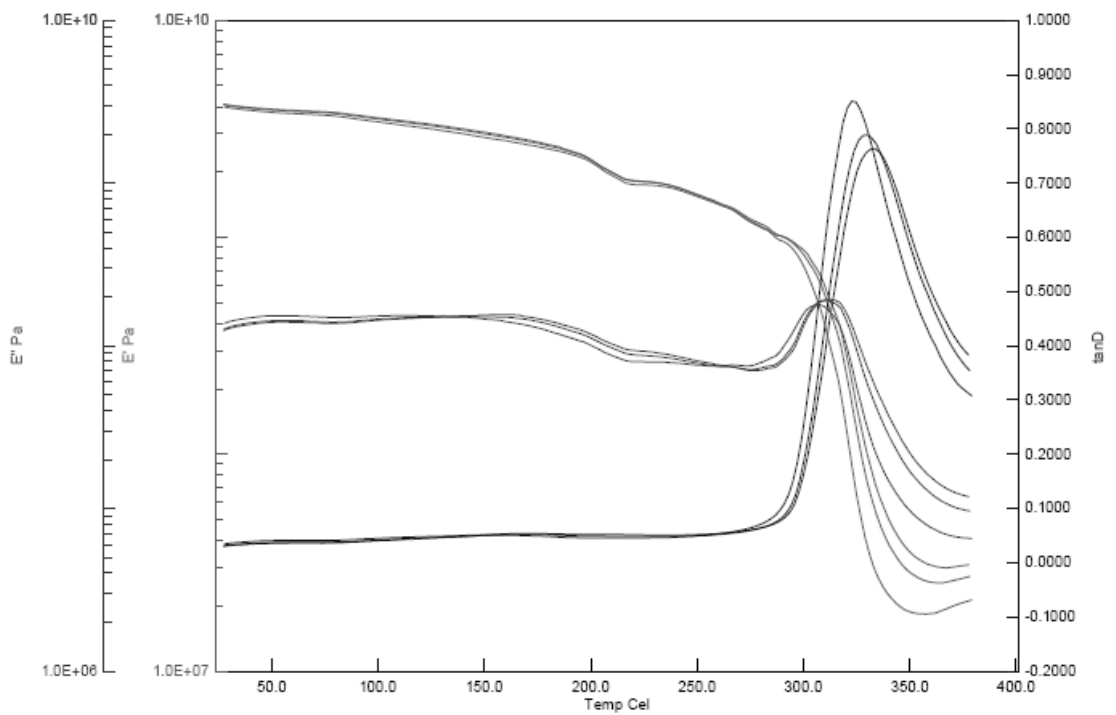


Figure B.4 DMA curve of PI25-C1.0

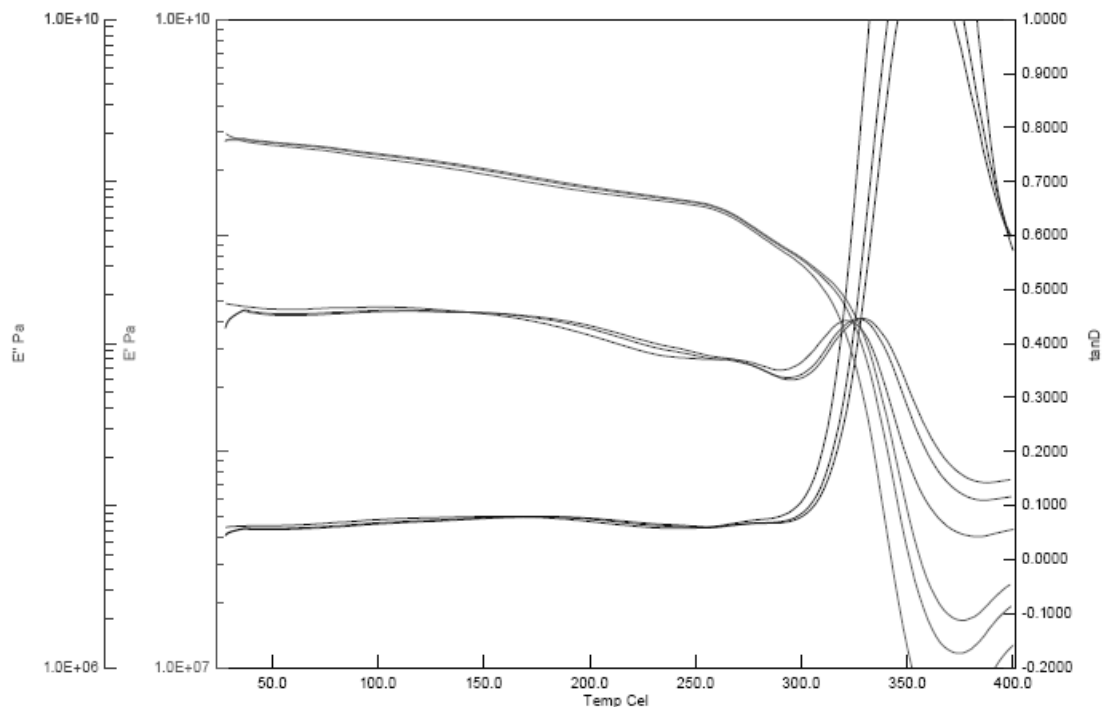


Figure B.5 DMA curve of PI50

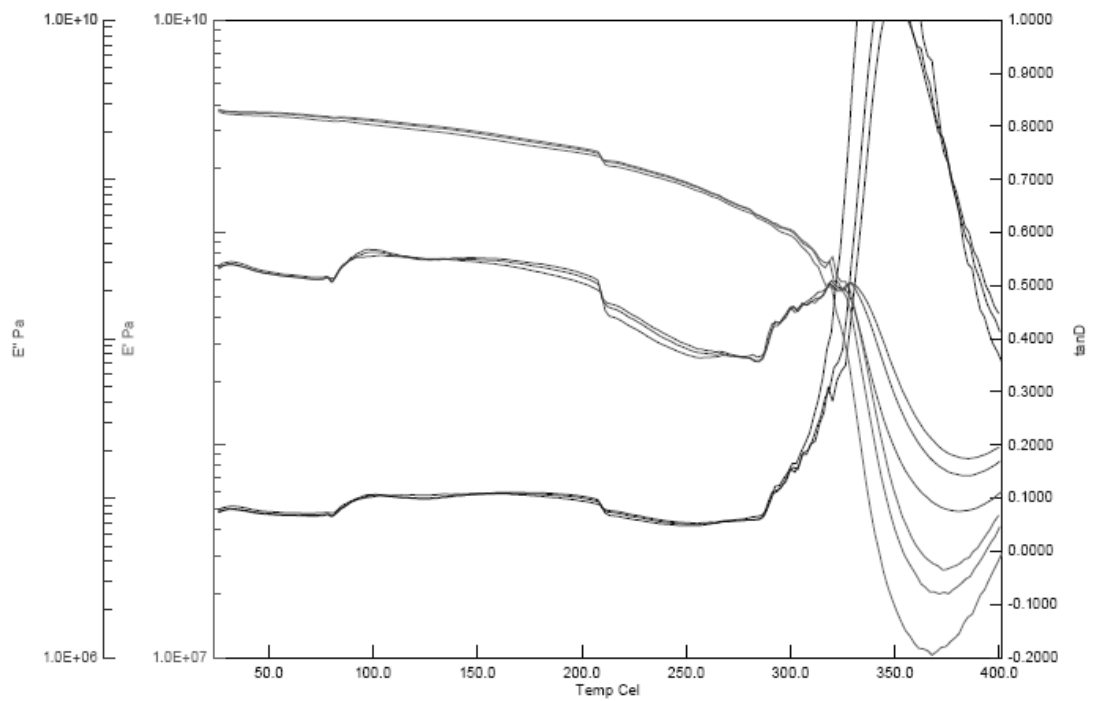


Figure B.6 DMA curve of PI50-C0.1

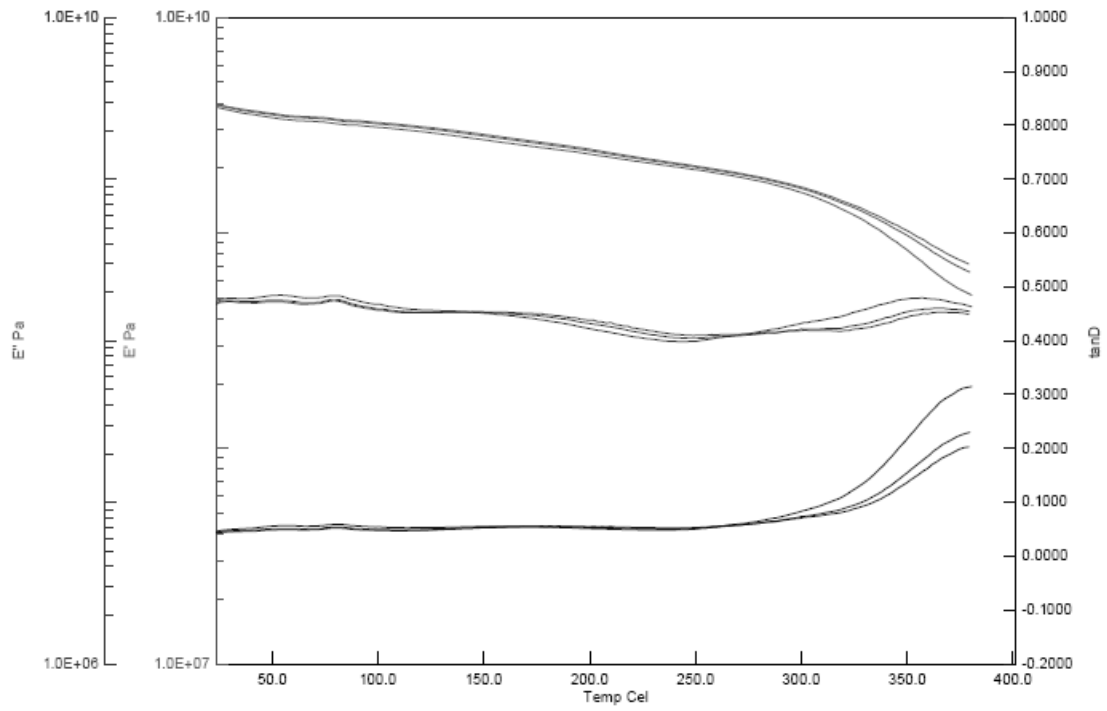


Figure B.7 DMA curve of PI50-C0.5

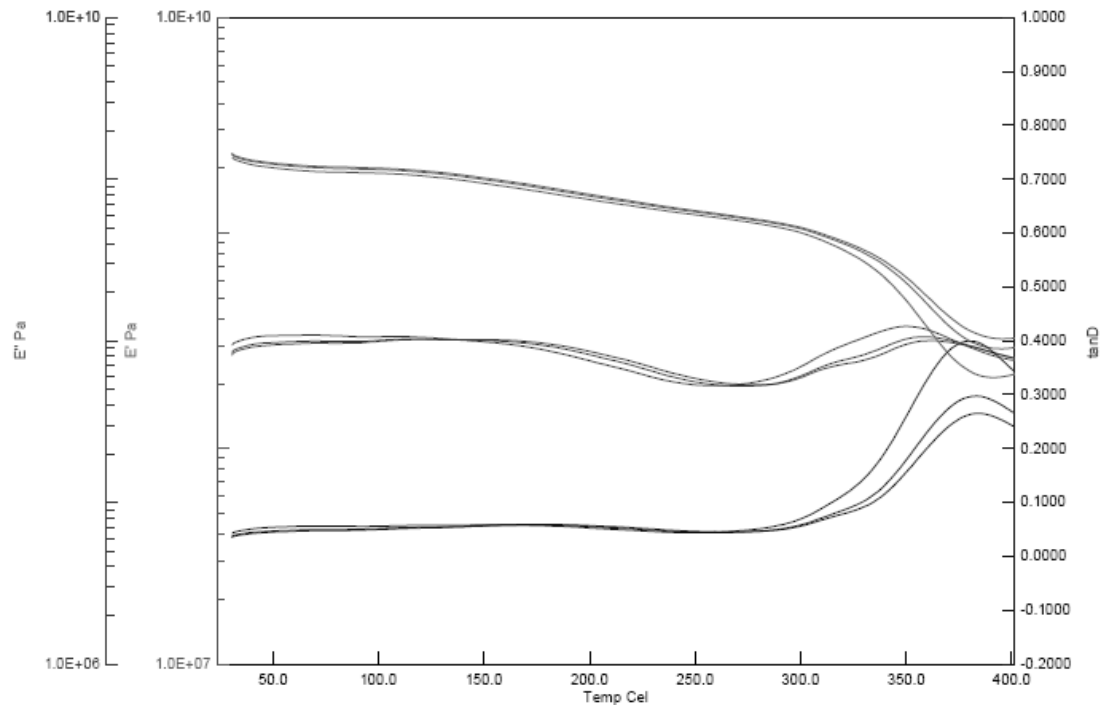


Figure B.8 DMA curve of PI50-C1.0

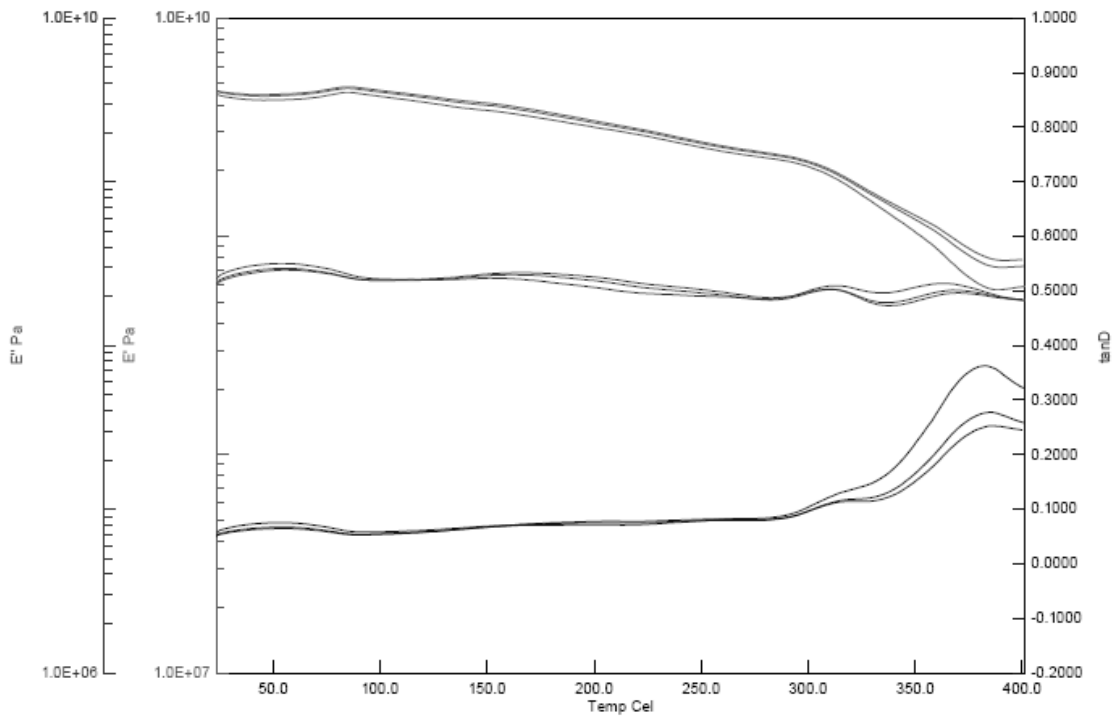


Figure B.9 DMA curve of PI75

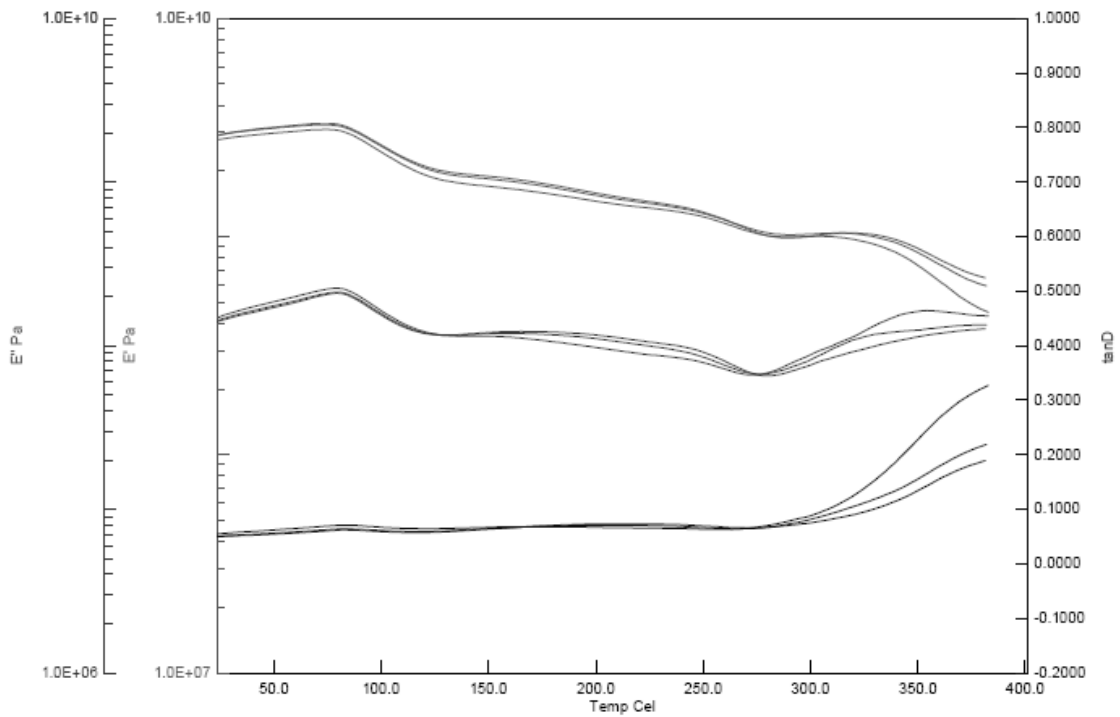


Figure B.10 DMA curve of PI75-C0.1

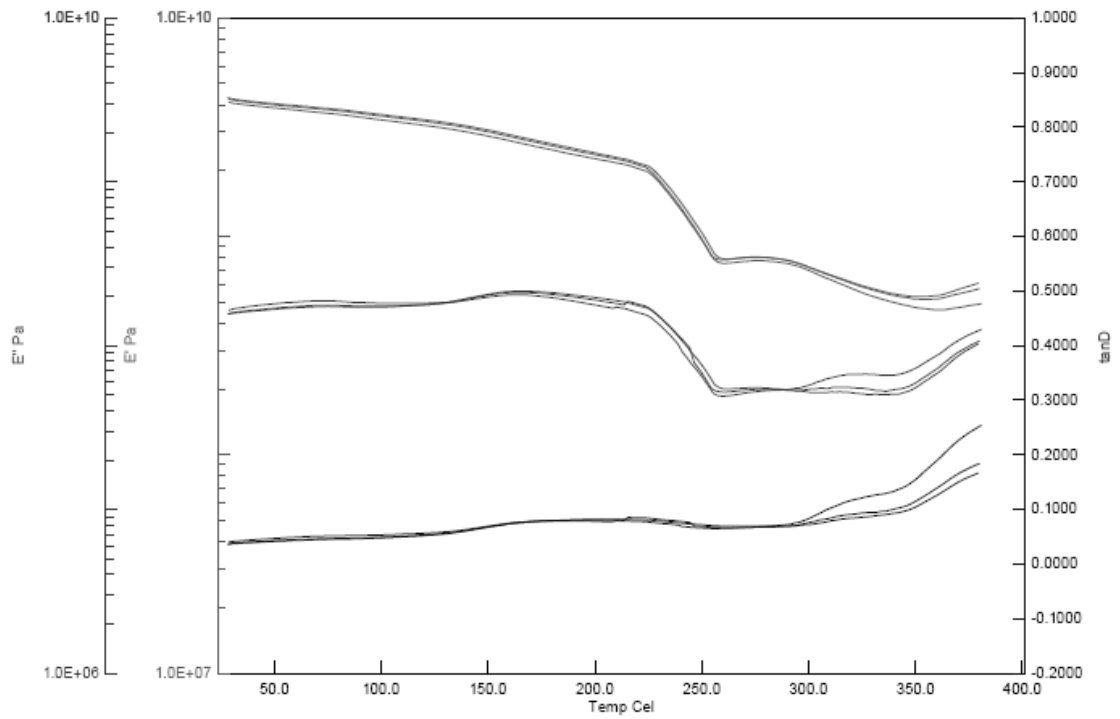


Figure B.11 DMA curve of PI75-C0.5

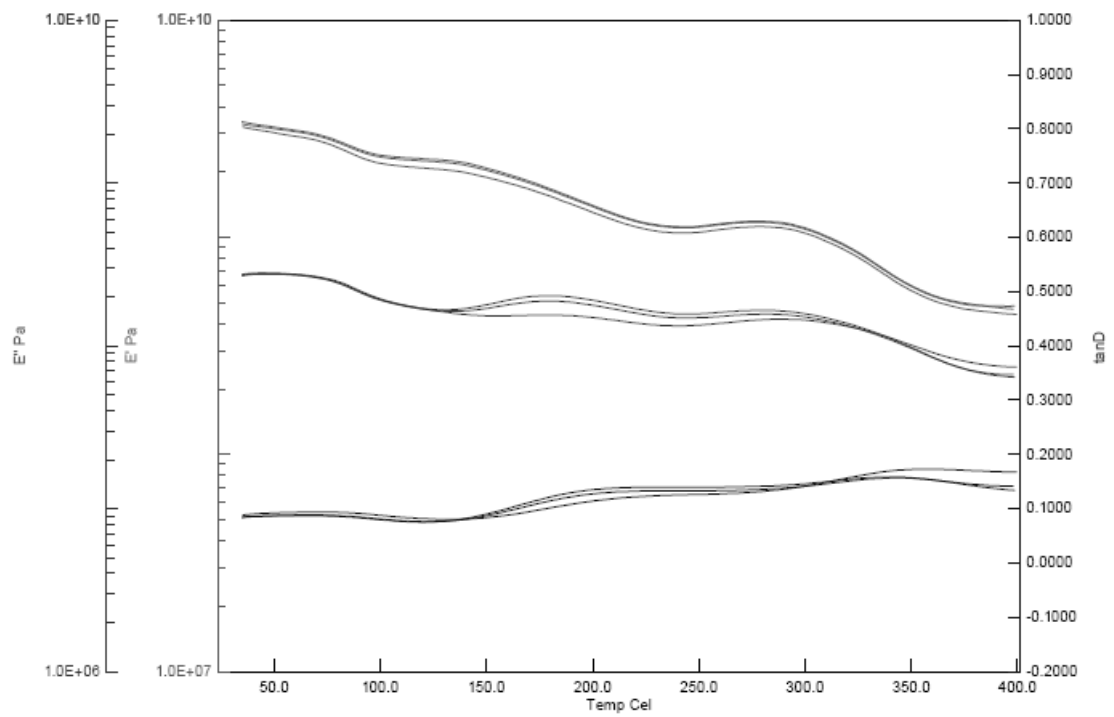


Figure B.12 DMA curve of PI100

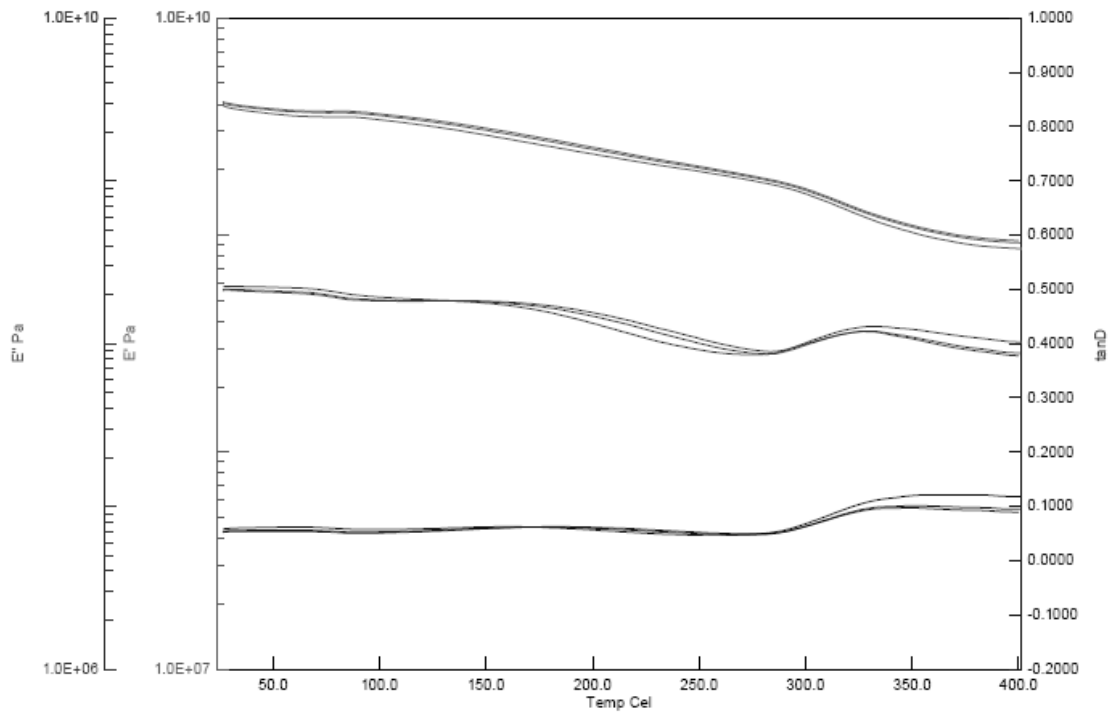


Figure B.13 DMA curve of PI100-C0.1

Appendix C
TGA Characterization under N₂ atmosphere

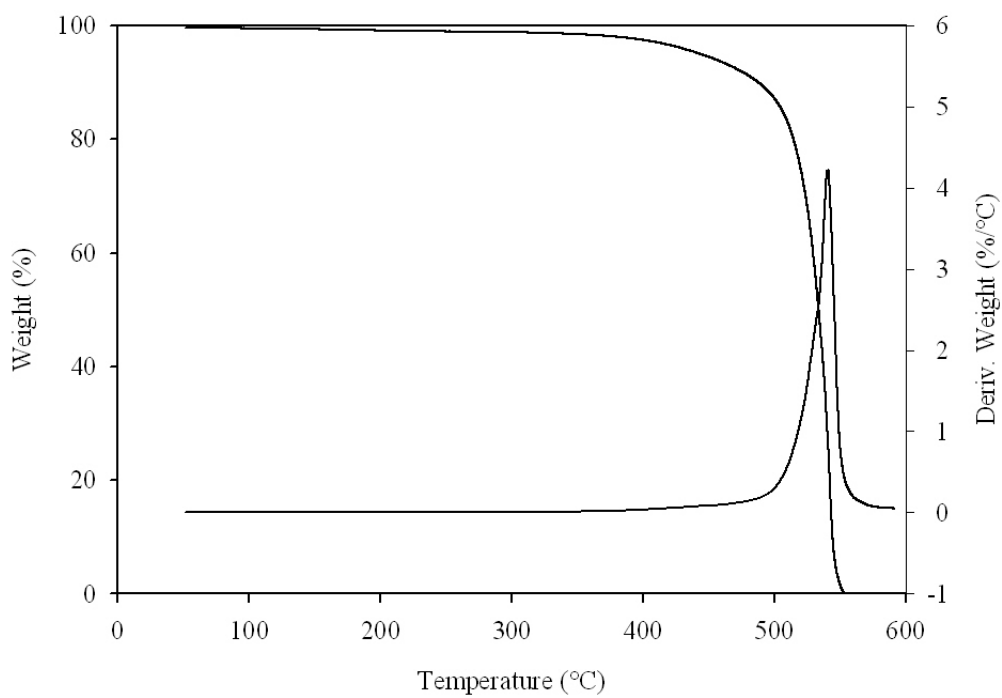


Figure C.1 TGA curve of PI25

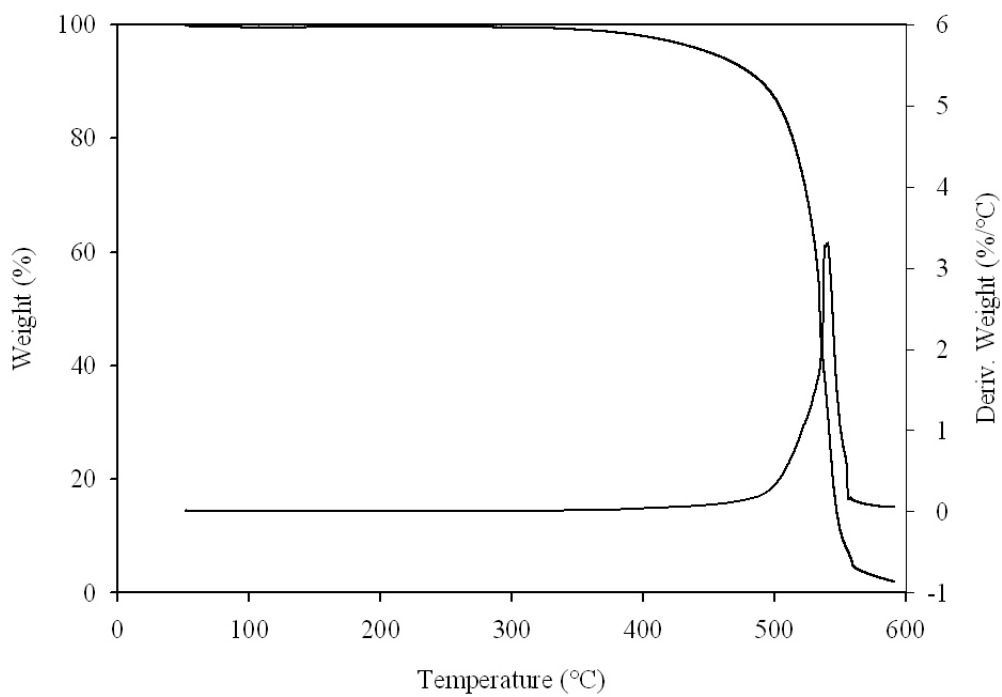


Figure C.2 TGA curve of PI25-C0.1

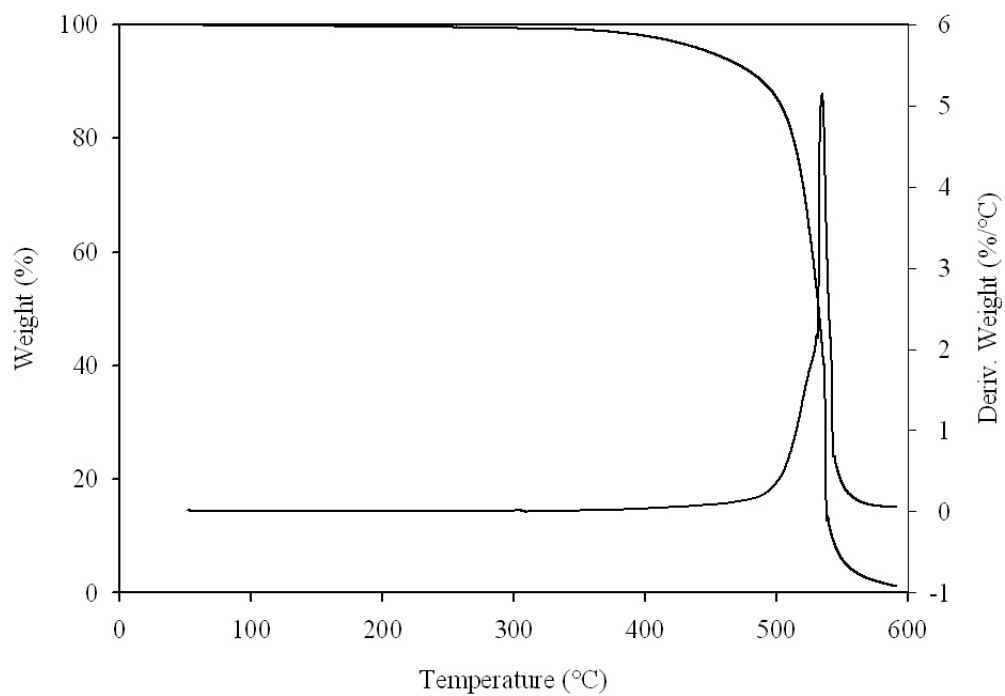


Figure C.3 TGA curve of PI25-C0.5

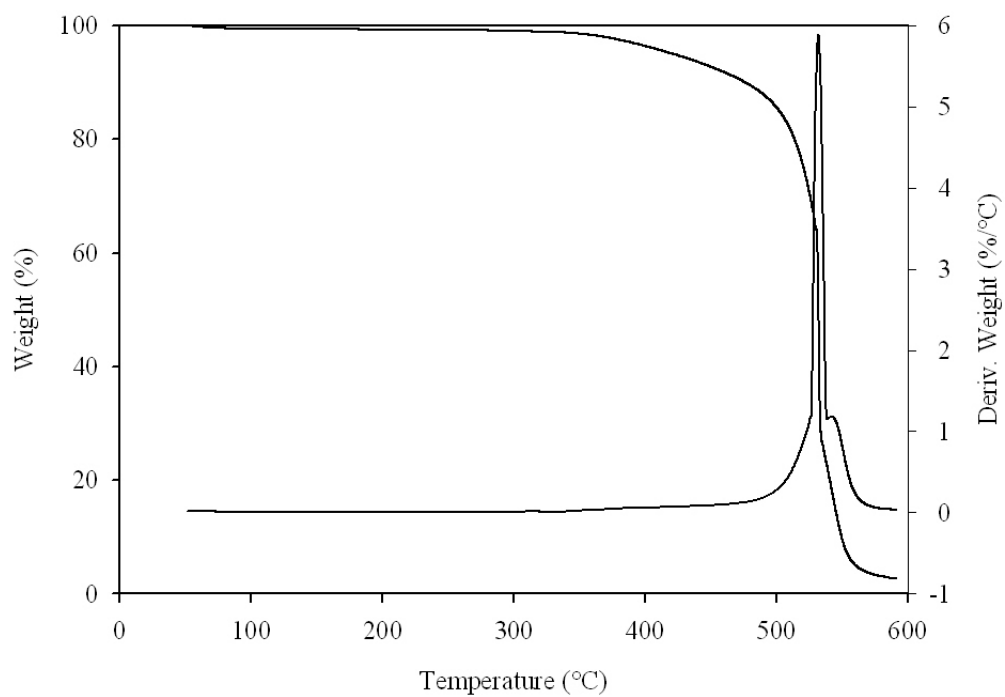


Figure C.4 TGA curve of PI25-C1.0

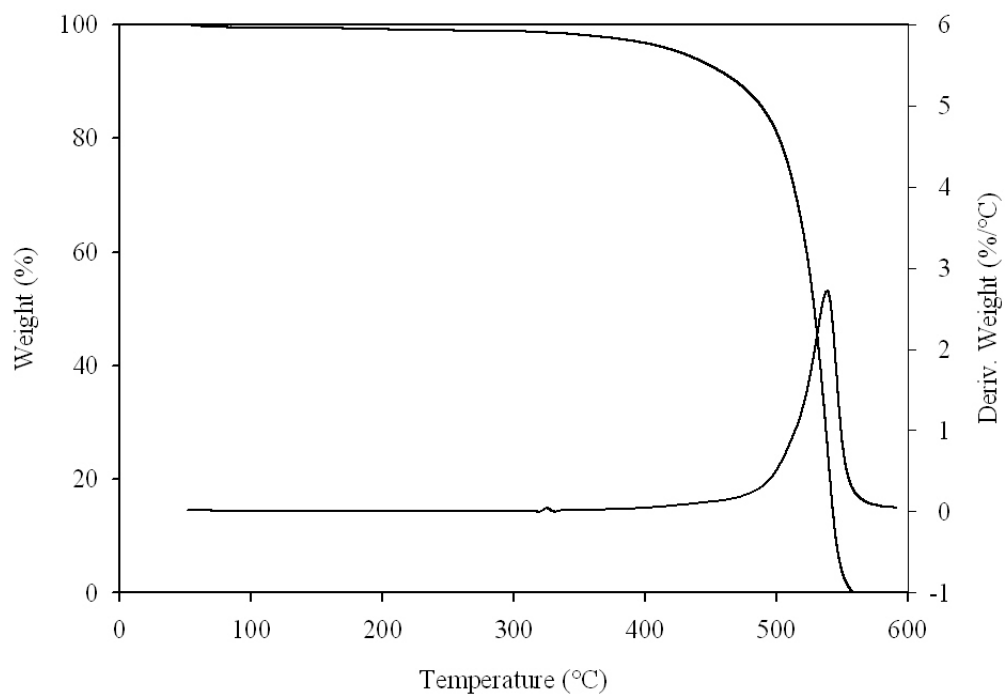


Figure C.5 TGA curve of PI50

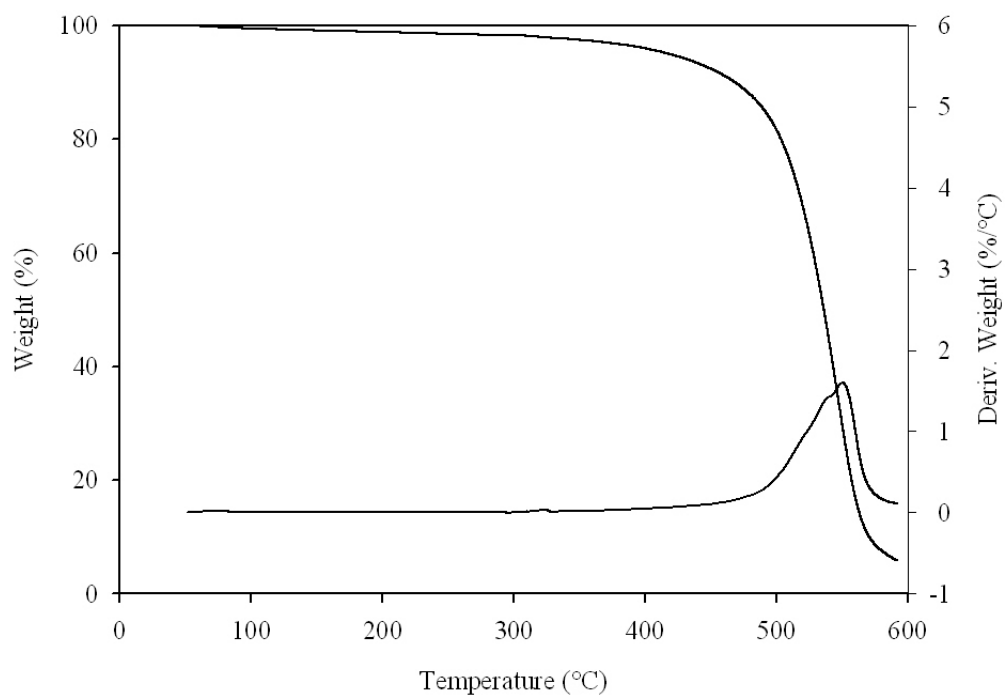


Figure C.6 TGA curve of PI50-C0.1

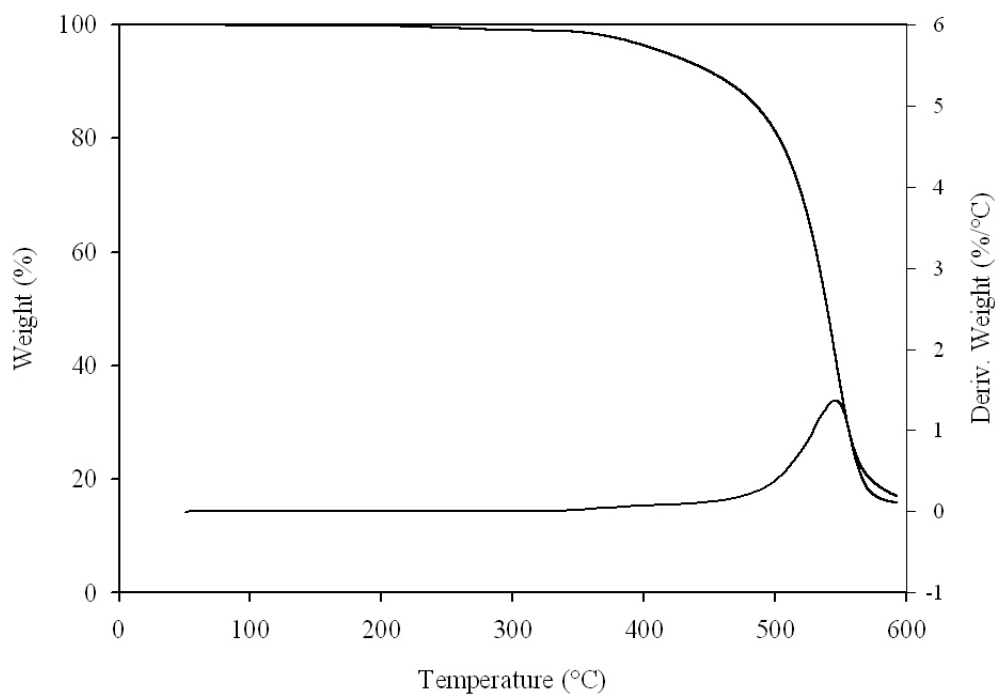


Figure C.7 TGA curve of PI50-C0.5

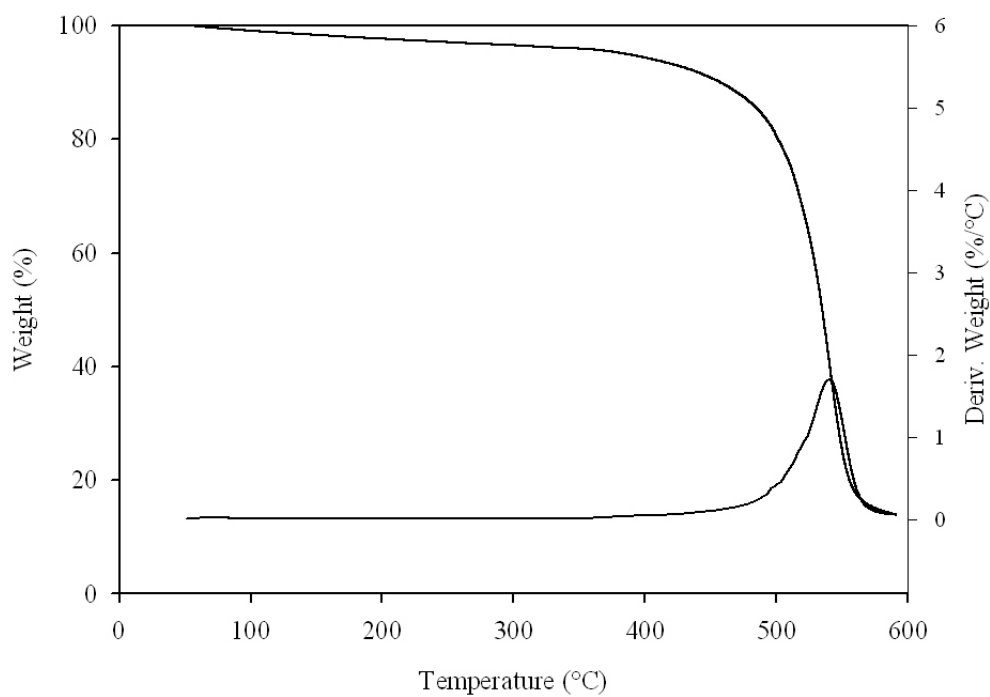


Figure C.8 TGA curve of PI50-C1.0

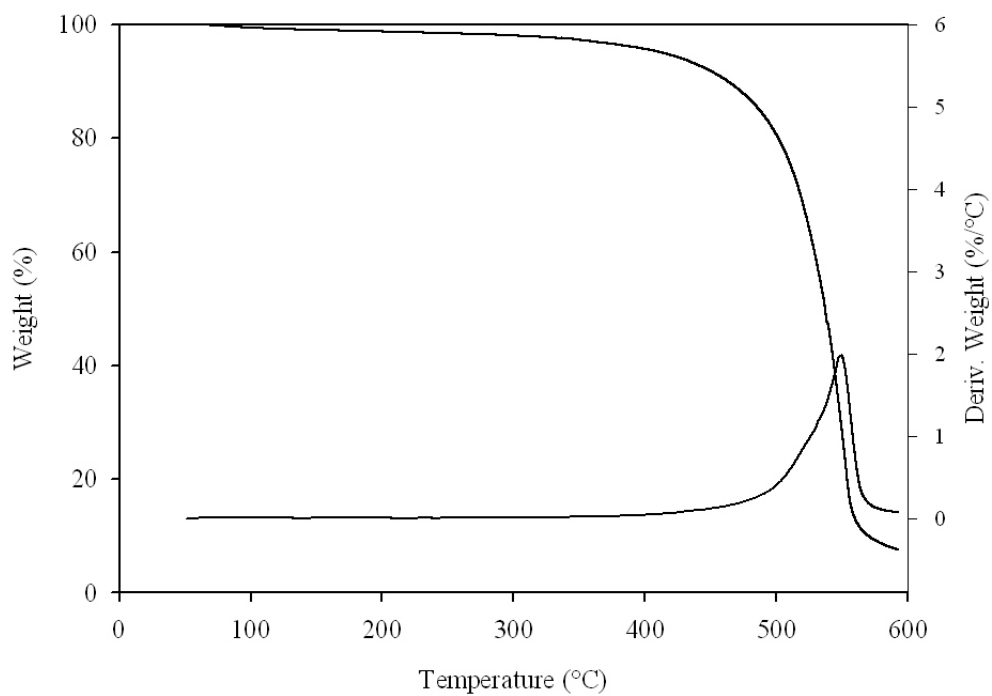


Figure C.9 TGA curve of PI75

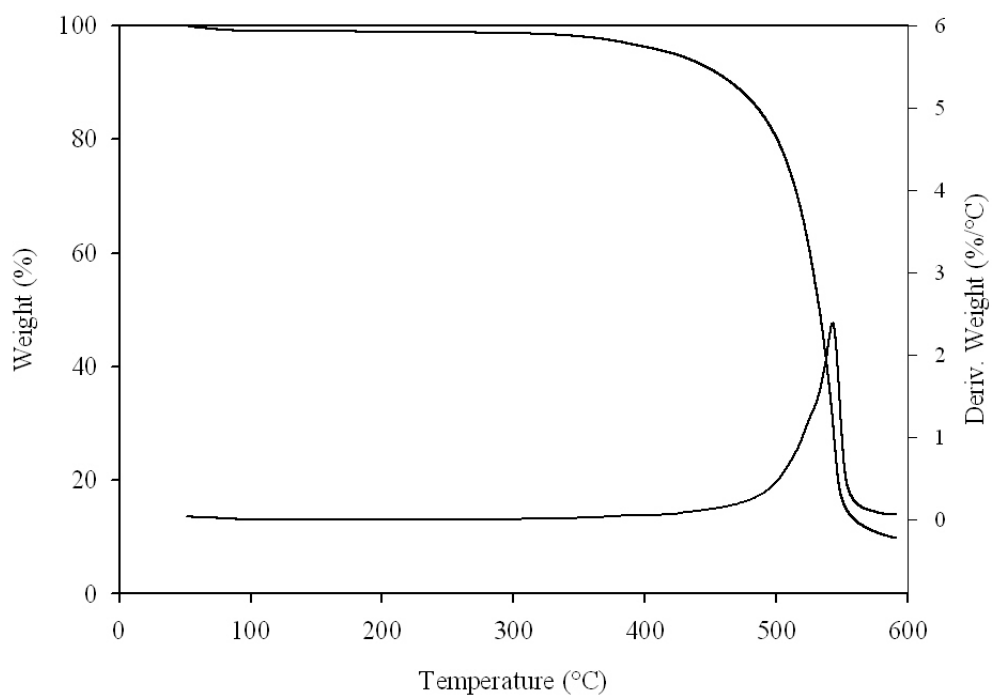


Figure C.10 TGA curve of PI75-C0.1

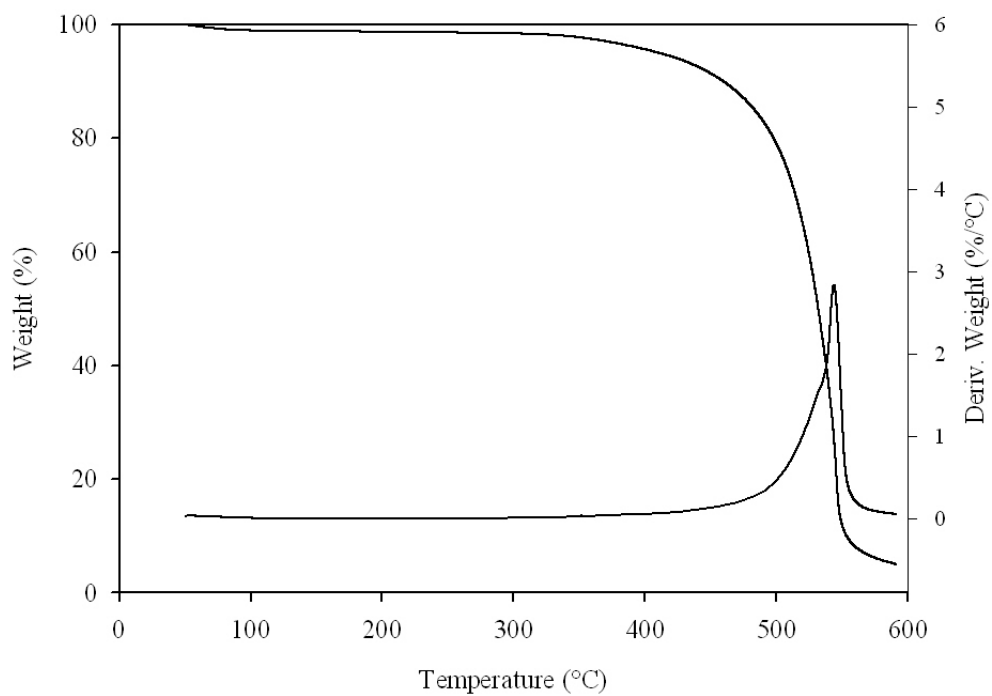


Figure C.11 TGA curve of PI75-C0.5

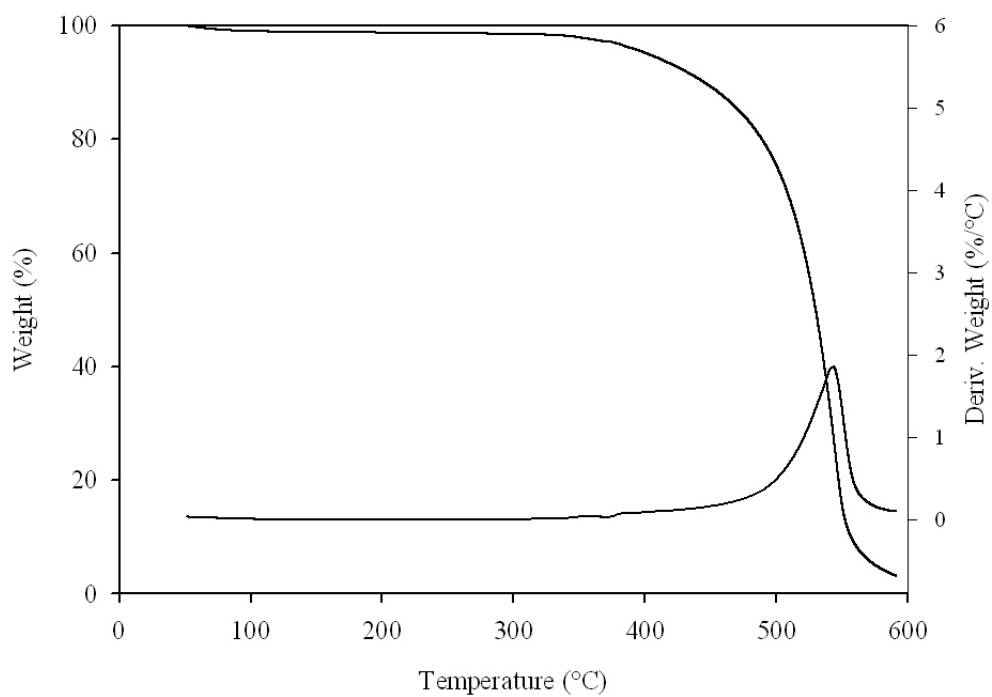


Figure C.12 TGA curve of PI75-C1.0

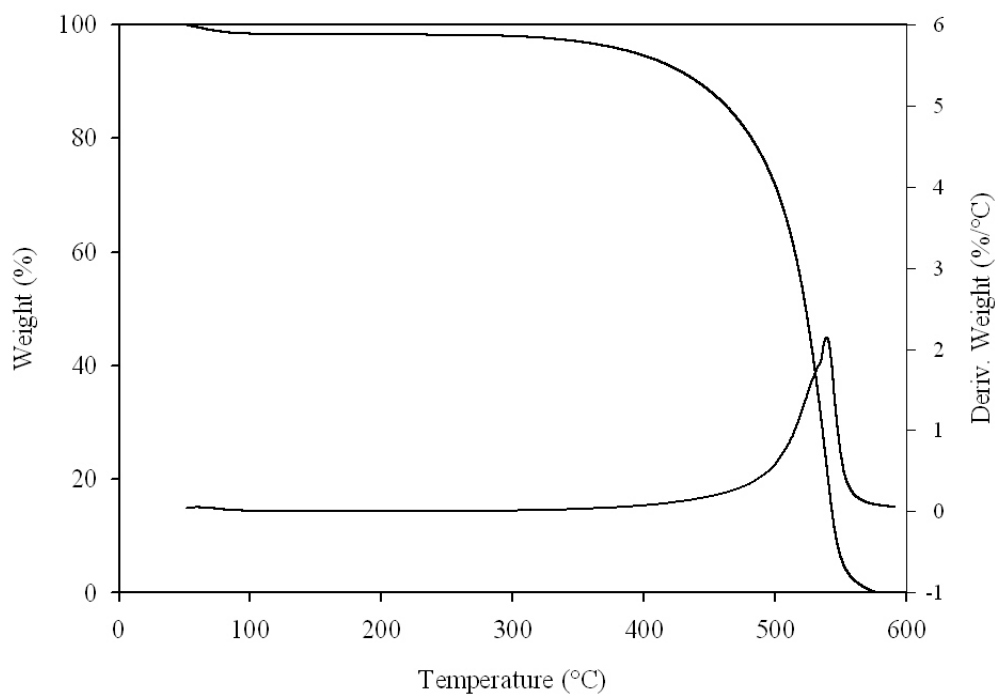


Figure C.13 TGA curve of PI100

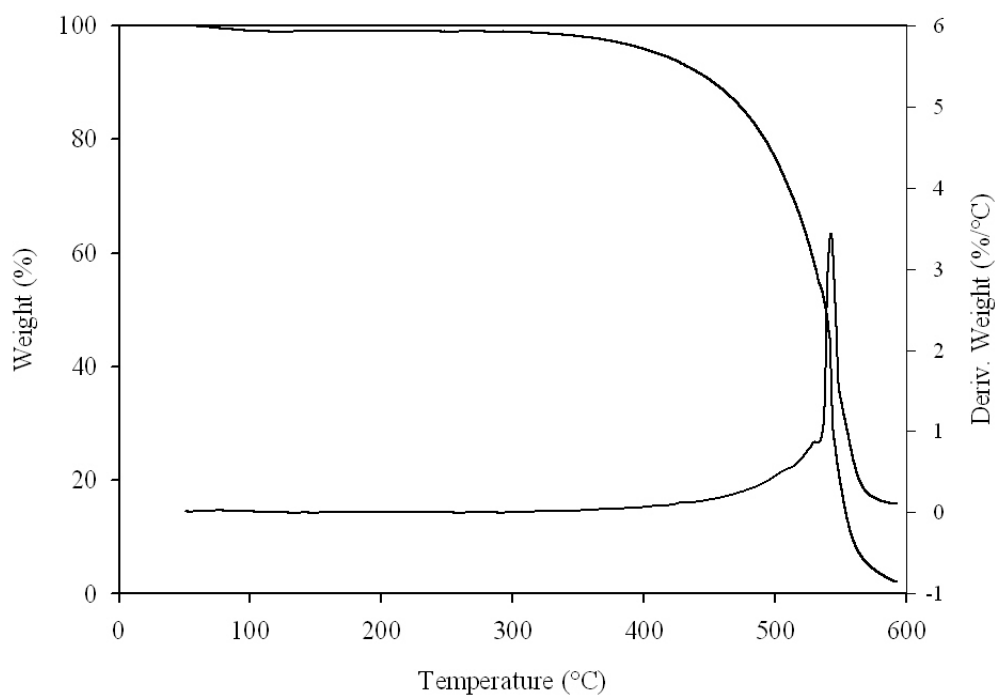


Figure C.14 TGA curve of PI100-C0.1

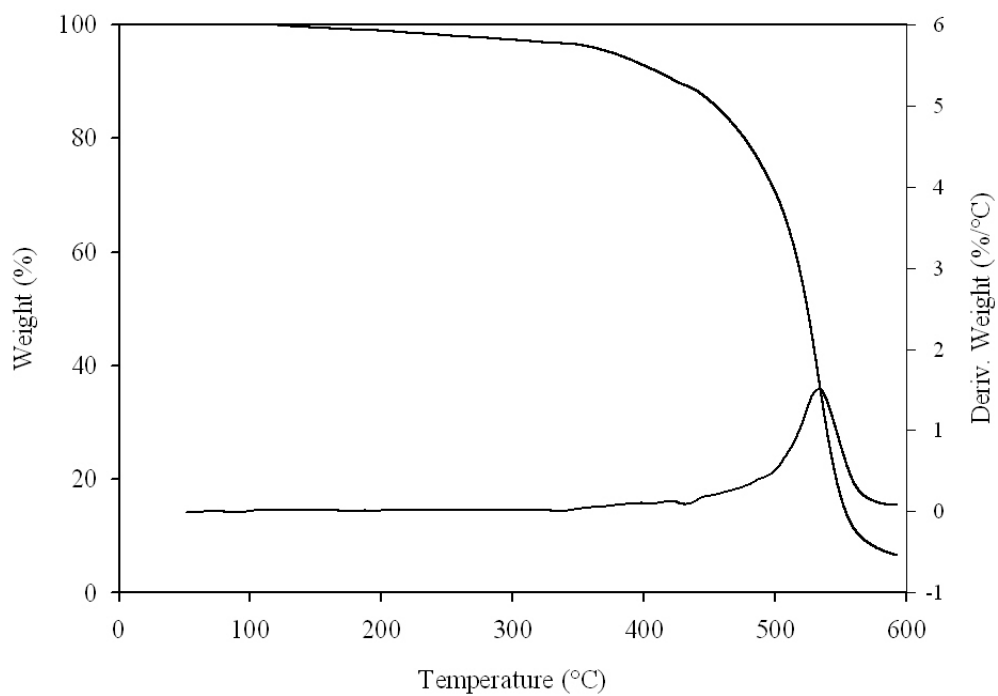


Figure C.15 TGA curve of PI100-C0.5

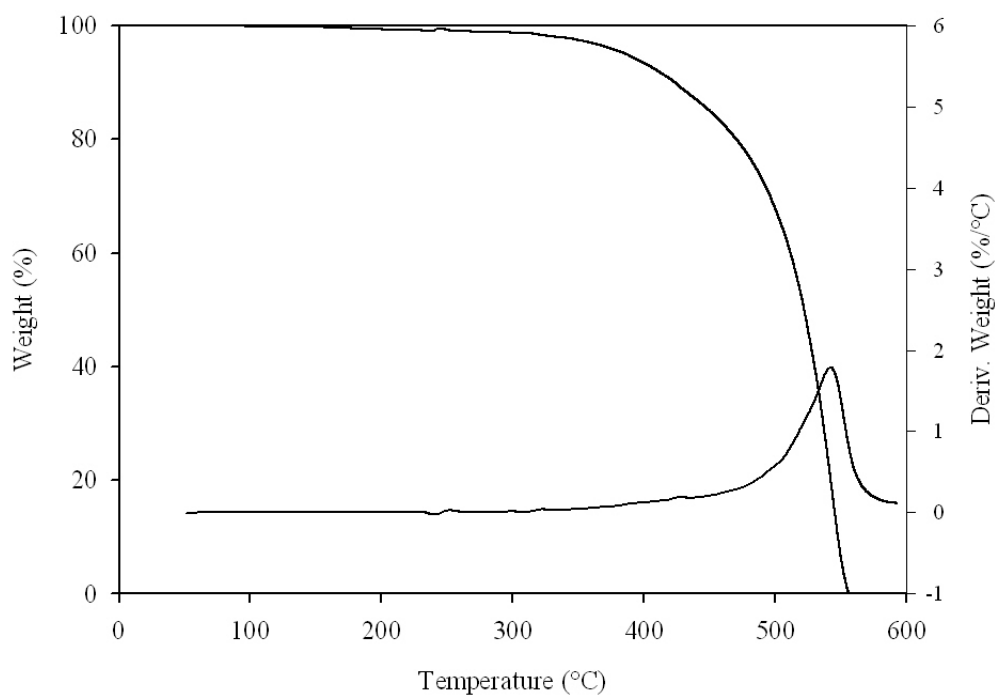


Figure C.16 TGA curve of PI100-C1.0

VITA

Mr. Sirichai Reeyakad was born on March 27, 1983 in Samutprakarn, Thailand. He received the Bachelor's Degree of Chemical Engineering from the Department of Chemical Technology, Faculty of Science, Chulalongkorn University in May 2005, He continued his Master's study at Chulalongkorn University in June, 2005.